Vibration-based condition monitoring of rotating machines in nonstationary regime

Dany Abboud

▶ **To cite this version:**

Dany Abboud. Vibration-based condition monitoring of rotating machines in nonstationary regime. Mechanics [physics.med-ph]. INSA de Lyon, 2015. English. NNT : 2015ISAL0106 . tel-01370989

HAL Id: tel-01370989
https://theses.hal.science/tel-01370989

Submitted on 23 Sep 2016

HAL is a multi-disciplinary open access archive for the deposit and dissemination of scientific research documents, whether they are published or not. The documents may come from teaching and research institutions in France or abroad, or from public or private research centers.

L'archive ouverte pluridisciplinaire **HAL**, est destinée au dépôt et à la diffusion de documents scientifiques de niveau recherche, publiés ou non, émanant des établissements d'enseignement et de recherche français ou étrangers, des laboratoires publics ou privés.

N° d'ordre 2015ISAL0106
Année 2015

Thèse

Vibration-based condition monitoring of rotating machines in nonstationary regime

Présentée devant
L'institut national des sciences appliquées de Lyon

Pour obtenir
Le grade de docteur

Formation doctorale
Mécanique

École doctorale
Ecole Doctorale Mécanique Energétique Génie civil et Acoustique (MEGA)

Par
Dany Abboud

Soutenue le 22 Octobre 2015 devant la Commission d'examen

Jury MM.

M Thomas	Professeur (École de Technologie Supérieure, Montréal), Rapporteur
M. Elbadaoui	Professeur (Université Jean Monnet), Rapporteur
R. Zimroz	Professeur (Université de technologie de Wroclaw)
C. Capdessus	Maître de conférences (IUT de Chartres)
P. Borghesani	Maître de conférences (Université de technologie de Queensland), invité
S. Sieg-Zieba	Ingénieur-docteur (CETIM), encadrant CETIM
M. Eltabach	Ingénieur-docteur (CETIM) , Co-directeur de thèse
J. Antoni	Professeur (INSA de Lyon), Directeur de thèse

Laboratoire de recherche : Laboratoire de Vibrations Acoustique (LVA)

Cette thèse est accessible à l'adresse : http://theses.insa-lyon.fr/publication/2015ISAL0106/these.pdf
© [D. Abboud], [2015], INSA Lyon, tous droits réservés

Surveillance vibratoire des machines tournantes en régime non-stationnaires

Résumé

Dans les dernières décennies, la surveillance vibratoire des machines tournantes a acquis un intérêt particulier fournissant une aide efficace pour la maintenance dans l'industrie. Aujourd'hui, de nombreuses techniques efficaces sont bien établies, ancrées sur des outils puissants offerts notamment par la théorie des processus cyclostationnaires. Cependant, toutes ces techniques reposent sur l'hypothèse d'un régime de fonctionnement (c.à.d. vitesse et/ou charge) constant ou éventuellement fluctuant d'une façon stationnaire. Malheureusement, la plupart des machines surveillées dans l'industrie opèrent sous des régimes non stationnaires afin de remplir les tâches pour lesquelles elles ont été conçues. Dans ce cas, ces techniques ne parviennent pas à analyser les signaux vibratoires produits. Ce problème a occupé la communauté scientifique dans la dernière décennie et des techniques sophistiquées de traitement du signal ont été conçues pour faire face à la variabilité du régime. Mais ces tentatives restent limitées, dispersées et généralement peu sountenues par un cadre théorique. Le principal objectif de cette thèse est de combler partiellement cette lacune sur la base d'une formalisation théorique du sujet et d'un développement systématique de nouveaux outils de traitement du signal. Dans ce travail, la non-stationnarité du régime est limitée à celle de la vitesse— c.à.d. vitesse variable et charge constante— supposée connue a priori. Afin d'atteindre cet objectif, la méthodologie adoptée consiste à étendre le cadre cyclostationnaire avec ses outils dédiés. Nous avons élaboré cette stratégie en distinguant deux types de signatures. Le premier type comprend des signaux déterministes connus comme cyclostationnaires au premier ordre. La solution proposée consiste à généraliser la classe cyclostationnaire au premier ordre à la classe cyclo-non-stationnaire au premier ordre qui comprend des signaux déterministes en vitesse variable. Le second type comprend des signaux aléatoires périodiquement corrélés connus comme cyclostationnaires au deuxième ordre. Trois visions différentes mais complémentaires ont été proposées pour traiter les variations induites par la non-stationnarité de la vitesse de fonctionnement. La première adopte une approche cyclostationnaire angle\temps, la seconde une solution basée sur l'enveloppe et la troisième une approche cyclo-non-stationnaire (au second ordre). De nombreux outils ont été conçus dont les performances ont été testées avec succès sur des signaux vibratoires réels et simulés.

Cette thèse est accessible à l'adresse : http://theses.insa-lyon.fr/publication/2015ISAL0106/these.pdf
© [D. Abboud], [2015], INSA Lyon, tous droits réservés

Mots-Clés: cyclostationnaire – cyclo-non-stationnaire – cyclostationnaire en angle\temps – régime non-stationnaire – analyse vibratoire – surveillance d'état.

Vibration-based condition monitoring of rotating machines in nonstationary regimes

Abstract

In the last decades, vibration-based condition monitoring of rotating machine has gained special interest providing an efficient aid for maintenance in the industry. Nowadays, many efficient techniques are well-established, rooted on powerful tools offered in particular by the theory of cyclostationary processes. However, all these techniques rely on the assump-tion of constant— or possibly fluctuating but stationary— operating regime (i.e. speed and/or load). Unfortunately, most monitored machines used in the industry operate under nonstationary regimes in order to fulfill the task for which they have been designed. In this case, these techniques fail in analyzing the produced vibration signals. This issue, therefore, has occupied the scientific committee in the last decade and some sophisticated signal processing techniques have been conceived to deal with regime variability. But these works remain limited, dispersed and generally not supported by theoretical frameworks. The principal goal of this thesis is to partially fill in this gap on the basis of a theoretical formalization of the subject and a systematic development of new dedicated signal processing tools. In this work, the nonstationarity of the regime is confined to that of the speed— i.e. variable speed and constant load, assumed to be known *a priori*. In order to reach this goal, the adopted methodology consists in extending the cyclostationary framework together with its dedicated tools. We have elaborated this strategy by distinguishing two types of signatures. The first type includes deterministic waveforms known as first-order cyclostationary. The proposed solution consists in generalizing the first-order cyclostationary class to the more general first-order cyclo-non-stationary class which enfolds speed-varying deterministic signals. The second type includes random periodically-correlated waveforms known as second-order cyclostationary. Three different but complementary visions have been proposed to deal with the changes induced by the nonstationarity of the operating speed. The first one adopts an angle\time cyclostationary approach, the second one adopts an envelope-based solution and the third one adopts a (second-order) cyclo-non-stationary approach. Many

Cette thèse est accessible à l'adresse : http://theses.insa-lyon.fr/publication/2015ISAL0106/these.pdf
© [D. Abboud], [2015], INSA Lyon, tous droits réservés

tools have been conceived whose performances have been successfully tested on simulated and real vibration signals.

Mots-Clés: cyclostationary – cyclo-non-stationary – angle\time cyclostationary – nonstationary regime – vibration analysis – condition monitoring.

Cette thèse est accessible à l'adresse : http://theses.insa-lyon.fr/publication/2015ISAL0106/these.pdf
© [D. Abboud], [2015], INSA Lyon, tous droits réservés

To my parents
To all those who are dear to me

Cette thèse est accessible à l'adresse : http://theses.insa-lyon.fr/publication/2015ISAL0106/these.pdf
© [D. Abboud], [2015], INSA Lyon, tous droits réservés

Preface

This PhD thesis contains the result of research undertaken at the laboratory of vibration and acoustic (LVA) of the National institute of applied science (INSA) of Lyon – France, in collaboration with and financed by the technical center of mechanical industries (CETIM) of Senlis – France. Undoubtedly, most of the results in this dissertation were the fruit of a collaborative work which includes, aside from me, scientific and technical experts from both university and industry.

I would like to express my special appreciation and thanks to my supervisors: Prof. Jérôme Antoni, Dr. Mario Eltabach and Dr. Sophie Sieg-Zieba, you have been great mentors for me. Your great scientific culture and human qualities are all elements that have strengthened me throughout the progress of my work. Your advices on both researches as well as on my career have been priceless. Also, I appreciate the time you gave for me disregarding your busy schedules.

I also want to express my gratitude to Prof. Didier Remond and Dr. Sophie Baudin from LaMCoS - INSA of Lyon, as well as Mr. Olivier Sauvage from PSA Peugeot Citroen- Paris, with whom we have done an interesting job. Again, I want to thank Prof. Jérôme Antoni who initiated this collaboration.

Also, thanks to my colleagues in LVA and CETIM for their scientific and technical advices.

Special thanks to my family. Words cannot express how grateful I am to my mother, my father and my two brothers for all of the sacrifices that you have made on my behalf.

Eventually, I wish to thank my girlfriend Marina for the patient and priceless support she has shown me, throughout this thesis.

Cette thèse est accessible à l'adresse : http://theses.insa-lyon.fr/publication/2015ISAL0106/these.pdf
© [D. Abboud], [2015], INSA Lyon, tous droits réservés

Contents

Cette thèse est accessible à l'adresse : http://theses.insa-lyon.fr/publication/2015ISAL0106/these.pdf
© [D. Abboud], [2015], INSA Lyon, tous droits réservés

Cette thèse est accessible à l'adresse : http://theses.insa-lyon.fr/publication/2015ISAL0106/these.pdf
© [D. Abboud], [2015], INSA Lyon, tous droits réservés

Acronyms

CM	condition monitoring
CS	cyclostationary
NS	Nonstationary
CETIM	Technical center of mechanical industries
REB	Rolling element bearings
CS1	First-order cyclostationary
CS2	Second-order cyclostationary
SNR	Signal-to-noise ratio
PDF	Probability distribution function
SC	Spectral correlation
SCoh	Spectral coherence
PSD	Power spectral density
CMS	Cyclic modulation spectrum
SES	Squared envelope spectrum
LTI	Linear time-invariant
CNS	Cyclo-non-stationary
ISA	Improved synchronous average
CNS1	First-order cyclo-non-stationary
GSA	Generalized synchronous average
CPW	Cepstrum prewhitening
AT-CS	Angle\time cyclostationary
OFSC	Order-frequency spectral correlation
OFSCoh	Order-frequency spectral coherence
CNS2	Second-order cyclo-non-stationary
SDSC	Speed dependent spectral correlation

Cette thèse est accessible à l'adresse : http://theses.insa-lyon.fr/publication/2015ISAL0106/these.pdf
© [D. Abboud], [2015], INSA Lyon, tous droits réservés

List of Figures

Cette thèse est accessible à l'adresse : http://theses.insa-lyon.fr/publication/2015ISAL0106/these.pdf
© [D. Abboud], [2015], INSA Lyon, tous droits réservés

List of Tables

Cette thèse est accessible à l'adresse : http://theses.insa-lyon.fr/publication/2015ISAL0106/these.pdf
© [D. Abboud], [2015], INSA Lyon, tous droits réservés

1 General introduction

1.1 General context

Rotating machines exist in a wide variety of industrial applications such as power production, vehicle transportation, process manufacturing and certainly others. Often, they operate under various conditions for a long time in a continuous chain of production. Thus, they are prone to failure in one or more of their components, causing a decrease in the system efficiency and, ultimately, a complete breakdown. Such inconvenient will not only add significant charges to the operation cost of the system, but also could result in serious risks to workers and users in some critical applications (e.g. aeronautic applications). From here comes the need for a maintenance activity to ensure a continuous operation of the system. As defined by AFNOR, maintenance is the process of maintaining or restoring a good in a specified state so that it is able to provide a specific service. Historically, maintenance was seen either as corrective or preventive. The corrective maintenance is carried out after breakdown and, consequently, results in an unscheduled downtime [Morow 1952]. For this reason, it is the most expensive approach since an additional cost related to the outage time of the system is generally counted. The preventive maintenance came in this context aiming to prevent this disadvantage. In this case, the maintenance activity is carried out at predetermined intervals or according to prescribed criteria recommended by the supplier [Quinion 2015]. The main advantage of this approach is the significant reduction of the probability of failure of the system. However, such an approach does not ensure a full exploitation of the component lifetimes: maintenance tasks are established more frequently than necessary and the full life of various components is not exhausted. A sophisticated version of the preventive maintenance, called the predictive maintenance, was developed lately to solve the mentioned inconvenient. It is designed to help in determining the condition of in-service equipment in order to allow convenient scheduling of the maintenance actions while preventing unexpected failures [Jardine 2006]. Predictive maintenance is thus based on a condition monitoring (CM) system whose role is to produce ac-

Cette thèse est accessible à l'adresse : http://theses.insa-lyon.fr/publication/2015ISAL0106/these.pdf
© [D. Abboud], [2015], INSA Lyon, tous droits réservés

tionable information (i.e. commands for maintenance actions) according to a certain analysis of various types of inputs measured by sensors (temperature, pressure, vibrations, current, voltage, etc.). The efficiency of such an approach mainly relies on the precision and reliability of the CM system.

When it comes to rotating machinery, vibration analysis is a widely accepted technique for CM in a variety of industries. Indeed, rotating machine vibrations are likely to convey a lot of information about the internal forces in the system. These internal forces are often related to some fault mechanisms and exhibit distinctive vibration symptoms widely referred as mechanical signatures [Braun 1986]. The measured vibrations can be divided into three general types according to the used sensor. First, displacement sensors measure the vibration displacement (its unit is meter) being the total distance travelled by the vibration body from one peak to peak. Second, velocity sensors measure the vibration velocity defined as the change of the displacement per unit time (its unit is m/s) of a surface as the machine vibrates. Third, the most common sensor in use nowadays is the piezoelectric accelerometer which measures the acceleration (its unit is m/s^2). The latter sensor is applicable to a broad range of frequencies, being cheap, robust, and available in a wide range of sizes and configurations [McGowin 2006]. In the present PhD thesis, analyses are exclusively performed on acceleration signals.

In the literature, there is a wide variety of signal processing tools used for the analysis of vibration signals, starting from the classic spectral [McFadden 1986] [Randall 1982] and envelope [Darlow 1974] [McFadden 1984b] [Ho 2000] analysis techniques, passing by parametric [Bardou 1994] [Sherman 1995] [VanZante 1996] and time-frequency [Staszewski 1997] [Adewusi 2001] [Belsak 2007] techniques, up to more sophisticated techniques such as those based on the cyclostationary (CS) theory [Antoni 2004a] [Antoni 2009]. Their common goal is to enable a better characterization of mechanical signatures, making them good candidates to be fed to an automatic decision system. Noteworthy is the fact that the effectiveness of these techniques is confined to the case of (quasi-) stationary operating regime. It should be clear from the beginning that, in the field of rotating machine vibration analysis, the terminology “stationary regime” generally refers to a stationary speed and load wherein the corresponding profiles remain merely constant during the operation of the system. The vibration signals, however, are typically nonstationary (NS) due to (i) the periodicity of the excitation mechanisms intrinsically related with the machine kinematics and (ii) the produced transient signatures (wide-band waveforms) generally related to the dynamical properties of the system. This explains

Cette thèse est accessible à l'adresse : http://theses.insa-lyon.fr/publication/2015ISAL0106/these.pdf
© [D. Abboud], [2015], INSA Lyon, tous droits réservés

why the spectral analysis—which is based on the stationary assumption—is not generally enough to characterize all rotating machine faults.
In practice, most monitored machines used in industry operate under NS regimes in order to fulfill the task for which they have been designed. A typical example is a wind turbine whose speed is mostly dependent on the random behavior of the wind [Urbanek 2013]. Another example is a mining machine wherein the nonstationarity of the load is induced by the nonstationarity of technological process of mining (variation of external load caused by an operating bucket wheel, a time-varying stream of materials transported by conveyors, etc.) [Zimroz 2008]. In these cases, most of the classical techniques, including those based on the CS theory, fail in analyzing the produced vibration signals. The present thesis comes into this context aiming to develop new signal processing tools for the vibration-based CM of rotating machines in NS conditions.

1.2 Problematic and objective

The technical center of mechanical industry (CETIM) is engaged in a large project with the intent of developing a CM system for rotating machines when operating under NS and severe conditions. This particularly includes the development of advanced signal processing tools dedicated to fault diagnosis, the fusion of data returned by different sensors (vibrations, temperature, currents, torques, etc.), and the embedding of an intelligent surveillance system. Being a part of this project, this PhD thesis is precisely centered on the development of new signal processing tools for the vibration-based CM of rotating machines when operating under NS conditions. The concerned vibrations are exclusively accelerations. In the industry, there are two existing CM approaches to deal with the issue of the nonstationarity of the regime. The first approach controls the acquisition system in order to acquire stationary regime records and data are then processed by means of classical diagnostic tools. However, in some applications, the permanent acquisition of (quasi-) constant speed records is not always feasible. For example, the operating speed of a wind turbine is mostly unpredictable as it depends on the random behavior of the wind. This restriction, for instance, prohibits this approach from being a versatile solution in the general setting. The second approach uses sophisticated signal processing techniques able to accommodate with the variations of the regime. Actually, the development of such tools has occupied the scientist committee in the last few years. Some efficient tools have been developed in the literature to deal with the regime variability within the record. But these works remain limited and generally not supported by theoretical frameworks. It is

Cette thèse est accessible à l'adresse : http://theses.insa-lyon.fr/publication/2015ISAL0106/these.pdf
© [D. Abboud], [2015], INSA Lyon, tous droits réservés

the principal object of this thesis to partially fill in this gap. In this work, the nonstationarity of the regime will be confined to that of the speed— i.e. variable speed and constant load. Also, it will be assumed that an accurate measure of the speed profile exists. Though the applications are constrained to vibration signals produced by a gearbox (principally gear and rolling element bearing (REB) vibrations), the applicability of the developed tools is intended to cover a wide variety of mechanical signals. Having defined the goals of this manuscript, the next subsection sets the accredited strategy to reach them.

1.3 General strategy and guidelines

Most of the vibrational processes generated by rotating machines are cyclostationary (CS), i.e. they exhibit periodic statistical properties. The reason is that the related excitation forces are often connected with the cyclic motion of the rotating shaft and, consequently, produce statistically periodic vibrations when the machine operates under stationary conditions. Depending on the machine design and the excitation phenomena, the emitted signals may belong to two main CS subclasses, namely, first-order cyclostationary (CS1) and second-order cyclostationary (CS2) classes [Antoni 2009] [Antoni 2004a] [Raad 2008]. CS1 signals are characterized by a periodic mean and they are related to deterministic and repetitive excitations such as those generated by imbalances, misalignments, flexible coupling, etc. CS2 signals are characterized by a zero mean and periodic (co-) variance and they are related to random and repetitive excitations such as those generated by wear, friction forces, impacting forces, fluid motions, combustion forces, etc. [Antoni 2004a].

Even if it slightly complicates the theoretical framework, the CS theory provides a rigorous framework from which many signal processing tools can be derived [Gardner 1990]. These tools provide more descriptive representations of mechanical signatures, thus enabling better characterization of the faults [Antoni 2004a]. In fact, their practical robustness stems from the consideration of the information redundancy across the cycles, thus making them suitable to reveal weak fault signatures when embedded in strong stationary noise. From here was our motivation to take advantage of this theory whose applications in the mechanical field have reached an advanced state of maturity [Antoni 2009]. Therefore, our strategy to deal with the problematic of the speed variability is to systematically extend the CS class together with its dedicated tools. We believe that this way is more straightforward than separately generalizing existing diagnostic tools. For this purpose, our work is principally oriented towards the extension of the first-

Cette thèse est accessible à l'adresse : http://theses.insa-lyon.fr/publication/2015ISAL0106/these.pdf
© [D. Abboud], [2015], INSA Lyon, tous droits réservés

and second-order CS classes. Although these generalizations do not include higher-orders, it often happens that the first two orders are enough to cover most practical purposes in mechanical engineering applications. Nevertheless, there is no doubt that similar lines can be followed to generalize higher-orders. In order to reach our goal, the treatment of the thesis problematic must respect the following elements:

i. Some reflections regarding the changes in the vibration signals induced by the nonstationarity of the speed and, accordingly, the extension of CS classes to enfold the associated vibration signals.

ii. Extension of dedicated statistical tools and proposal of consistent estimators.

iii. Demonstrating their usefulness for rotating machine fault diagnosis in NS regime. This specifically requires their validation on simulated and real vibration signals on one hand, and the comparison with classical CS tools on the other hand.

iv. Comparison between the developed tools and some sophisticated tools previously proposed to deal with NS regime

Having defined the general strategy of our research, the next subsection discusses the organization of the thesis.

1.4 Organization of the thesis

This thesis is divided into 4 chapters.

In chapter 1, we start the thesis with a general introduction. We delineate the framework, the problematic and the objective of this work. We equally set a general strategy with some guidelines to solve the issues.

In chapter 2, we recall the theoretical background of "cyclostationarity" which is a prerequisite for the development of advanced tools (see section 1.3). It is an important property that characterizes the vibratory processes induced by rotating machines. We point out on distinguishing among two main sub-classes, namely the first- and the second-order CS classes. The related tools are then revised and investigated on a Fourier based signal modal. We then investigate the vibrations emitted by gears and REBs, while highlighting their CS property. Also, we discuss some practical peculiarities of the CS nature of rotating machine signals.

In chapter 3, we describe the research methodology followed to reach the thesis objective defined in section 1.2. The principal contributions of this thesis are presented in five independent articles, logically connected among each other and enclosed in the appendices. This chapter establishes the link between these publications and the research methodology according to the general strategy and guidelines provided in section 1.3. In particular, it

Cette thèse est accessible à l'adresse : http://theses.insa-lyon.fr/publication/2015ISAL0106/these.pdf
© [D. Abboud], [2015], INSA Lyon, tous droits réservés

classifies the solution into 4 principal gates. The first one is concerned with the extension of the CS1 framework, whereas the three others are concerned with the extension of the CS2 framework according to three different, but complementary, visions.
In chapter 4, we seal this thesis with a general conclusion and some perspectives.

Cette thèse est accessible à l'adresse : http://theses.insa-lyon.fr/publication/2015ISAL0106/these.pdf
© [D. Abboud], [2015], INSA Lyon, tous droits réservés

2 State of the art on cyclostationarity

Cette thèse est accessible à l'adresse : http://theses.insa-lyon.fr/publication/2015ISAL0106/these.pdf
© [D. Abboud], [2015], INSA Lyon, tous droits réservés

2.1 Introduction

The vibration analysis of rotating machine signals was historically established under the assumption of stationarity benefiting from the many ‘‘on-the-shelf’’ tools offered by that framework. By definition, the stationary hypothesis assumes a constant statistical behavior in time of the evaluated signals. This assumption is unrealistic when it comes to rotating machine signals as these are likely to witness varying statistics due to some sequential changes in the excitation mechanisms. Generally speaking, a succession of events mostly occurs within the machine cycle so as to release energy on a rhythmic basis. Some examples are the meshing of teeth in gears, impacts due to a local fault, combustion of gas in internal combustion engines, turbulence around fan blades, etc. [Antoni 2004a] [Antoni 2009]. Such phenomena are likely to produce transient signatures (i.e. wide-band waveforms) carrying critical information on the machine health. A typical example is a REB subjected to a local fault in one of its components wherein cyclic impacts— generated when the defect strikes a mating surface— excite (wide-band) structural resonances. In fact, it is the presence of these transients that makes the signal NS and this nonstationarity is intimately related to the concept of information (e.g. the nature of the excitation, the properties of the transfer functions, etc.). Because of their short duration, transients are extremely difficult to track inside the machine cycle. Their investigation was historically made under the local stationarity assumption using time-frequency tools. These tools are well-established nowadays and widely used as *analysis tools*, but not as *processing tools*. This may return to the fact that these tools are ineffective when analyzing low signal-to-noise (SNR) ratio signals. Thus, they are generally unable to propose a versatile methodology that applies to all mechanical signals in all circumstances. Nevertheless, the use of these tools is more a matter of convenience than of actuality.

Cyclostationarity comes into this context by defining a certain type of nonstationarity whose statistics evolve on a periodic basis. It also provides a rigorous framework to signal processing tools that extends the classical stationary tools. The practical robustness of cyclostationary tools follows from the consideration of the information redundancy across the cycles (as opposed to the approaches based on local stationarity), thus making it suitable to reveal weak cyclic signatures even when embedded in strong stationary noise. Therefore, this theory has proved its leading role for different types of rotating machine vibration analysis and in multiple fields of application such as machine diagnostics, identification of mechanical systems and sep-

Cette thèse est accessible à l'adresse : http://theses.insa-lyon.fr/publication/2015ISAL0106/these.pdf
© [D. Abboud], [2015], INSA Lyon, tous droits réservés

aration of mechanical sources. In particular, vibration-based diagnostic is perhaps the field which has most benefited from cyclostationarity during the last two decades.

The principal object of this chapter is to review the CS theory, some of its tools and its applications on rotating machine diagnostic (precisely for gears and REBs). Section 2.2 provides a Fourier based definition of CS processes with the aim to unambiguously describe its properties. Also, different types of cyclostationarity are discussed while underlining their physical differences. Section 2.3 reviews some CS1 tools, namely Fourier domain calculation techniques, synchronous averaging and blind filters. Section 2.4 reviews some CS2 tools, namely the instantaneous autocovariance function, the Wigner-Ville spectrum, the spectral correlation and others. Section 2.5 reviews and investigates the nature of the vibrations emitted by gears and REBs from a CS point of view. For this purpose, simple models are first reviewed before being analytically evaluated by means of CS tools. Section 2.6 discusses some practical peculiarities of the CS nature of rotating machine signals. Finally, this chapter is sealed with a conclusion in section 2.7.

2.2 Cyclostationary processes

2.2.1 Basic definitions

CS processes are a special case of NS processes that carry hidden periodicities in their structure. Formally speaking, a stochastic process $X(t)$ is said *CS* with *period* T (also coined as *cycle*) if its joint probability density function (PDF) is periodic in t with T, i.e.

$$p_X(X_1, \dots, X_n; t, \tau_1, \dots \tau_{n-1}) = p_X(X_1, \dots, X_n; t + T, \tau_1, \dots \tau_{n-1}), \quad (1)$$

where $\{X_i\}_{i=1}^{i=n}$ are realizations of the process $X(t)$. Despite its valuable theoretical significance, this definition does not clearly reveal the structure of CS signals. Therefore, various generative models have been proposed in the literature, some with physical origins [George 1992] and other with grounds in telecommunication engineering [Gardner 1990]. Of particular interest is the Fourier series based model [Gardner 1975] which decomposes the signal into a set of *random* coefficients modulated by a set of periodic exponential basis:

$$X(t) = \sum_{k\in\mathbb{Z}} c_X^k(t) e^{j2\pi kt/T} \quad (2)$$

Cette thèse est accessible à l'adresse : http://theses.insa-lyon.fr/publication/2015ISAL0106/these.pdf
© [D. Abboud], [2015], INSA Lyon, tous droits réservés

where $\mathbb{Z}$ is the set of all integers, the Fourier coefficients $c_X^k(t)$ are jointly stationary signals and the complex exponentials are parameterized by cyclic frequencies k/T. This insightful representation makes explicit the existence of hidden periodicities in the form of periodic modulations of the random carriers $c_X^k(t)$. The order of cyclostationarity is dictated by the order of the joint stationarity of the coefficients. In a general manner, the first two orders are usually investigated in signal processing as they cover most practical purposes in engineering applications. The following subsections investigate their definitions and statistical properties.

2.2.11 First-order cyclostationary signals

The most basic CS signal is when the coefficients $c_X^k(t)$ are first-order stationary. This implies that their mean is constant, i.e.

$$\mathbb{E}\{c_X^k(t)\} = \bar{c}_{1X}^k. \tag{3}$$

where symbol $\mathbb{E}$ denotes the ensemble averaging operator. In this case, $X(t)$ is said *CS1* and enjoys a periodic mean of cycle T. Thus, the latter accepts a Fourier series with non-zero *deterministic* coefficients

$$M_{1X}(t) \stackrel{\text{def}}{=} \mathbb{E}\{X(t)\} = \sum_k M_{1X}^k e^{j2\pi kt/T}, \tag{4}$$

where

$$M_{1X}^k = \bar{c}_{1X}^k, \tag{5}$$

stand for the *cyclic means* of signal X.

2.2.12 Second-order cyclostationary signals

A more general CS signal is when the coefficients $c_X^k(t)$ are mutually second-order stationary. This implies that the autocovariance or the cross-covariance of any two coefficients is strictly dependent on the time-lag τ, i.e.

$$\mathbb{E}\left\{\left(c_X^k(t+\tau/2) - M_{1X}^k\right)\left(c_X^{k'}(t-\tau/2) - M_{1X}^{k'}\right)^*\right\} = \bar{c}_{2X}^{k,k'}(\tau) \quad for\ all\ k, k'. \tag{6}$$

In this case, $X(t)$ is said *CS2* and enjoys a periodic autocovariance function of cycle T. Thus, the latter accepts a Fourier series with non-zero *deterministic* coefficients

$$C_{2X}(t,\tau) \stackrel{\text{def}}{=} \mathbb{E}\{X_c(t+\tau/2)X_c(t-\tau/2)^*\} = \sum_k C_{2X}^k(\tau) e^{j2\pi kt/T} \tag{7}$$

Cette thèse est accessible à l'adresse : http://theses.insa-lyon.fr/publication/2015ISAL0106/these.pdf
© [D. Abboud], [2015], INSA Lyon, tous droits réservés

where $X_c = \mathrm{X}(t) - M_{1X}(t)$ stands for the centered signal and

$$C_{2X}^{k}(\tau) = \sum_{k'} \bar{c}_{2X}^{k+k',k'}(\tau) \tag{8}$$

stand for the *cyclic autocovariance functions* of X. It is worth noting that Eq. (7) separates the autocovariance function into two sets of deterministic functions with different physical meanings: the "Fourier coefficients" and the "exponential kernels". Whereas the latter is exclusively dependent on the temporal variable and reflects the periodic evolution of the waveform, the former is exclusively dependent on the time-lag and reflects the property of a stationary carrier.

2.2.2 Types of cyclostationarity

The model provided in Eq. (2) defines a strict CS process at the cyclic frequency $\alpha = 1/T$. This cyclostationarity relies on the existence of a unique and finite cycle with respect to which the process is periodic. This definition can be extended to accept multiple CS contributions whose basic cycles, say T_i, are not multiple of each other's. Such signals are called poly-CS and can still be modeled via a Fourier series of random coefficients as:

$$X(t) = \sum_i \sum_{k_i \in \mathbb{Z}} c_X^{k_i}(t) e^{j2\pi k_i t/T_i} = \sum_{v \in \mathcal{A}} c_X^{v}(t) e^{j2\pi v t/T}, \tag{9}$$

where stands for the index referring to the CS contribution number, $c_X^{k_i}(t)$ stands for the kth coefficient associated with the ith CS contribution and $\mathcal{A} = \{k_i.T/T_i | k \in \mathbb{Z}\ and\ i = 1,2,\dots\}$ denotes the cyclic order set with respect to the *reference period* T. Another type of cyclostationarity is obtained through a different kind of interactions between multiple CS contributions whose cycles are not integer multiple of each other. Such signals are called quasi-CS and can still be modeled via a Fourier series as:

$$X(t) = \sum_{v \in \mathcal{B}} c_X^{v}(t) e^{j2\pi v t/T}, \tag{10}$$

where $\mathcal{B} \subset \mathbb{R}$ denotes the cyclic order set whose elements may take any real value ($\mathbb{R}$ is the set of real values).

It is worth noting that the difference between poly- and quasi-cyclostationarity is physical rather than mathematical. In fact, they are mathematically equivalent: the cyclic order set $\mathcal{A}$ of Eq. (9) can be equivalent to $\mathcal{B}$ in Eq. (10) if T_i and k_i are suitably chosen. In general, poly-CS signals are induced by additive combinations of different CS sources whose common cycle is extremely long (i.e. incommensurate) and virtually impos-

Cette thèse est accessible à l'adresse : http://theses.insa-lyon.fr/publication/2015ISAL0106/these.pdf
© [D. Abboud], [2015], INSA Lyon, tous droits réservés

sible to be observed. This is typically the case of complex gearbox vibrations where the least common cycle is a multiple of the cycles of every gear in the system and thus can take many hours to be completed. On the other hand, quasi-CS signals are generally induced by multiplicative combinations of different CS sources whose common cycle is infinite. This is, for instance, the case of REB vibrations which witness modulations between distinct and not phase-locked rotating components. At any rate, poly- and quasi-CS signals should not be considered as a no trouble because the set of their Fourier coefficients is simply the combination of all the basic CS signals that they are compounded of. Therefore, they can still be statistically treated— to some extent— similarly to CS signals. In the following, poly- and quasi-cyclostationarity will be referred to cyclostationarity in general without distinguishing between these different subtleties *if not necessary*.

2.2.3 Cycloergodicity

Previously, the expected value—either used for the mean value or the auto-covariance function—always refers to an ensemble average. This means that the averaging operation is applied on realizations of the same process from repeated experiments. Contrary to the ergodic assumption of stationary signals, the ensemble averaging operator cannot be replaced by the time averaging operator when only one realization of the process exists. This can be checked by calculating the mean value of a pure sine which equals itself but not its time average (because the time average returns zero). Since the statistics of CS signal varies on a periodic basis, the concept of the expected value is intimately linked with a deterministic periodic waveform which can be extracted by the $\mathcal{P}$-operator [Antoni 2004a][1]. This equivalence implicitly exploits the cyclic redundancy of the information in the signal, giving birth to the paradigm of *cycloergodicity*. Cycloergodicity of CS processes is equivalent to what ergodicity is to stationary processes: it is the condition under which the ensemble averaging $\mathbb{E}$ equals the $\mathcal{P}$-operator. This assumption is of high practical importance as it allows to build useful operators and consistent estimators. Sections 2.3 and 2.4 presents some of these operators.

[1]The $\mathcal{P}$-operator is that which extracts all the periodic components of a signal. A detailed exposition of this operator is provided in Ref. [Antoni 2004], while a brief review of this operator is given in subsection 2.3.1.

Cette thèse est accessible à l'adresse : http://theses.insa-lyon.fr/publication/2015ISAL0106/these.pdf
© [D. Abboud], [2015], INSA Lyon, tous droits réservés

2.3 First-order tools

First order tools are those dedicated to the extraction of the first-order moment of a CS signal. The aim of this paragraph is to briefly review some dedicated signal processing tools while highlighting their capacity to deal with different types of cyclostationarity.

2.3.1 Fourier domain calculation

The most natural way to compute the mean value of a CS signal is to select the Fourier coefficients (i.e. cyclic means) associated with the cyclic frequency set, before reconstructing the mean signal by combining them with the associated exponential kernels. This defines the $\mathcal{P}$-operator of a CS signal:

$$m_X(t) = \mathcal{P}\{X(t)\} = \sum_{v\in\mathcal{B}} \left\{ \lim_{W\to\infty} \frac{1}{W} \int_{-W/2}^{+W/2} X(u)\, e^{-j2\pi vt/T} du \right\} e^{j2\pi vt/T}. \quad (11)$$

Note that this operator does not put restrictions on the cyclic order set, thus it can deal with all types of cyclostationarity, the reason why the cyclic order $\mathcal{B}$ (see Eq. (10)) was used to ensure a generic definition. However, *a priori* knowledge of the corresponding cyclic order set is required. The practical implementation of this operator can be performed using a numerical filter after a discrete Fourier transform (using the fast Fourier transform algorithm) of the digitized signal. The filter can be designed as a comb filter of gain equal to unit at the cyclic frequencies, with minimum gain elsewhere and with impulse responses not greater than the signal length [Antoni 2004a]. However, the continuous nature of such transfer functions does not allow the signal to be perfectly periodic. For this purpose, it is preferable to replace the comb filter by Dirac deltas which have a discrete transfer function and, thus, returns a (quasi-) periodic signal.

2.3.2 Synchronous average

The synchronous average (SA)— widely termed as the time synchronous average [Braun 1975][Braun 2011]— is another efficient technique for the extraction of periodic waveforms from a noisy signal. Based on prior knowledge of the desired component, it consists of segmenting the temporal signal into blocks of length equal to the signal period and averaging them together to extract the periodic waveform. By construction, the applicability of the SA is confined to the case when the signal is strictly CS,

Cette thèse est accessible à l'adresse : http://theses.insa-lyon.fr/publication/2015ISAL0106/these.pdf
© [D. Abboud], [2015], INSA Lyon, tous droits réservés

having a *finite* and *known* period. The SA of a signal $X(t)$ with respect to the period T is defined as:

$$m_X(t) = \mathcal{P}_T\{X(t)\} = \lim_{M\to\infty} \frac{1}{2M+1} \sum_{m=-M}^{m=+M} X(t+mT). \qquad (12)$$

Viewed differently, Eq. (12) is equivalent to a special case of Eq. (11) when the cyclic order set $\mathcal{B}$ is replaced by the set of all integers $\mathbb{Z}$— i.e. in the case of strict CS signal [Antoni 2004a]. The estimator of the SA is simply the *cyclic arithmetic mean* computed over a limited number of cycles. The principle of the synchronous average is illustrated in Fig. 1. Despite their equivalence, the practical implementation of the SA (i.e. Eq. (12) is computationally cheaper than that based on the Fourier domain (i.e. Eq. (11). Note that the SA is also suitable for poly-CS signal as it may be successively applied with respect to each basic cycle, yet care should be taken to not extract a several time the same harmonic [Antoni 2004a].

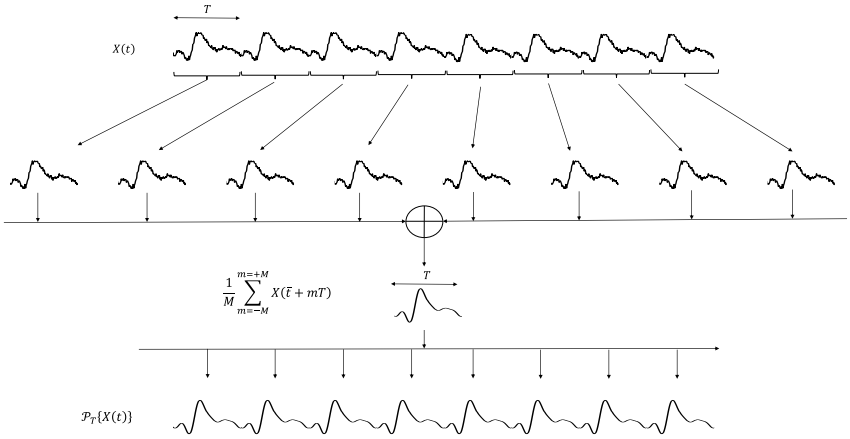

Figure 1 *Principle of the synchronous average.*

2.3.3 Blind filters

Blind filters are basically conceived to estimate the mean value of poly-CS signals when the basic cycles are unknown. In this realm, the "linear adaptive enhancer" [Zeidler 1978], the "adaptive noise canceller" [Widrow 1985] and the "self-adaptive noise canceller" [Randall 1995] provide efficient solutions for this issue. The frequency domain version of the latter is coined "discrete random separator" [Antoni 2003b]; it significantly reduces the computational cost of the algorithm [Antoni 2003a]. In general, the transfer function of such filters are similar to that of the comb filters but where the maxima are not necessarily harmonically related and can there-

Cette thèse est accessible à l'adresse : http://theses.insa-lyon.fr/publication/2015ISAL0106/these.pdf
© [D. Abboud], [2015], INSA Lyon, tous droits réservés

fore blindly adjust to any set of harmonics in a signal. The main drawback of these techniques is the dependence of their performance on the SNR ratio. Another drawback is the continuous nature of the transfer function which disrupts the exact (quasi-) periodicity of the filtered signal—just like the case of comb filters.

2.4 Second-order tools

Second-order tools are based on the use of the autocovariance function. The aim of this paragraph is to briefly review some dedicated signal processing tools.

2.4.1 Instantaneous covariance function

The instantaneous autocovariance function is the most basic tool that follows directly from the autocovariance function (see Eq. (7)) by replacing the ensemble average operator by the $\mathcal{P}$-operator:

$$C_{2X}(t,\tau) = \mathcal{P}\{X_c(t+\tau/2)X_c(t-\tau/2)^*\}. \quad (13)$$

It is worth noting that the $\mathcal{P}$-operator is applied with respect to the time variable t for each time lag τ. If $X(t)$ is a CS2 signal, the instantaneous autocovariance function is (quasi-) periodic and accepts a Fourier series whose coefficients are non-zero and depend on the time-lag—see Eq. (7). In the case of strict cyclostationarity, the $\mathcal{P}$-operator can be replaced by the SA, giving birth to the synchronous autocovariance function defined as $C_{2X}(t,\tau) = \mathcal{P}_T\{X_c(t-\tau/2)X_c(t+\tau/2)^*\}$.

2.4.11 Instantaneous variance function

The instantaneous variance function is a particular case of the instantaneous autocovariance function when the time-lag is nil, viz

$$SE_X(t) = C_{2X}(t,\tau=0) = \mathcal{P}\{|X_c(t)|^2\}. \quad (14)$$

It can be either viewed as a measure of the instantaneous energy or as the mean squared envelope of the (centered) signal. If $X(t)$ is a CS2 signal, the instantaneous variance is (quasi-) periodic and accepts a Fourier series with non-zero coefficients:

$$SE_X(t) = \sum_{v\in\mathcal{B}} SE_X^v e^{j2\pi vt/T} \quad (15)$$

Cette thèse est accessible à l'adresse : http://theses.insa-lyon.fr/publication/2015ISAL0106/these.pdf
© [D. Abboud], [2015], INSA Lyon, tous droits réservés

where SE_X^{υ} stands for the cyclic variance. In the case of strict cyclostationarity, the $\mathcal{P}$-operator can be replaced by the SA, giving birth to the synchronous variance function defined as $SE_X(t) = \mathcal{P}_T\{|X_c(t)|^2\}$.

2.4.2 Time-Frequency distributions

2.4.21 Wigner-Ville spectrum

The Wigner-Ville spectrum is a joint time-frequency energy distribution for NS signals. It is defined as the expected value of the Wigner-Ville distribution that was originally introduced for the time-frequency analysis of finite energy deterministic signals [Martin 1982]. It is also equivalent to the Fourier transform of the autocovariance function with respect to the time-lag variable, i.e.

$$WV_{2X}(t,f) \stackrel{\text{def}}{=} \mathcal{F}_{\tau\to f}\{C_{2X}(t,\tau)\} = \mathcal{F}_{\tau\to f}\left\{\mathcal{P}\left\{X_c\left(t+\frac{\tau}{2}\right)X_c\left(t-\frac{\tau}{2}\right)^*\right\}\right\} \quad (16)$$

where $\mathcal{F}_{\tau\to f}\{*\}$ is the Fourier transform. For CS2 signals, the Wigner-Ville spectrum is (quasi-) periodic with respect to t and accepts a Fourier series with non-zero coefficients,

$$WV_{2X}(t,f) = \sum_{\upsilon\in\mathcal{B}} WV_{2X}^{\upsilon}(f)e^{j2\pi\upsilon t/T}, \quad (17)$$

where $S_{2X}^{\upsilon}(f) = \mathcal{F}_{\tau\to f}\{C_{2X}^{\upsilon}(\tau)\}$ stands for the cyclic power spectrum. The principal advantage of this quantity over the Wigner-Ville distribution is its ability to minimize the presence of negative interference terms thanks to the averaging effect of the autocovariance function (ensured by the $\mathcal{P}$-operator). For instance, the Wigner-Ville spectrum $W_{2(X_1+X_2)}$ of a sum of two independent signals X_1 and X_2 is exactly the sum of the Wigner-Ville spectra $W_{2X_1}$and $W_{2X_2}$of X_1 and X_2. This follows from the fact that the interferences $W_{X_1X_2}$ and $W_{X_2X_1}$are zero as the cross-covariance of X_1 and X_2 is nil. This is in plain contrast with most of quadratic time-frequency representations where interference terms always lead to misleading interpretations. The estimation of this quantity will not be addressed herein; interested readers are invited to read Ref. [Antoni 2007a] [Antoni 2007b]. Another important feature is its similarity to a time-dependent version of the Wiener–Khinchin theorem, thus supporting the interpretation of Wigner-Ville spectrum as an instantaneous spectrum at time t.

2.4.22 Instantaneous power spectrum

Another way to present a time-frequency distribution is by computing the instantaneous variance (or the mean power) at a narrow bandpass filtered signal while scrutinizing the whole spectral content by moving the carrier.

Cette thèse est accessible à l'adresse : http://theses.insa-lyon.fr/publication/2015ISAL0106/these.pdf
© [D. Abboud], [2015], INSA Lyon, tous droits réservés

In this way, the periodic modulations are presented for each spectral carrier or, conversely, the power spectrum is presented at each instant. Formally speaking, let us consider $X_{\Delta f}(t;f)$ the filtered version of $X_c(t)$ through a frequency band of width Δf centered on frequency f. Now using the $\mathcal{P}$-operator, the mean instantaneous power resided through that frequency band is

$$P_X(t,f;\Delta f) = \mathcal{P}\left\{\left|X_{\Delta f}(t;f)\right|^2\right\}. \tag{18}$$

The principle of the mean instantaneous power is illustrated in Fig. (2). The principal disadvantage of such a representation is that it is faced with the uncertainty principle so that the time and frequency resolutions cannot be made arbitrarily and independently small. Precisely, the frequency resolution Δf and the time resolution, say Δt, are interrelated by the inequality

$$\Delta f.\Delta t \geq \frac{1}{4\pi}. \tag{19}$$

Stated differently, the filter bandwidth Δf should be larger than $1/4\pi\Delta t$ in order to be able to track small temporal variations of duration Δt. Note that the Wigner-Ville spectrum is free from this shortcoming. For CS2 signals, the instantaneous power spectrum is (quasi-) periodic with respect to t and accepts a Fourier series with non-zero coefficients:

$$P_X(t,f;\Delta f) = \sum_{v\in\mathcal{B}} P_X^v(f;\Delta f)e^{j2\pi vt/T}. \tag{20}$$

Note that the Fourier coefficients $P_X^v(f;\Delta f)$ are parametrized by the choice of the filter bandwidth predefined by the user. This is what prevents the instantaneous power spectrum from being a density: it is directly linked to the energy of the filtered waveform.

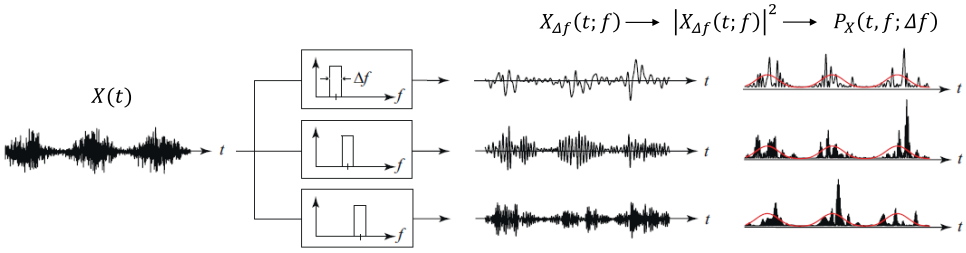

Figure 2 *Academic illustration of the instantaneous power spectrum as the energy flow measured at the output of a filterbank [Antoni 2009].*

Cette thèse est accessible à l'adresse : http://theses.insa-lyon.fr/publication/2015ISAL0106/these.pdf
© [D. Abboud], [2015], INSA Lyon, tous droits réservés

2.4.3 Frequency-Frequency distributions

2.4.31 Spectral correlation

The most prominent way to reveal the statistical information in the auto-covariance function is to present them in the dual Fourier domain. Specifically, the double Fourier transforms relatively to the time t and the time-lag τ defines the spectral correlation function (SC),

$$S_{2X}(\alpha, f) = \underset{\tau \to f}{\mathcal{F}_{t \to \alpha}}\{C_{2X}(t, \tau)\} = \mathcal{F}_{t \to \alpha}\{W_{2X}(t, f)\}, \tag{21}$$

which can be also seen as the Fourier transform of the Wigner-Ville spectrum with respect to the time variable. The SC in Eq. (21) is a frequency-frequency distribution with respect to both the cyclic frequency α, linked to the cyclic evolution of the waveforms and the spectral frequency f, linked to the waveforms in the signal. While the former reflects the frequency of the modulations, the latter describes the frequency of the carriers. An alternative way of defining the SC is

$$S_{2X}(\alpha, f) = \lim_{W \to \infty} \frac{1}{W} \mathbb{E}\left\{X_W^*\left(f - \frac{\alpha}{2}\right) X_W\left(f + \frac{\alpha}{2}\right)\right\}, \tag{22}$$

where $X_W(f) = \mathcal{F}_W\{X(t)\} = \int_{-W/2}^{+W/2} X(t) e^{+j2\pi t f} dt$ stands for the Fourier transform of signal $X(t)$ over a time interval of finite duration W. This expression provides another interpretation of the SC, which actually justifies its name: it is a measure of the correlation between the frequency components of the signal at $f - \alpha/2$ and $f + \alpha/2$. Note that this presentation is very helpful to build performant estimators such as the averaged cyclic periodogram [Antoni 2007a]. In the special case of a CS2 signal, it takes the discrete form

$$S_{2x}(\alpha, f) = \sum_{v \in \mathcal{B}} S_{2X}^{v}(f) \delta(\alpha - {}^{v}/_{T}) \tag{23}$$

with $S_{2X}^{v}(f) = WV_{2X}^{v}(f)$. Expression (23) evidences that the SC of a CS signal is discretely distributed along spectral lines parallel to the f-axis and positioned at the cyclic frequencies $\alpha = v/T$. This unique signature makes the SC a powerful and robust tool for detecting the presence of and characterizing cyclostationarity in engineering applications [Antoni 2007a]. An illustration presenting the relationship among the instantaneous autocovariance function, the Wigner-Wile spectrum and the SC of a (strict) CS signal is provided in Fig. 3.

Cette thèse est accessible à l'adresse : http://theses.insa-lyon.fr/publication/2015ISAL0106/these.pdf
© [D. Abboud], [2015], INSA Lyon, tous droits réservés

2.4.32 Spectral coherence

A related operator is the spectral coherence (SCoh) which has the property of measuring the degree of correlation between two spectral components independently of the signal power spectrum. The SCoh is defined as:

$$\gamma_{2X}(\alpha,f)=\frac{S_{2X}(\alpha,f)}{\left[S_{2X}\left(0,f-\frac{\alpha}{2}\right)S_{2X}\left(0,f+\frac{\alpha}{2}\right)\right]^{1/2}}=\frac{S_{2X}(\alpha,f)}{\left[S_{2X}\left(f-\frac{\alpha}{2}\right)S_{2X}\left(f+\frac{\alpha}{2}\right)\right]^{1/2}}, \quad (24)$$

with $S_{2X}(f)$ the power spectral density (PSD) of signal $X(t)$. Just like the regular correlation coefficient, $|\gamma_{2X}(\alpha,f)|^2$ is normalized between 0 and 1: the closer it is to the unity, the stronger the CS component at cyclic frequency α. Therefore, when a CS signal of cycle $1/\alpha$ is embedded in stationary noise, the squared magnitude of its SCoh, $|\gamma_{2X}(\alpha,f)|^2$, can be seen as an indication of the SNR. In the special case of a CS2 signal, the SCoh also takes a discrete form

$$\gamma_{2X}(\alpha,f)=\sum_{v\in\mathcal{B}}\gamma_{2X}^{v}(f)\delta(\alpha-{}^{v}/_{T}), \quad (25)$$

where

$$\gamma_{2X}^{v}(f)=\frac{S_{2X}^{v}(f)}{\left[S_{2X}\left(f-\frac{v}{2}\right)S_{2X}\left(f+\frac{v}{2}\right)\right]^{1/2}} \quad (26)$$

stand for the *cyclic coherence function*s.

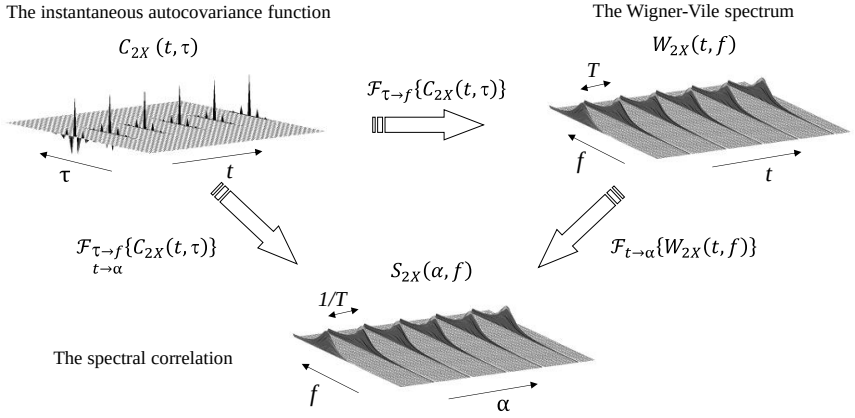

Figure 3 *Academic illustration of the relationship among the instantaneous autocovariance function, the Wigner-Wile spectrum and the spectral correlation of a strict-CS signal.*

Cette thèse est accessible à l'adresse : http://theses.insa-lyon.fr/publication/2015ISAL0106/these.pdf
© [D. Abboud], [2015], INSA Lyon, tous droits réservés

2.4.33 Cyclic modulation spectrum

A similar distribution to the SC is the *cyclic modulation spectrum* (CMS) which can be obtained by applying the Fourier transform on the instantaneous power spectrum with respect to the time variable t, viz

$$P_X(\alpha, f; \Delta f) = \mathcal{F}_{t\to\alpha}\{P_X(t, f; \Delta f)\}. \tag{27}$$

The principle of the mean instantaneous power is illustrated in Fig. (4). Also, the CMS is faced with the uncertainty principle which, in this case, limits the maximal cyclic frequency which can be scanned. Specifically, noting that the reciprocal of the time resolution Δt is the largest cyclic frequency α_{max} that can be scanned in the filtered signal $X_{\Delta f}(t; f)$, the uncertainty principle reads

$$\alpha_{max} \leq 4\pi\Delta f. \tag{28}$$

Conversely, the spectral frequency resolution Δf should be chosen sufficiently coarse so that α_{max} becomes bigger than the higher cyclic frequency to be evaluated. Interestingly, the SC is free from this shortcoming. For CS2 signals, the CMS takes the discrete form

$$P_X(\alpha, f; \Delta f) = \sum_{v\in\mathcal{B}} P_X^v(f; \Delta f)\delta\left(\alpha - {}^{v}/_{T}\right), \tag{29}$$

providing also a symptomatic distribution of parallel spectral lines $P_X^v(f; \Delta f)$ at the cyclic orders v. Last, it is worth noting that the magnitude of this distribution is not unique as it explicitly depends on the Δf defined by the user. Similarly to the instantaneous power spectrum, this also prevents the CMS from being a density.

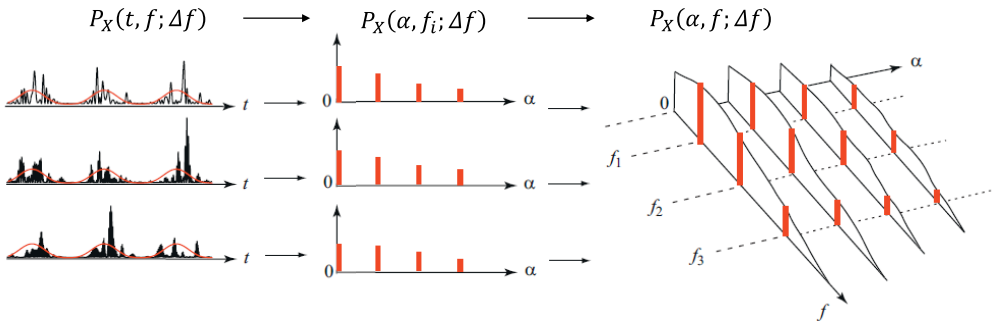

Figure 4 *Academic illustration of the cyclic modulation spectrum [Antoni 2009].*

Cette thèse est accessible à l'adresse : http://theses.insa-lyon.fr/publication/2015ISAL0106/these.pdf
© [D. Abboud], [2015], INSA Lyon, tous droits réservés

2.4.4 Squared envelope spectrum

The squared envelope spectrum (SES) is simply the Fourier transform of the instantaneous variance function. It is also equivalent to the integration of the SC over the spectral frequency axis:

$$SES_X(\alpha) = \mathcal{F}_{t\to\alpha}\{SE_X(t)\} = \int_{-\infty}^{+\infty} S_{2x}(\alpha, f)df. \quad (30)$$

It represents an averaged view of cyclic content of the energy flow carried by all the frequencies. For CS2 signals, the SES takes the discrete form

$$SES_X(\alpha) = \sum_{v\in\mathcal{B}} SE_X^v \delta(\alpha - \frac{v}{T}). \quad (31)$$

2.5 Cyclostationarity in gear and REB vibrations

The inherent periodicities in the kinematics of rotating machines are prone to make vibrations CS. In this context, many precursory works have been reported on modelling rotating machine signals as CS e.g. [Capdessus 2000] [Bouillaut 2001] [McCormick 1998] [Randall 2001]. In particular, the vibration-based diagnostic of gears and REBs was undoubtedly the main beneficiary field. The aim of this section is to review and investigate the nature of the vibrations emitted by these components from a CS point of view.

2.5.1 Gear case

The aim of this subsection is to investigate the nature of the vibrations emitted by a pair of parallel axis gear and to show how it is possible to take advantage of CS tools— particularly the SA— for gear diagnosis.

2.5.11 Preliminaries

A gear is an element of rotating machines having cut teeth which mesh with another toothed part to transmit torque. This can produce a mechanical advantage through a gear ratio by increasing the speed or the torque. Of particular interest are the spur gears which are the simplest and the most widely used type of gears. They consist of a cylinder with the teeth projecting radially, and although they are not straight-sided in form, the edge of each tooth is straight and aligned parallel to the axis of rotation. Sometimes, multiple spur gears are used in sequence to create larger gear ratios [Nice 2000]. The presence of a fault alters the normal functioning conditions causing higher vibration levels as well as a decrease in the transmission ef-

Cette thèse est accessible à l'adresse : http://theses.insa-lyon.fr/publication/2015ISAL0106/these.pdf
© [D. Abboud], [2015], INSA Lyon, tous droits réservés

ficiency. In general, these defects are divided into geometrical or teeth defects. Whereas the former type includes manufacturing errors, mounting errors, installation errors, etc., the latter includes errors that occur during the operation of the gear [Chaari 2011]. Another classification of these defects can be made through their distributions over contact surfaces, namely the distributed and the local defects. Distributed faults affect all the teeth (e.g. wear), while localized faults typically affect a particular tooth (e.g. tooth cracks, spalling, pitting, etc.). Often, local faults progressively develop and lead to the breakage of the tooth. Obviously, such defects are more dangerous and critical than the distributed defects. The next subsections review a simple vibration model of a faulty spur gear and demonstrate how it is possible to take advantage of CS1 tools for their diagnosis.

2.5.12 Vibration model

The principal source of vibratory excitation of a pair of spur gears is relative to the meshing forces resulting from the shock between the teeth of the two wheels. The meshing force is generally modulated by the rotation of the two wheels due to systematic variation of their stiffness. The variation of the stiffness results from the deviation of the teeth shape (due to a fault) from their ideal shape. Since these deviations are different from one tooth to another, it is expected that the modulation induced by each wheel is periodic with a period equal to its rotation. Neglecting frequency modulations, the excitation of a pair of parallel and fixed axis gears operating under constant speed and load can be modeled as:

$$\Sigma_g(t) = m(t)\big(1 + p_1(t) + p_2(t)\big) = m(t) + p'_1(t) + p'_2(t), \quad (32)$$

where $p_i(t) = p_i(t + T_i)$ stands for the modulation induced by the wheel i (with $i = 1{,}2$ and T_i the rotation period of wheel i), $m(t) = m(t + T_m)$ stands for the meshing signal (with $T_m = T_i/Z_i$ is the meshing period and Z_i is the number of teeth of wheel i) and $p'_i(t) = m(t)p_i(t) = p'_i(t + T_i)$. The vibration response acquired by the accelerometer can be obtained by filtering the excitation by a linear time-invariant (LTI) system, say $h_g(t)$, that physically model the transfer function of the transmission path from the excitation to the sensor

$$x_g(t) = \Sigma_g(t) \otimes h_g(t) + n(t) = m''(t) + p''_1(t) + p''_2(t) + n(t), \quad (33)$$

where $\otimes$ stands for the convolution product and $n(t)$ is a purely random signal (including potential higher-order CS components). It is worth noting that the responses of the periodic components $m(t), p'_1(t)$ and $p'_2(t)$ are also periodic with their basic periods i.e. $m''(t) = m(t) \otimes h_g(t) = m''(t + T_m)$ and $p''_i(t) = p'_i(t) \otimes h_g(t) = p''_i(t + T_i)$.

Cette thèse est accessible à l'adresse : http://theses.insa-lyon.fr/publication/2015ISAL0106/these.pdf
© [D. Abboud], [2015], INSA Lyon, tous droits réservés

2.5.13 Cyclostationary analysis of gear signals

For healthy gears, the modulations $p_i(t)$ induced by the gear imperfection are typically weak. The strength of the modulation induced by the wheel i increases when a local defect occurs. Generally speaking, the strength of the modulation $p_i(t)$ increases with the advancement of the fault, leading to an increase in the associated vibration component $p''_i(t)$. Therefore, the systematic separation of the vibrational components provides valuable diagnostic information which can feed an automatic decision system. Accordingly, it is clear that gear vibrations are generally first-order poly-CS as their deterministic component is a combination of two components of different periods, namely, T_1 and T_2. In general, a common period does exist but, in most situations, it is too long to be fully observable in practice. For this reason, the CS analysis can be fairly accomplished by applying successively the SA relative to the existing periods. Specifically, the vibration component associated with the gear meshing can be extracted by applying the SA with respect to the period T_m:

$$\mathcal{P}_{T_m}\{x_g(t)\} = m''(t). \tag{34}$$

On the other hand, the application of the SA with respect to a wheel period returns

$$\mathcal{P}_{T_i}\{x_g(t)\} = p''_i(t) + m''(t). \tag{35}$$

Therefore, the vibration component relative to the modulation of the wheel i is obtained as

$$p''_i(t) = \mathcal{P}_{T_i}\{x_g(t)\} - \mathcal{P}_{T_m}\{x_g(t)\}, \tag{36}$$

which provides individual diagnostic information relative to the wheel i. In many applications, the elimination of the deterministic component is crucial in order to properly investigate the random part. In the literature, this issue is coined as “discrete\random separation”. According to the introduced model, the random component can be obtained as

$$n(t) = x_g(t) - \left(\mathcal{P}_{T_1}\{x_g(t)\} + \mathcal{P}_{T_2}\{x_g(t)\} - \mathcal{P}_{T_m}\{x_g(t)\}\right). \tag{37}$$

Eventually, this simple analysis was reported on a pair of parallel shaft gears, yet it can be simply extended to the case of multiple-stage gearboxes following the same lines. A particular difficulty is encountered in planetary gearboxes where the transmission path varies periodically. In this case, a

Cette thèse est accessible à l'adresse : http://theses.insa-lyon.fr/publication/2015ISAL0106/these.pdf
© [D. Abboud], [2015], INSA Lyon, tous droits réservés

kinematic study is mandatory in order to identify the mechanical signature of the fault. However, the SA would be insufficient in some cases where the basic periods of the meshing components and the modulations are not integer multiple. In this case, the signal turns quasi-CS—instead of being poly-CS— and the SA must be replaced by the $\mathcal{P}$-operator.

2.5.2 REB case

This subsection is dedicated to study the vibrations emitted by a local fault in a REB. It starts with some preliminaries about the constitution and the operation of REBs, as well as their failure mode and their distinct vibrational signature. A general model is then adopted to analytically study the statistical properties of such signals. At first, the failure of the classical spectral analysis is analytically explained, while the convenience of some CS2 tools is eventually underlined.

2.5.21 Preliminaries

A REB is a mechanical component devised to provide relative positioning and rotational freedom while transmitting a load between two structures. Typically, it is constituted of inner and outer races between which rolling elements (such as balls or rollers) are mounted in a cage spin. The cage is placed between the races and has the role of reducing friction by hindering the elements from scrubbing against each other. The load is carried by the rolling motion that significantly decreases the frictional resistance [Hamrock 1983]. For this reason, most of rotating machines are equipped with REBs to support the load and maintain the clearances between stationary and rotating machinery elements. During their operation, REBs are prone to fail for many reasons such as manufacturing errors, improper assembly, overloading, operation under harsh environment, fatigue, etc... The failure of these components may lead to a total shutdown in the system, thus its diagnostic is crucial to anticipate such costly downtimes. Among different techniques, the vibration analysis proved itself as a reliable and effective technique.

In most cases, REB faults start with a local loss of material (pitting, spalling, corrosion, rubbing, contamination) on a matting surface (inner/outer race, rolling elements) [McFadden 1984] [Antoni 2007b]. As a defect strikes a mating surface, an abrupt change in the contact stress occurs at the interface (also called shock), producing a sharp impulse that excites some structural resonance either related to the REB structure or to the vibration transducer itself. Because of the rotating motion of the REB, these impacts are regularly repeated resulting in a series of impulse responses whose temporal spacing depends on the fault type and the geometry of the REB.

Cette thèse est accessible à l'adresse : http://theses.insa-lyon.fr/publication/2015ISAL0106/these.pdf
© [D. Abboud], [2015], INSA Lyon, tous droits réservés

This series of broadband impulse responses is possibly amplitude modulated owing to the passage of the fault into and out of the load zone. Some common fault and modulation frequencies (also called characteristic frequencies) are given in Table 1 [Randall 2011a] [Su 1992]. Note that these relationships are established considering that the outer race is stationary and that the inner race rotates at the shaft speed. Also, they assume a pure rolling motion of the rolling element, whereas in reality the rolling elements are subjected to some slips. In details, the contact angle Φ varies with the position of each rolling element in the REB since the ratio of local radial to axial load varies. As a consequence, each rolling element will have a different rolling diameter and try to roll at different speed, while the cage limits the deviation of the rolling elements from their mean position, thus causing some random slip [Randall 2011]. Thus, the actual characteristic frequencies are likely to deviate from their theoretical values in practical applications.

Table 1 Typical fault frequencies, where f_r =speed of the shaft, d =REB roller diameter,D =pitch circle diameter, N =number of rolling elements, Φ =contact angle.

Ballpass frequency, inner race (BPFI)	$\frac{N}{2} f_r \left(1 + \frac{d}{D} \cos \Phi\right)$
Ballpass frequency, outer race (BPFO)	$\frac{N}{2} f_r \left(1 - \frac{d}{D} \cos \Phi\right)$
Fundamental train frequency (FTF)	$\frac{f_r}{2} \left(1 - \frac{d}{D} \cos \Phi\right)$
Ball spin frequency (BSF)	$f_r \frac{D}{d} \left(1 - \left(\frac{d}{D} \cos \Phi\right)^2\right)$

Generally speaking, an outer race fault experiences a constant modulation, inner race a periodic amplitude modulation at the period of the inner race rotation, and a rolling-element fault a periodic amplitude modulation at the period of the cage rotation. The vibration signals and the corresponding envelopes[2] of these faults are illustrated in Fig. 5. Obviously, the amplitude modulations presented in the envelope results in distinct *mechanical signatures* in the corresponding spectrum for each fault type. These mechanical

[2]The reason why the envelope is used in the illustration instead of the signal itself is that the periodicity of the modulations is more obvious in the former. This will be properly explained in the next subsections.

Cette thèse est accessible à l'adresse : http://theses.insa-lyon.fr/publication/2015ISAL0106/these.pdf
© [D. Abboud], [2015], INSA Lyon, tous droits réservés

signatures are valuable diagnostic information that helps not only in detecting the fault, but also in identifying its nature. After this introductory paragraph, the next subsections evaluate in-depth the nature of the vibrations emitted by a local fault in a REB and show how some CS2 tools are able to exhibit the corresponding mechanical signature.

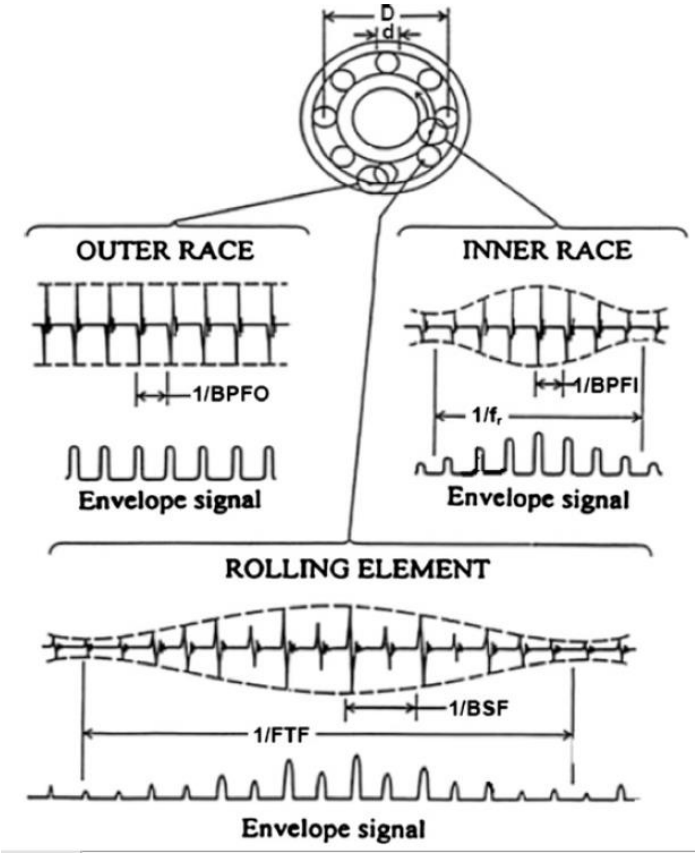

Figure 5 Typical signals and envelope signals from local faults in REBs [Randall 2011].

2.5.22 Vibration model

The first model for vibration signal emitted by a localized fault in a REB dates back to McFadden & Smith [McFadden 1984] [McFadden 1985]. In these references, the excitation is modeled as a periodic train of Dirac deltas expressing the repetitive impacts generated by the defect. Also, this modeling includes possible amplitude modulations such as those generated by the radial load distribution and the moving location of impact forces, thus providing a straightforward understanding of the fault signature in the envelope spectrum. Later on, Ho &Randall adjusts the McFadden's model by adding slight random fluctuations to the inter-arrival times of the impact so that the train of Dirac delta becomes random instead of being periodic.

Cette thèse est accessible à l'adresse : http://theses.insa-lyon.fr/publication/2015ISAL0106/these.pdf
© [D. Abboud], [2015], INSA Lyon, tous droits réservés

These fluctuations can be justified by the presence of necessary random slips (as indicated in 2.5.21), possible speed fluctuations, and variations of the axial to radial load ratio [Antoni 2007b]. Also, they pointed out the presence of random fluctuations in the impulse magnitudes due to the non-exactly reproducible microscopic conditions when the fault impacts a rolling surface. Building on this, the vibration signal may be expressed as [Antoni 2007b]

$$x_b(t) = \sum_{i=-\infty}^{+\infty} A_i q(iT).h_b(t - T_i) + n(t), \;\; with \;\; T_i = iT - \tau_i \qquad (38)$$

where $h_b(t)$ stands for the impulse response to a single impact as measured by the sensor, $q(t) = \sum_l q_l e^{j2\pi lt/P}$ is the periodic modulation of period P due to the load distribution (this includes periodic changes in the impulse response as the distance and orientation of the impacts moves towards and backwards the sensor, as well as for possible bearing unbalance or misalignment), T is the fault characteristic frequency, $\mathrm{A_i}$ is the amplitude modulation modelled as a delta-correlated random sequence with $\mathbb{E}\{\mathrm{A_i}\} = 1$ and $\mathrm{Var}\{\mathrm{A_i}\} = \sigma_\mathrm{A}^2$, τ_i are the inter-arrival time fluctuations modelled as a zero-mean delta-correlated random variable[3] with $\mathbb{E}\{\tau_\mathrm{i}\} = 0$ and $\mathrm{Var}\{\tau_\mathrm{i}\} = \sigma_\mathrm{A}^2$ having the PDF $\Phi(\tau)$, and $n(t)$ accounts for an additive background noise that embodies all other vibration sources.

2.5.23 Insufficiency of the first-order analysis

This subsection analytically evaluates the PSD of the REB vibration model to make clear why the classical spectral analysis may fail to reveal the existing periodicity. According to Ref. [Antoni 2007b], the PSD writes as:

$$S_{x_b}(f) = \frac{1}{T}|H_b(f)|^2 \left[|\Phi(f)|^2 \sum_{k,l=-\infty}^{+\infty} q_l \delta\left(f - \frac{k}{T} - \frac{l}{P}\right) + (1 + \sigma_A^2 - |\Phi(f)|^2) q_{20}\right] + S_n(f), \qquad (39)$$

where $H_b(f)$ stands for the Fourier transform of $h_b(t)$, $\delta(f)$ is the Dirac delta pulse, $\Phi(f)$ stands for the Fourier transform of the PDF $\Phi(\tau)$ of the random variable τ_i, q_{20} stands for the mean square of the modulating function $q(t)$ and $S_n(f)$ is the PSD of the noise. Obviously, $S_{x_b}(f)$ decomposes as the spectrum of a forcing function—the terms into the brackets—multiplied by the system transfer function $|H_b(f)|^2$. The (quasi-) periodic vibration part is due to the first term in the forcing function (i.e. $|\Phi(f)|^2 \sum_{k,l=-\infty}^{+\infty} q_l \delta(f - k/T - l/P)$). Indeed, it carries the diagnostic in-

[3] It was shown in Ref. [Antoni 2003c] that having uncorrelated inter-arrival time differences $T_{i+1} - T_i$ is physically more realistic than imposing uncorrelated (white) jitters on the arrival times. However, as stated in the same reference, this leads to extra complications while not fundamentally changing the resulting properties of the vibration signal. This explains the choice of this simplistic modeling of the jitter.

Cette thèse est accessible à l'adresse : http://theses.insa-lyon.fr/publication/2015ISAL0106/these.pdf
© [D. Abboud], [2015], INSA Lyon, tous droits réservés

formation and assigns uniquely a distinctive spectral signature to each REB fault. As a result, the (quasi-) periodic vibration part is simultaneously weighted by the function $|H_b(f)|^2$ and $|\Phi(f)|^2$. The latter function is the Fourier transform of a PDF and, thus, can be seen as a transfer function of a low-pass filter: the larger the random fluctuations the shorter the band-width. The former function (i.e.$|H_b(f)|^2$) can be seen of a high-pass or high-frequency band-pass nature. As a consequence, the product $|H_b(f)|^2|\Phi(f)|^2$ will certainly attenuate the discrete structure in the spectrum and, eventually, the presence of a strong additive background noise $S_n(f)$ will completely mask it. On the other hand, the second term in the bracket (i.e. $(1+\sigma_A^2-|\Phi(f)|^2)$) is a continuous spectrum weighted by a high-pass function $(1+\sigma_A^2-|\Phi(f)|^2)$ and $|H_b(f)|^2$, thus amplifying the frequency range spanned by the transfer function. Building on this, one can approximate the PSD of a REB signal as,

$$S_{x_b}(f) \cong \frac{1}{T}|H_b(f)|^2(1+\sigma_A^2-|\Phi(f)|^2)q_{20}+S_n(f), \tag{40}$$

which a continuous function of frequency without characteristic peaks. This explains why, in practice, classical spectral analysis often fails to detect REB faults. This is illustrated in Fig. 6 [Antoni 2007b].

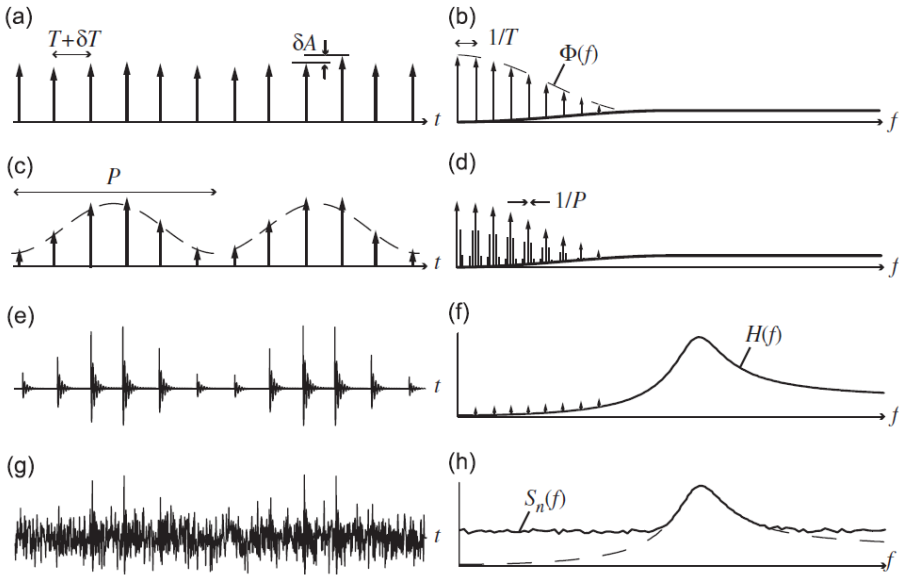

Figure 6 Synthesis of the vibration signal produced by a localized fault as seen in the time domain (left) and in the frequency domain (right): (a,b) a series of impact forces with slight random fluctuations in their inter-arrival times (mean value =T) and in their magnitudes; (c,d) possible modulation by shaft or cage rotation (period =T); (e,f) filtering by a structural or transducer resonance; (g–h) additive noise from other vibration sources [Antoni 2007b].

Cette thèse est accessible à l'adresse : http://theses.insa-lyon.fr/publication/2015ISAL0106/these.pdf
© [D. Abboud], [2015], INSA Lyon, tous droits réservés

2.5.24 Cyclostationary based solution

As previously shown, the classical spectral analysis is unable to reveal the presence of diagnostic information in the presence of masking noise. The aim of this paragraph is to show how CS2 tools are able to reveal the hidden periodicities. In particular, the SC, the SCoh and the SES will be analytically investigated using the vibration model of Eq. (38).

2.5.241 Spectral correlation

Inserting Eq. (38) into Eq. (22), it can be shown that the SC of a REB signal takes the particular form [Antoni 2007b]:

$$S_{2x_b}(\alpha,f) \cong \frac{1}{T} H_b\left(f+\frac{\alpha}{2}\right) H_b\left(f-\frac{\alpha}{2}\right)^* \left(\Phi(\alpha)(1+\sigma_A^2) - \Phi\left(f+\frac{\alpha}{2}\right)\Phi\left(f-\frac{\alpha}{2}\right)^*\right) \times \sum_{k,l=-\infty}^{+\infty} q_{2l}\,\delta\left(\alpha-\frac{k}{T}-\frac{l}{P}\right) + \delta(\alpha) S_n(f), \quad (41)$$

where q_{2l} stands for the l[th] Fourier coefficient of $q^2(t)$— i.e. $q^2(t) = \sum_l q_{2l} e^{j2\pi lt/P}$. Note that the $\cong$ sign comes from the fact that the (quasi-) periodic contribution was neglected, thus by setting $\alpha = 0$, the SC $S_{x_b}(0,f)$ boils down to the PSD of the random part (see Eq.(40)). Note that $S_{2x_b}(\alpha,f)$ enjoys a continuous spectrum in the f-variable at the cyclic frequency set $\alpha = k/T + l/P$. More interestingly, the hidden periodicity that carries the diagnostic information is fully disclosed when looking at the SC as a function of α, returning a discrete spectrum $\sum_{k,l=-\infty}^{+\infty} q_{2l}\delta(f - k/T - l/P)$ weighted by the Fourier coefficients of the square of the modulation function $q^2(t)$.

2.5.242 Spectral coherence

Assuming the transfer function and the noise power density are smooth enough and $\alpha \ll f$, one can accept the following approximations

$$\begin{cases} H_b\left(f \pm \frac{\alpha}{2}\right) \cong H_b(f) \\ S_n\left(f \pm \frac{\alpha}{2}\right) \cong S_n(f) \\ \Phi\left(f \pm \frac{\alpha}{2}\right) \cong 0. \end{cases} \quad (42)$$

Taking these approximations into account, the SCoh can be easily found as

$$\gamma_{2x_b}(\alpha,f) \cong \left|\frac{SNR(f)}{1+SNR(f)}\right|^2 |\Phi(\alpha)|^2 \times \sum_{k,l=-\infty}^{+\infty} \left|\frac{q_{2l}}{q_{20}}\right|^2 \delta\left(\alpha-\frac{k}{T}-\frac{l}{P}\right), \quad (43)$$

Cette thèse est accessible à l'adresse : http://theses.insa-lyon.fr/publication/2015ISAL0106/these.pdf
© [D. Abboud], [2015], INSA Lyon, tous droits réservés

where $SNR(f)$ denotes the SNR ratio of the fault component,

$$SNR(f) = \frac{S_{x_R}(f)}{S_n(f)} = \frac{(1+\sigma_A^2)q_{2l}}{T}\frac{|H_b(f)|^2}{S_n(f)}, \quad (44)$$

and $S_{x_R}(f) = 1/T\,|H_b(f)|^2(1+\sigma_A^2 - |\Phi(f)|^2)q_{20}$ stands for the PSD of the cyclic random contribution which carries the diagnostic information in the signal (see the left side term in Eq. (40)). Interestingly, when read as a function of the f-variable, the SCoh returns a measure of the SNR of the fault normalized between 0 and 1. As a consequence, the magnitude of the SCoh in the spectral frequency domain can serve as a relative measure of the fault severity. When read as a function of α, the SCoh displays the fault signature and, consequently, the diagnostic information that are now fully revealed in the cyclic frequency domain.

2.5.243 Squared envelope spectrum

The SES can be obtained by simply integrating Eq. (41) over the f-axis,

$$SES_{x_b}(\alpha, f) \cong \frac{1}{T}H_{2b}(\alpha)\Phi(\alpha)(1+\sigma_A^2) \times \sum_{k,l=-\infty}^{+\infty} q_{2l}\delta\left(\alpha - {}^{k}/_{T} - {}^{l}/_{P}\right) + \sigma_n^2\delta(\alpha), \quad (45)$$

where $H_{2b}(\alpha) = \mathcal{F}_{t\to\alpha}\{|h_b(t)|^2\}$ and $\sigma_n^2(f) = \int_{-\infty}^{+\infty} S_n(f)df$ stands for the mean square value of the noise $n(t)$. As expected, the SES presents a discrete distribution with non-zero Fourier coefficients at the (non-zero) cyclic frequencies associated with the REB fault type. Indeed, this explains why the envelope analysis was historically recognized as a powerful technique for REB diagnosis.

2.6 Peculiarities of the cyclostationarity of rotating machine signals

2.6.1 Temporal versus angular domain

The cyclostationarity in rotating machine signals is principally due to the cyclic mechanisms that produce them. These mechanisms are related to the machine kinematics, being intrinsically phase-locked with the rotational angle. Therefore, the true variable of interest is actually the *angle* of rotation of the machine rather than *time*. With stationary signals, time or angle makes little difference since the signal statistics are constant by definition. However, with CS signals, the two descriptions are not equivalent in general. Strictly speaking, the periodicities induced by the rotation of the machine should be described according to the angular variable, say θ, and time

Cette thèse est accessible à l'adresse : http://theses.insa-lyon.fr/publication/2015ISAL0106/these.pdf
© [D. Abboud], [2015], INSA Lyon, tous droits réservés

t substituted for the latter in all the above definitions. In particular, the Fourier series representation of a CS signal then becomes

$$\tilde{X}(\theta) = X\big(t(\theta)\big) = \sum_{v\in\mathcal{B}} c_X^k\big(t(\theta)\big)e^{j2\pi k\theta/\Theta}, \tag{46}$$

where it has been assumed that a full cycle corresponds to Θ (in radians). Strictly speaking, this defines an angle-CS signal only if $c_X^k\big(t(\theta)\big)$ is stationary in angle. Such an approach has been pursued in several research works [Antoni 2004a] where the signals were either *directly* sampled in angle or *indirectly* by numerically resampling afterwards from time to angle [André 2010]. This subject is properly addressed in the next subsection. At any rate, this was shown to be central for order spectrum analyses and order tracking methods [Fyfe 1997] [Bonnardot 2005], mainly concerned with analyzing first-order angle-CS signals. If angular sampling is not possible or even inappropriate in some particular applications, then it is necessary to investigate under which conditions an angle-CS signal remains CS in the time domain. The answer to this question was provided in Ref. [Antoni 2004a] which came to the following conclusion: the CS property holds if the machine speed is periodic, stationary or CS. Another peculiarity in analyzing rotating machine signals is the effect of the transmission path from the source to the sensor. Indeed, although rotating machine signals are intrinsically generated by angle-CS forces, they may depart form this characteristic once they arrive at the sensors after passing through structural filters or preprocessing analogic filters that are governed by time differential equations. Therefore, it was important to investigate under which conditions an angle-CS signal remains angle-CS after passing through a LTI system. In this context, it was also shown in Ref. [Antoni 2004a] that the angle-cyclostationarity holds if the speed profile is periodic, stationary or CS.
In summary, the CS assumption is valid for rotating machine signals either considered in the time or angle domain provided that the speed profile is periodic, stationary or CS. In all other cases, the resulting signal loses its CS property, which invalidates the application of traditional CS tools presented in sections 2.3 and 2.4.

2.6.2 Order tracking

The aim of this subsection is to investigate the nature of the vibrations emitted by a pair of parallel axis gears and to show how it is possible to take advantage of CS tools—particularly the SA—for gear diagnosis.
As previously pointed out, the cyclostationarity in rotating machine signals is intrinsically phase-locked to the rotation angle of the machine. The cy-

Cette thèse est accessible à l'adresse : http://theses.insa-lyon.fr/publication/2015ISAL0106/these.pdf
© [D. Abboud], [2015], INSA Lyon, tous droits réservés

clic frequencies are thus synchronized with the fundamental frequency of the machine which, in turn, would undergo some fluctuations. This issue was identified in the sixties of the last century in the field of communication and electronics [Millar 1968] [Weinberg 1974] [Ferrero 1992]. First solutions were based on the "synchronous sampling" technique. This technique consists in synchronizing the data acquisition system with the sampling clock using a hardware structure in the acquisition system [Klapper 1972] [Bin 2010]. This necessarily includes a ratio synthesizer and an anti-aliasing tracking filter. The principle of synchronous sampling system is illustrated through the block diagram in Fig. 7 [Fyfe 1997]. The rotating machine is tracked to obtain the so-called "keyphasor signal", which is typically a once-per-shaft revolution event that is used to measure the shaft speed. The ratio synthesizer is used to adjust the number of pulse per revolution and eventually control the cut-off frequency of the tracking filter. Note that the tracking filter is an analog low-pass filter whose cutoff frequency is adjustable. The frequency counter block, however, is optional and generally used to monitor the shaft speed.

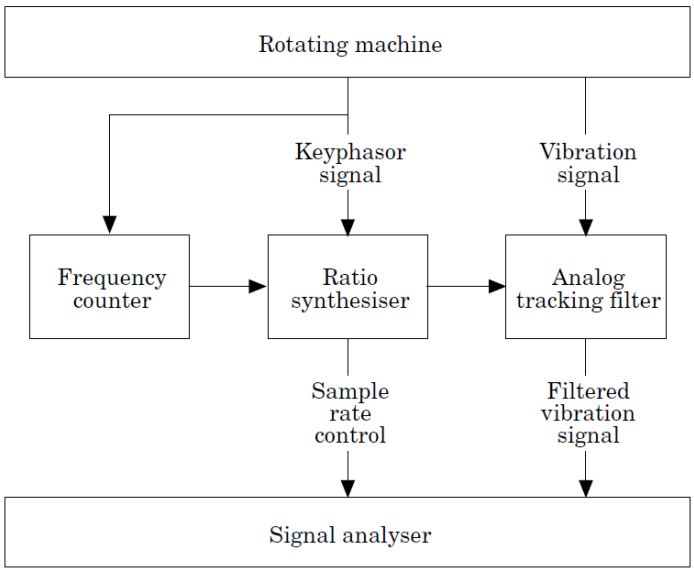

Figure 7 Block diagram of the synchronous sampling technique [Fyfe 1997].

Cette thèse est accessible à l'adresse : http://theses.insa-lyon.fr/publication/2015ISAL0106/these.pdf
© [D. Abboud], [2015], INSA Lyon, tous droits réservés

Thanks to the revolutionizing advances in digital signal processing in the late eighties, considerable improvements in terms of cost and hardware complexity were achieved. The first attempts date back to Refs. [Potter 1989] [Potter 1990], wherein the "computed order tracking" technique has been introduced. In this technique, signals are sampled with constant-time increments before being digitally post-processed (or "resampled") in order to obtain the angular domain transformation. The principle of synchronous sampling system is illustrated through the block diagram in Fig. 8. Later on, this method was deeply examined by Fyfe & Munck in Ref. [Fyfe 1997] who investigate key processing issues. In particular, it was shown that the use of higher sampling rates on keyphasor and data signals improves the result accuracy as it significantly reduces the interpolation errors. Another important finding is the relationship between the interpolation order and the operation accuracy: the higher the interpolation order, the more accurate the operation. For instance, the use of a block cubic spline interpolation reduces background noise by almost two orders of magnitude as compared to the linear interpolation.

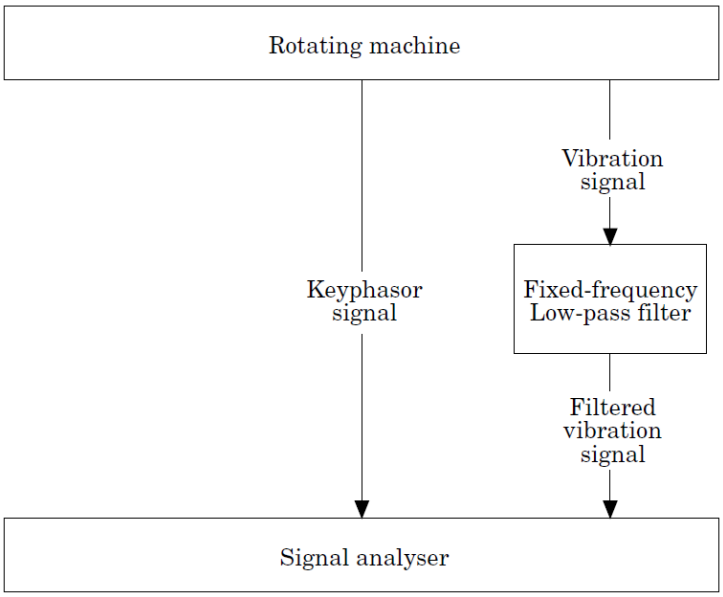

Figure 8 Block diagram of the computed order tracking technique [Fyfe 1997].

A second order tracking family is that based on the Vold-Kalman filter, being based on non-casual narrow-band filtering operations used to track a specific waveform within multiple harmonic time signals [Leuridan 1995] [Feldbauer 2000][Pan 2007]. In this technique, the speed signal must be sampled at a sufficiently high rate and resampled (e.g. by cubic spline) to acquire the arrival time in order to relate the signal to the order domain

Cette thèse est accessible à l'adresse : http://theses.insa-lyon.fr/publication/2015ISAL0106/these.pdf
© [D. Abboud], [2015], INSA Lyon, tous droits réservés

[Fair 1998]. The third order tracking family is based on the Fourier transform with proper adjustments in the kernel [Blough 1997] [Blough 2003] [Capdessus 2013] [Borghesani 2013a]. The object of these transforms is the direct passage from the time to the order domain without the need of passing through the interpolation step.

2.7 Conclusion

This chapter provided a review of the CS theory and its application in the field of rotating machine vibration analysis. A Fourier based model was first adopted in subsection 2.2 to provide a general model for CS signals of gears and REBs, to describe their characteristics and to theoretically investigate their statistical properties. Also, some of their dedicated tools were presented in subsections 2.3 and 2.4. Afterwards, it was shown in subsection 2.5 how to take advantage of CS tools in the field of vibration-based diagnosis of gears and REBs. In particular, it was shown that CS1 tools (particularly the SA) are efficient to separate vibrational components (i.e. meshing and fault components). Also, it was shown that REB vibrations exhibit CS2 signal owing to some fluctuations in the inter-arrival time between impacts. In accordance, the suitability of the SC, the SCoh and the SES to detect the presence of a fault was analytically investigated. Last, two main peculiarities of the cyclostationarity for rotating machine signals were addressed in 2.6. The first one is the fluctuating nature of the speed, while the other is concerned with the transmission path effect. However, when the speed profile is strongly NS, vibration signals undergo significant variations in their properties, thus making the CS framework insufficient to describe and analyze such signals. This issue is properly addressed in the next chapter which proposes some original solutions.

Cette thèse est accessible à l'adresse : http://theses.insa-lyon.fr/publication/2015ISAL0106/these.pdf
© [D. Abboud], [2015], INSA Lyon, tous droits réservés

3 Research methodology

3.1 Introduction

This PhD thesis is a part of a large project whose intent is to develop a CM system for rotating machines when operating under NS and severe conditions.
Having reviewed the CS theory, some of its tools and its applications for rotating machine diagnostic, this chapter describes the research methodology followed to solve the thesis problematic and reach the objective defined in section 1.2. The principal contributions of this thesis are presented in five independent publications, logically connected among each other. These publications are as follow:

1) Pub#1: a copy of this paper is enclosed in appendix A
   - Title: Deterministic-Random separation in nonstationary regimes
   - Journal: Accepted in the Journal of Sound and Vibrations, Elsevier
   - Authors: D. Abboud, J. Antoni, S. Sieg-Zieba, M. Eltabach

Cette thèse est accessible à l'adresse : http://theses.insa-lyon.fr/publication/2015ISAL0106/these.pdf
© [D. Abboud], [2015], INSA Lyon, tous droits réservés

2) Pub#2: a copy of this paper is enclosed in appendix B
   - Title: The spectral analysis of cyclo-non-stationary signals
   - Journal: Accepted in the journal of Mechanical System and Signal Processing, Elsevier
   - Authors: D. Abboud; S. Baudin; J. Antoni; D. Rémond; M. Eltabach; O. Sauvage

3) Pub#3: a copy of this paper is enclosed in appendix C
   - Title: Angle\Time cyclostationarity for the analysis of rolling element bearing vibrations
   - Journal: Accepted in the journal of Measurement, Elsevier
   - Authors: D. Abboud, J. Antoni, S. Sieg-Zieba, M. Eltabach

4) Pub#4: a copy of this paper is enclosed in appendix D
   - Title: Envelope analysis of rotating machine vibrations in variable speed conditions: a comprehensive treatment
   - Journal: Submitted to the journal of Mechanical System and Signal Processing, Elsevier
   - Authors: D. Abboud, J. Antoni, S. Sieg-Zieba, M. Eltabach

5) Pub#5: a copy of this paper is enclosed in appendix E
   - Title: The speed dependent spectral correlation
   - Conference: presented at the international conference on structural engineering dynamics 2015 (ICEDyn 2015)
   - Authors: D. Abboud, J. Antoni, S. Sieg-Zieba, M. Eltabach.

This chapter establishes the link between these publications and the research methodology according to the general strategy and guidelines provided in section 1.3. In particular, it classifies the solution into 4 principal gates. The first one is concerned with the extension of the CS1 framework, whereas the three others are concerned with the extension of the CS2 framework according to three different, but complementary, visions. In details, the extension of the CS1 class is addressed in section 3.2. The extension of the CS2 class, however, is made according to three visions. Section 3.3 addresses the first vision which adopts an angle\time approach. Section 3.4 addresses the second view which adopts an envelope-based solution. Section 3.5 addresses the third view which adopts a “cyclo-non-stationary” (CNS) solution by considering the speed as a supplementary variable. This chapter is sealed with a conclusion in section 3.6.

Cette thèse est accessible à l'adresse : http://theses.insa-lyon.fr/publication/2015ISAL0106/these.pdf
© [D. Abboud], [2015], INSA Lyon, tous droits réservés

3.2 First-order solutions

This section describes the solution adopted to deal with the changes in the CS1 component induced by the nonstationarity of the operating speed.

3.2.1 Preliminaries

The deterministic\random separation of vibration signals carries substantial benefits in machine diagnostic and, particularly, for that based on "differential diagnosis" [Antoni 2004b] [Randall 2011]. It allows the separation of mechanical contributions issued from distinct phenomena. For constant operating speed, the signal is time-CS and its deterministic part is periodic in the temporal domain. This explains why the SA is widely accepted as a powerful CS1 tool for extracting deterministic components in rotating machine vibrations [Braun 1975] [McFadden 2000] [Braun 2011]. In practice, the operating speed often undergoes some fluctuations which, despite being low, jeopardize the effectiveness of the SA. Since repetitive patterns in rotating machines are intrinsically phase-locked to specific angular positions, the straightforward solution was to proceed in the angular domain (by synchronizing the SA with respect to *angle* rather than to *time*). In practice, the transformation from the time-domain to the angle domain is performed by order tracking the signal as discussed in subsection 2.6.2. This implicitly assumes the signal to be angle-CS and, consequently, the deterministic component to be angle-periodic. Nevertheless, as discussed in subsection 2.6.1, this requires the speed fluctuation to be periodic, stationary or CS [Antoni 2004a].

3.2.2 Problem identification

The present PhD is particularly concerned by the general case of NS speed profiles. In this case, vibration signals are subjected to significant distortions that alter their statistics [Wang 2002] [Heyns 2011] [Heyns 2012]. These distortions are basically introduced by (i) variations of the machine power intake and (ii) the effect of LTI transfers. Whereas the first effect essentially results in *amplitude modulation* [Jardine 2006] [Heyns 2011], the second one also induces *phase modulation* [Stander 2006] [Borghesani 2012]. The latter phenomenon was originally inspected in Ref. [Stander 2006], before being revisited in Ref. [Borghesani 2012] through a comprehensive theoretical analysis. In the details, accelerometers are mostly remoted from the sources due to non-intrusion constraints, thus there is often a transmission path effect characterized by the transfer function of the

Cette thèse est accessible à l'adresse : http://theses.insa-lyon.fr/publication/2015ISAL0106/these.pdf
© [D. Abboud], [2015], INSA Lyon, tous droits réservés

structure. Consequently, the measured signal is to be interpreted as the output of an LTI system. This system is characterized by ordinary differential equations in time, independently of the excitation nature. When the excitation is angle-CS (as commonly assumed in rotating machines [Antoni 2004a]), the transmission path induces maximum amplification and phase shift when the frequency content of the excitation coincides with a resonance of the transfer function. The corresponding response is *instantaneously* delayed and amplified/attenuated [Heyns 2006] according to the fluctuating amplitude and frequency content of the input signal. From a temporal view, the system response is the convolution of a NS excitation with a LTI transfer function: it is therefore NS as well. Conversely, from an angular point of view the order content of the excitation remains constant, yet the transfer function becomes *angle-varying;* therefore, the response of the system to an angle-CS excitation is generally NS in the angular domain (i.e. neither stationary nor CS). This necessary invalidates the application of traditional CS tools such as the SA. The next subsection discusses some previously proposed solutions that deal with this issue.

3.2.3 Some previous work

After inspecting the problem of phase blur, Stander and Heyns were the first who proposed a solution for this issue in Ref. [Stander 2006]. They proposed an enhanced version of the SA— coined "phase domain averaging"— comprising a phase correction of the cycles before the averaging operation. The phase information was returned by Hilbert demodulation of a high-energy harmonic (such as a meshing order) of the resampled acceleration signal. Later, a simpler variant was provided in Ref. [Coat 2009], coined the "improved synchronous average" (ISA), which consists in resampling the signal with a virtual tachometer signal synthesized via the demodulated phase. This work was inspired from Ref. [Bonnardot 2005] which introduced a technique to perform angular resampling using the acceleration signal of a gearbox operating under limited speed fluctuation. Recently, the same technique was used in Ref. [Borghesani 2012] to identify the optimal demodulation band for deterministic/random separation in speed varying conditions. Moreover, the authors in Ref. [Daher 2010] provided a parametric approach in an attempt to generalize the SA to the CNS case. Using Hilbert space representation, they decomposed the deterministic component on to a set of periodic functions multiplied by speed-dependent functions apt to capture long-term evolution over consecutive cycles. Yet, their method carries the general disadvantages of parametric approaches, namely, the critical dependence on the basis order. Another attempt was made in Ref. [Antoni 2013] where the aim was to remove the de-

Cette thèse est accessible à l'adresse : http://theses.insa-lyon.fr/publication/2015ISAL0106/these.pdf
© [D. Abboud], [2015], INSA Lyon, tous droits réservés

terministic part of the vibrations produced by an internal combustion engine in runup regimes. Assuming a first-order Markov dependence of the CNS signal, the authors introduced an operator –coined the "cyclic difference"– based on subtracting each cycle from the previous one in the resampled signal. Despite the good compliance of this method for the particular addressed application, it suffers from high variability in the more general setting.

3.2.4 Proposed solution

A solution of the problems identified in subsection 3.2.2 was the subject of "Pub#1" enclosed in appendix A. The first step toward the solution starts by understanding the changes undergone by the vibration signal and its connection with the operating regime. Thus, the first object of the paper is to investigate the nature of the nonstationarity induced by the response of a LTI system subjected to speed varying excitation. In details, It is shown that the operating speed significantly influence the signal statistics, while preserving an angle-periodic behavior. For this purpose, the concept of first-order cyclo-non-stationarity is proposed by considering the speed as a supplementary variable, with the aim of extending the class of CS1 signals to NS speed conditions. In details, the first-order cyclo-non-stationary (CNS1) class is defined through a CNS1 field, being a collection of angle-CS1 processes of common angular-period but with speed-dependent statistics. This intuitive generalization has allowed us to develop a signal model for CNS1 signals, which happens to be a trajectory in this field exclusively dictated by the speed profile. This model consists of Fourier series whose complex exponentials are functions of the angle variable and whose coefficients are only dependent on the speed.

Having derived a signal model for CNS1 signals, the second step is to use this model to conceive a first-order operator— namely the generalized synchronous average" (GSA) — to replace the SA in variable speed conditions. This operator is bi-variable of the angle and the speed: it returns the mean value of a CNS signal for each operating speed. Two non-parametric estimators of the GSA have been proposed, namely the *raw estimator* and the *smooth estimator*. The first one provides the synchronous average of the signal at predefined discrete operating speeds. Similarly to the histogram estimators in statistics, the raw estimator is based on a systematic discretization of the speed into a set of regimes, then averaging the cycles according to their global pertinence to a regime (cycles whose mean speed values fall in a regime interval are averaged together). A brief statistical study is then performed on this estimator with the aim to provide the user with confidence intervals that reflect the "quality" of the estimator according to the

Cette thèse est accessible à l'adresse : http://theses.insa-lyon.fr/publication/2015ISAL0106/these.pdf
© [D. Abboud], [2015], INSA Lyon, tous droits réservés

SNR and the estimated speed. The second estimator returns a smoothed version of the latter by enforcing continuity over the speed axis. The continuity can be imposed by a classical interpolation method (e.g. kernel density estimation method, polynomial interpolation, etc.). The smoothed estimator was particularly conceived to reconstruct the deterministic components by tracking a specific trajectory dictated by the speed profile (assumed to be known *a priori*). The proposed approach as well as the theoretical findings is evaluated on numerical and real vibration signals. In particular, the application part reports a typical example in the field of rotating machine diagnostics where deterministic gear related components contribute to the (order-domain) SES and mask the REB fault signature— originally random. The aim is to show how to take advantage of the GSA to enhance the envelope-based diagnosis of REB when operating under NS regime. The obtained results evidence the efficiency of the GSA and its superiority over the classical SA (when applied in the angle domain).
It is worth noting that a comparison between the GSA, the ISA and the cepstrum prewhitening (CPW) is made in "Pub#4" enclosed in Appendix D. The comparison, however, has been evaluated according to their ability to eliminate the deterministic part of a CNS signal. It has been shown that the GSA can be an efficient alternative of the ISA, while the preference between the former and the CPW is dependent on the nature of the application.

3.3 Second-order solution: angle\time based approach

This section describes the solution adopted to deal with the changes in the CS2 components induced by the nonstationarity of the operating speed according to an angle\time vision.

3.3.1 Preliminaries

In rotating machines, a succession of events is likely to occur within the machine cycle so that the released energy varies on a rhythmic basis. These events are likely to produce *transient signatures* in vibration signals which, in turn, carry critical information on the machine health [Antoni 2009]. The periodicity of the events is generally related to the *machine kinematics*, while the transients are related to the system dynamics. Let us insist on the fact that the concept of *diagnostic information* is related to (i) the periodicity of the events and (ii) the properties of the transients, thus their identification is of high importance for *machine diagnostics*. A typical example is the vibration signal emitted by a local fault in a REB. Indeed, it can be

Cette thèse est accessible à l'adresse : http://theses.insa-lyon.fr/publication/2015ISAL0106/these.pdf
© [D. Abboud], [2015], INSA Lyon, tous droits réservés

viewed as a series of cyclic impacts phase-locked to the shaft angle and exciting structural resonances. Clearly, the positions of the impact excitations are dictated by the shaft angle while the resonance responses are governed by differential equations that impose time-invariant properties (e.g. natural frequencies and relaxation times). In the constant-speed case, the fault signature appears as periodically correlated components phase-locked to the rotational shaft speed via the fault characteristic frequency. This makes convenient the application of CS2 tools on these signals to reveal the diagnostic information. In particular, it was found that the SC—or equally its normalized form coined as the SCoh— provides an optimal description of such signals. Precisely, in the case of a faulty REB signal, the SC returns a symptomatic distribution of parallel spectral lines discretely located at the cyclic frequencies associated with the REB fault frequencies and whose distribution along the spectral frequency axis is often intensified around the system resonances (see subsection 2.5.24).

3.3.2 Problem identification

NS speed variations of rotating machines are typically seen as nonstationarities from the receiver point of view. Indeed, the corresponding signals are no longer CS, although they are still exhibiting rhythms produced by some cyclic phenomena. Let us come back to the REB signal example where, in the presence of speed variations, the periodicity of the impacts is no longer consistent in time due to varying spacing between each other. Nevertheless, the spacing of the impacts would be constant in angle, but the resulting signal would still not exhibit periodic behavior in angle: the response to each impact has constant time characteristics which would become varying in angle. Generally speaking, the angle-periodicity holds for mechanisms resulting from the rotation of mechanical elements whatever the rotational speed. Yet, physical phenomena governed by time-dependent dynamical characteristics should still be described in time. Consequently, the SC fails to describe such signals whether applied in the temporal or the angular domain. Indeed, if a temporal domain description was adopted, the cyclic frequency of the "temporal" SC would be unable to identify the angle-dependent modulations even though the spectral frequency would identify the carrier characteristics. Conversely, if an angular domain description[4] was adopted (see subsection 2.6.1), the *spectral order* of the "angular" SC would be unable to identify the time-invariant characteristics of the

[4] It is meant by an "angular domain description" that signals are processed in the angle domain before applying classical CS tools. This strictly implies an angle-CS modeling of the vibration signal. In practice, the change of variable is commonly applied through an angular (re)sampling operation.

Cette thèse est accessible à l'adresse : http://theses.insa-lyon.fr/publication/2015ISAL0106/these.pdf
© [D. Abboud], [2015], INSA Lyon, tous droits réservés

transient waveform even though the cyclic order would identify existing modulations. In conclusion, neither a temporal nor an angular domain description is sufficient alone to explore the full signal content.

3.3.3 Some previous work

It was shown in the previous subsection that the CS framework is generally insufficient to describe and analyze rotating machine signals when operating under variable speed conditions. A similar issue has been encountered in the field of telecommunication [Gardner 1994]. For instance, it has been shown that a signal subjected to a Doppler shift loses its CS properties due to the relative motion between transmitter and receiver. The novel class of "generalized almost-cyclostationary" processes has been introduced to embody this particular case [Izzo 1998] [Napolitano 2007] [Napolitano 2012]. Despite its relevance in the mentioned field, this generalization is not able to deal with the mechanical signals of interest.

In the last few years, efforts have been directed toward the extension of existing CS tools in NS regimes. In particular, Urbanek et al. [Urbanek 2013] proposed an angle-frequency distribution— namely the averaged instantaneous power spectrum— based on a time filtering step followed by an angle averaging operation of the squared output. A similar solution was proposed by Jabłoński et al. [Jabłoński 2013] who introduced the angular-temporal spectrum to jointly represent the angular and temporal properties of the signal. More interestingly, a prominent solution was proposed by Delia et al. [D'Elia 2010] who explored the order-frequency approach. Their idea was to replace the frequency-frequency distribution by a frequency-order distribution that jointly describes the time-dynamics and the angle-periodicities of the signal. They proposed intuitive algorithms to extent the SC to the so-called "α-synchronized spectral correlation density". Later on, a fast version of the latter estimator, called "speed correlation", was proposed in Ref. [Roussel 2013] wherein the speed transform was used in the algorithm.

3.3.4 Proposed solution

Notwithstanding the practical efficiency of these attempts, they still lack formalism with rigorous statistical definitions: all the proposed algorithms are fully intuitive and need to be supported by rigorous theoretical proofs. This has motivated us to extent the CS framework by adopting an angle\time approach, giving birth to so-called "angle/time cyclostationary (AT-CS)" class. This was the subject of two journal papers which will be described hereafter.

Cette thèse est accessible à l'adresse : http://theses.insa-lyon.fr/publication/2015ISAL0106/these.pdf
© [D. Abboud], [2015], INSA Lyon, tous droits réservés

The first paper, “Pub#2”, is enclosed in Appendix B. It starts by identifying the problematic of the speed variability and the shortcoming of the CS approach. After a brief review of stationary, CS and CNS signals, we proceed to the solution by inspecting the nature of the nonstationarity of the signal induced by the speed variability. This nonstationarity evidences a marked interaction between time and angle-dependent components. This interaction is materialized by the angle-periodicity of the correlation measure of two versions of the signals shifted by a constant time-lag. This gives birth to a novel class of processes, the AT-CS class, whose theoretical foundations are introduced. Precisely, a signal model is proposed to the signals that belong to this class, being based on a Fourier series decomposition of time-stationary coefficients and the complex exponentials are explicitly expressed in angle (i.e. periodic in angle). Then, the related second-order cumulant, namely “angle-time covariance function”, is defined by considering the correlation at two time instants phase-locked on a given angle position and spaced apart by a given time-lag. The double Fourier transform of the angle-time covariance function defines the “order-frequency spectral correlation” (OFSC) that jointly localizes angle-periodicity of the modulation and the spectral property of the carrier in Hertz. Also, its normalized form, coined the “order-frequency spectral coherence” (OFSCoh), is proposed as an extension of the classical SCoh. Afterwards, a Welch-based estimator is proposed together with its related statistics. These statistics had led us to build a hypothesis test to indicate the presence/absence of an AT-CS component. Finally, two very different applications have been considered to demonstrate the effectiveness of the proposed theory in the field of rotating machines operating under NS regimes. The first one is concerned with the diagnosis of REB whereas the second one is concerned with the detection of gear rattle noise. Interesting results have been obtained in both cases, demonstrating the adequacy of the AT-CS approach for vibration analysis of speed-varying signals.

The second paper, “Pub#3”, is enclosed in Appendix C. It is theoretically and experimentally oriented toward a REB application. The first object of this paper is to analytically characterize REB fault vibrations and explore its AT-CS property. To do so, a CS model of REB vibration is revised to account for speed variations. Then, an analytic study is performed on the model wherein the REB signal is shown to be AT-CS on average. The second object is to experimentally validate these results on real-world vibration signals and demonstrate the optimality of the AT-CS approach over classical approaches dedicated to REB diagnosis. For this purpose, a comparison between the OFSC, the temporal SC and the angular SC has been made. The obtained results demonstrate the superiority of the OFSC over

Cette thèse est accessible à l'adresse : http://theses.insa-lyon.fr/publication/2015ISAL0106/these.pdf
© [D. Abboud], [2015], INSA Lyon, tous droits réservés

the classical SC: the OFSC was able to clearly reveal the fault signature of the REB even when it is energetically weak. A brief comparison is then made with the order-domain SES widely used after some pre-processing steps for REB fault diagnosis in variable speed conditions. The obtained results equally demonstrate the superiority of the OFSC over the SES for REB fault detection.

3.4 Second-order solution: envelope based approach

This section describes the solution adopted to deal with the changes in the CS2 component induced by the nonstationarity of the operating speed according to the envelope-based vision.

3.4.1 Preliminaries

The envelope analysis has been recognized for long as a powerful technique for REB diagnosis in constant speed [McFadden 1984]. Typically, it consists of a bandpass filtering step around a high-frequency band wherein the impulsive excitation is amplified, before demodulating the obtained signal to form the envelope. The spectrum of the latter— known as the *envelope spectrum*— contains the desired diagnostic information, including the repetition rate of the fault and potential modulations [Randall 2011]. At the time, the filtering and the demodulation operations were performed using analogue techniques (e.g. [Darlow 1974]) with inherent limitations regarding the filter characteristics and the analogue rectifier [Randall 2001]. Thanks to the advances in digital signal processing, considerable improvement have been made taking advantages of the Hilbert transform. This latter returns the (complex) analytic signal whose modulus is the envelope. In this context, it was shown in Ref. [Ho 2000] that it is preferable to use the *squared envelope (SE)* instead of the envelope as the latter introduces extraneous components that appears as misleading peaks in the envelope spectrum. Since that time, the envelope spectrum was replaced with the SES which has become the benchmark technique for REB diagnostics exploiting its low computational cost [Randall 2011]. The relationship between (second-order) cyclostationarity and envelope analysis was established in Ref. [Randall 2001], which stated that the SES is equivalent to an integrated version of the SC over the spectral frequency variable.

3.4.2 Some previous work

In NS speed conditions, the SES is coupled with computed order tracking to obtain an order domain representation. In order to deal with the non-

Cette thèse est accessible à l'adresse : http://theses.insa-lyon.fr/publication/2015ISAL0106/these.pdf
© [D. Abboud], [2015], INSA Lyon, tous droits réservés

consistency of the dynamical response (i.e. time-invariant transients) and to eliminate potential interfering deterministic components, two general strategies were adopted. The first strategy filters the temporal signal around a high-frequency resonance band (or simply high-pass filtering the signal) [Borghesani 2013c] [Zhao 2013] [Cocconcelli 2013], while the second one eliminates the gear contribution with sophisticated deterministic random separation tools and directly applies the SES on the residual signal [Randall 2011] [Borghesani 2013c].

3.4.3 Proposed solution

When dealing with second-order signatures, the investigation of the SES is unescapable because of its simplicity, low computational cost and implementation easiness on one hand and the confidence gained through the decades in industries on the other hand. Undoubtedly, the previous works based on the envelope have proved to be efficient in multiple cases, yet most of them lack a formalism from which the efficiency of their applicability can be evaluated. For this reason, we approach this issue by organizing these dispersed works into an academic structured framework. This was the subject of a journal paper "Pub#4" which provides a general guideline on how to exploit the SES in rotating machine diagnosis as well as the required functioning conditions. In details, this paper revises the application of the SES on rotating machine signals in variable speed conditions and collects previously published materials into a unified academic framework. For this purpose, signal models have been proposed to describe the structure of vibration signals. This is the cornerstone towards the formalization of the subject for a comprehensive evaluation of existing strategies. Two potential challenges that may face the direct application of the SES have been identified. The first challenge is the spurious contribution of the deterministic component in the SES. The paper has addressed this issue by comparing three sophisticated methods, namely, the ISA, CPW and GSA, used for suppressing the deterministic part of vibration signals. The second challenge is the spurious contribution of other second-order components emitted by other sources. This issue was ignored in the literature where the SES is computed over the whole demodulation band after removing the deterministic part. For this purpose, a general envelope enhancement procedure is revised and adjusted. All theoretical findings and comparisons are experimentally validated on simulated and real-world vibration signals.

Cette thèse est accessible à l'adresse : http://theses.insa-lyon.fr/publication/2015ISAL0106/these.pdf
© [D. Abboud], [2015], INSA Lyon, tous droits réservés

3.5 Second-order solution: cyclo-non-stationary based approach

This section describes the solution adopted to deal with the changes in the CS2 component induced by the nonstationarity of the operating speed according to the CNS2 vision.

3.5.1 Problem identification

By construction, the AT-CS approach assumes that time-dependent components are independent of the operating speed, which may be accurate for modest speed variations. In practice, these components undergo structural changes as the speed widely varies, causing substantial changes in the frequency content of the carrier [Antoni 2013]. These changes may be induced by the passage of critical speeds, changes in the machine power intake, gyroscopic effects, non-linearity of the system and other phenomena. Indeed, they affect the statistical properties of the carrier (assumed to be time-stationary) which turn out to become NS. As a consequence, the AT-CS assumption is jeopardized and the signal turns out to become CNS [Antoni 2013]. This necessarily invalidates the working assumption of its tools (e.g. the OFSC, the OFSCoh…) which returns the average behavior of the carrier; thus, the obtained quantity is likely to depend on the corresponding speed profile.

3.5.2 Proposed solution

A solution of the problems identified in subsection 3.2.2 was the subject of "Pub#5" enclosed in Appendix E. This paper proposes a CNS-based strategy to deal with such signals. In particular, the angle-time covariance function of a second-order cyclo-non-stationary (CNS2) signal is modeled by means of a Fourier series whose Fourier coefficient explicitly depends on speed profile. This modeling has served to analytically understand the shortcoming of the OFSC: the distribution of the latter undergoes speed-dependent leakage around the spectral lines located at the cyclic orders. This modeling is reminiscent to that proposed for the GSA (see subsection 3.2.4 and appendix A for more details). Thus, we have proceeded by generalizing the (angle-time) covariance function to the so-called "speed-dependent covariance function" by adding the speed as a supplementary variable. The double Fourier transform of this quantity defines the "speed-dependent spectral correlation" (SDSC) which happens to be a generalization of the SC (or the OFSC) to the case of strong variable speed conditions. Afterwards, an adjusted version of the Welch estimator is proposed

Cette thèse est accessible à l'adresse : http://theses.insa-lyon.fr/publication/2015ISAL0106/these.pdf
© [D. Abboud], [2015], INSA Lyon, tous droits réservés

to estimate the SDSC. Eventually, the proposed approach is validated on real vibration signals wherein a comparison with the AT-CS is made.

3.6 Conclusion

This chapter has presented the research methodology adopted to conceive new signal processing tools for vibration-based diagnosis of rotating machines in NS regimes. We have addressed this issue by distinguishing two types of signatures.

The first type includes deterministic waveforms known in the CS framework as being CS1. The proposed solution consists in generalizing the CS1 class to the more general CNS1 class which could enfold speed-varying deterministic signals. This has led to the proposal of the GSA to replace the SA in variable speed conditions. Two estimators of the GSA have been proposed and validated on numerical and real vibration signals. Results have shown good compliance of the GSA as compared with the SA and other advanced techniques (such as the ISA and the CPW).

The second type includes random periodically correlated waveforms known in the CS framework as being CS2. Three visions have been proposed to deal with the changes in the CS2 component induced by the nonstationarity of the operating speed. The first vision adopted an angle\time approach and extends the CS2 class to the more general AT-CS class. Also, the SC and SCoh have been generalized to the SC and SCoh, respectively. Also, a Welch based estimator has been proposed together with its related statistics. This approach has been validated on simulated and real vibration and its superiority over classical approaches has been demonstrated in multiple applications and case studies. The second vision adopted an envelope-based solution. It proposes an envelope based strategy to express second-order signatures. The third view adopted a CNS solution which, similarly to the first-order solution, considers the speed as a supplementary variable, and extends the CS2 class to the more general CNS2 class. In this context, the "speed-dependent spectral correlation" has been proposed as a generalization of the SC. This approach has been validated on real vibration signals wherein a comparison with the AT-CS is made.

Cette thèse est accessible à l'adresse : http://theses.insa-lyon.fr/publication/2015ISAL0106/these.pdf
© [D. Abboud], [2015], INSA Lyon, tous droits réservés

4 General conclusion

4.1 Introduction

This PhD thesis is part of a large project whose intent is to develop a CM system for rotating machines when operating under NS and severe conditions. The aim was to respond an actual requirement in industry wherein rotating machines are likely to operate under NS speed. Even though CM of rotating machines is well-established nowadays, the NS of the operating speed raises several challenges as it completely alters the statistical properties of the vibrations. This topic, therefore, has gained particular interest in the last decade and some sophisticated signal processing techniques have been conceived to deal with the variability of the speed within the record. But these works remain limited, dispersed and generally not supported by theoretical frameworks. The principal object of this thesis was to partially fill in this gap on the basis of a theoretical formalization of the subject and a systematic development of new dedicated signal processing tools.

4.2 Principal contributions

The contributions of the thesis directly result from the research strategy (section 1.3) that has guided the direction of our work. In general, this strategy exploits the theory of CS processes by extending it to enfold speed-varying vibration signals. We proceeded to the solution through four principal gates. The first one was concerned with the extension of the CS1 framework, whereas the three others were concerned with the extension of the CS2 framework according to three different, but complementary, visions. The principal contributions were presented in five independent publications, enclosed in the appendices.

In the first gate, an extension of the CS1 class to the CNS1 class has been proposed in 'Pub#1'. As a consequence, a GSA was derived to extend the application field of the SA to the case of NS regime. In particular, it has been shown that the GSA is able to systematically discriminate the deterministic part from the random part. Regardless of the nature of the vibra-

Cette thèse est accessible à l'adresse : http://theses.insa-lyon.fr/publication/2015ISAL0106/these.pdf
© [D. Abboud], [2015], INSA Lyon, tous droits réservés

tional component of the fault, the use of the GSA is crucial to investigate it. In details, if this component is of deterministic nature, the GSA will increase its SNR; otherwise (i.e. the vibrational component of the fault is random), the GSA will attenuate the spurious contribution of the deterministic part and allows a more prominent evaluation of the random part. An example of the latter case was provided in the application part of 'Pub#1', wherein the deterministic gear component contributes in the envelope (order-) spectrum and masks the REB component (originally random). Contrary to the SA, the elimination of the gear component by the GSA has significantly enhanced the REB signature. Also, the GSA was compared with the ISA and CPW in 'Pub#4', according to their ability to eliminate the deterministic part of a CNS signal. The principal advantage of the GSA over the others is its ability to systematically discriminate the deterministic part from the random part with minimal distortion of the latter. This technique also has some drawback such as its inability to remove modulation sidebands whose angular period is incommensurate with the carrier period. This may limits its effectiveness, for instance, when analyzing vibration signals produced by planetary gearboxes.

In the second gate, an extension of the CS2 class to the AT-CS class has been proposed in 'Pub#2' by adopting an angle\time approach. This approach was based on a joint description of the random signal in angle and time: the first describes modulations typically related to the system kinematics, whereas the second describes the carrier (e.g. transients) typically related to the system dynamics. Accordingly, the OFSC has been conceived to extend the SC. It provided a detailed order-frequency distribution of the energy which jointly localizes (i) the angle-periodicity of the modulation by the cyclic order variable and (ii) the spectral property of the carrier by the spectral frequency variable. Its normalized form, namely the OFSCoh, has been equally proposed as a generalization of the SCoh. Also, a Welch-based estimator has been proposed together with its related statistics. These statistics had led us to build a hypothesis test to indicate the presence of an AT-CS component. The usefulness of this approach has been validated in two applications. The first one is concerned with the diagnosis of REB whereas the second one is concerned with the detection of gear rattle noise. Interesting results have been obtained in both cases, demonstrating the adequacy of the AT-CS approach for vibration analysis of speed-varying signals. The application of angle-time approach on REB has been retaken in a more detailed way in 'pub#3'. The AT-CS nature of REB vibrations has been analytically proved, and its superiority over classical CS approaches (being considered in the time or angle domain) has been experimentally demonstrated.

Cette thèse est accessible à l'adresse : http://theses.insa-lyon.fr/publication/2015ISAL0106/these.pdf
© [D. Abboud], [2015], INSA Lyon, tous droits réservés

In the third gate, the extension of the envelope analysis to NS regime has been revisited through a comprehensive treatment in 'Pub#4'. This work was intended to serve as a guideline on how to exploit the SES in rotating machine diagnosis and to optimize it under given operating conditions. A number of original results have been brought to provide a more comprehensive view of some previously published material. In particular, a critical comparison between envelope enhancement techniques is provided. Also, a general envelope enhancement procedure is revised and adjusted. All the theoretical findings and the qualitative comparisons have been validated on simulated and real vibration signals including various case studies.
In the fourth gate, an extension of the CS2 class to the CNS2 class has been proposed in 'Pub#5' by adopting a CNS approach. This extension is reminiscent to that of the first-order (see the first gate) as a supplementary variable of the speed is added to describe the statistical properties of the signal. This has led to a more advanced extension of the SC to a tri-variable quantity, namely the SDSC, which returns the SC (or the OFSC) for each speed. Also, an adjusted version of the Welch estimator is proposed to estimate the SDSC. This approach has been validated on real vibration signals wherein a comparison with the AT-CS is made.
Regarding the investigation of second-order signatures (gates 2 to 4), the AT-CS approach (gate 2) is the most optimal for modest speed variations in terms of precision and robustness: it provides a perfect localization of the signal energy and a detailed representation of all second-order components. The envelope based approach (gate 3) is the most optimal in terms of simplicity and computational cost. However, according to the provided methodology, a prior knowledge of high-SNR band associated with the evaluated component is required. This is a strong requirement as it calls for more complex and sophisticated techniques to identify these bands. The CNS based approach (gate 4) is the most optimal for large speed variations. However, this approach is computationally very expensive and complex inasmuch as its related quantities are typically tri-variable. Building on this, the choice among these approaches relies on the application and requires the knowledge of (i) the benchmark components, (ii) the profile of the operating speed and (iii) the practical requirement of the CM system (e.g. performance of the microprocessor, online or offline monitoring).

4.3 Future works

This section is dedicated to the proposal of some perspectives with the aim to orient future works. The proposed perspectives are the following:

Cette thèse est accessible à l'adresse : http://theses.insa-lyon.fr/publication/2015ISAL0106/these.pdf
© [D. Abboud], [2015], INSA Lyon, tous droits réservés

• Extension of the GSA to be able to remove modulation sidebands whose angular period is incommensurate with the carrier period (i.e. quasi-CNS1 signals). This can be established, for instance, by estimating the (speed-dependent) Fourier coefficients at a given speed after an appropriate ponderation in the signal. In other words, the vibration signal will be multiplied by a speed-dependent weighting function (e.g. Gaussian kernel) whose maximum value (typically equals 1) is reached at a given central speed and progressively decreases to reach zero for far speeds. Evidently, the notion of regime in this case will be equivalent to the standard deviation of the weighing function. Then, a Fourier transform will be optimized for the estimation of the coefficients at the central speed. Once the coefficients are estimated, the deterministic component could then be constructed in a similar way to that of the GSA.

• Extension of other CS2 tools (such as the instantaneous covariance, Wigner-Ville spectrum) according to the AT-CS and the CNS approaches; these extensions follow similar lines as those of the OFSC and the SDSC, respectively. For the AT-CS case, bivariable quantities will be obtained either being in angle\time-lag (the angle\time instantaneous covariance) or in angle/frequency (the angle-frequency Wigner-Ville spectrum). For the CNS case, tri-variables quantities will be obtained such as the generalized instantaneous covariance or the generalized Wigner-Ville spectrum.

• Derivation of suboptimal (bi-variable) CNS2 indicators exploiting the optimality of the SDSC (since the SDSC is a tri-variable operator). This can be obtained for instance by integrating the SDSC over a spectral frequency band or to evaluate it at a given cyclic order. This will consequently lead to an order/speed and a frequency/speed distribution, respectively. Note that the integration over the speed variable is not useful as it brings us back to the AT-CS framework.

• Extension of the “indicators of cyclostationarity” [Raad 2008] to the CNS case in order to measure the strength of the cyclo-non-stationarity in the signal. In the stationary regime case, the calculation of these indicators (particularly for spur gears) can be estimated by means of the SA. Now having generalizing the latter (the GSA), the extension of these indicators seems to be simple.

Cette thèse est accessible à l'adresse : http://theses.insa-lyon.fr/publication/2015ISAL0106/these.pdf
© [D. Abboud], [2015], INSA Lyon, tous droits réservés

• Evaluation of first- and second-CNS approaches on load-varying signals by replacing the speed variable by the load variable. We expect a good compliance of the GSA and SDSC on such signals as the load equally alters the signal statistics

• Application of the developed approaches on other mechanical applications (e.g. gear diagnostic, noise separation in IC engines, etc.) or even other types of signals such as (acoustic signals, current signals, pressure signals, etc.)

4.4 Conclusion

The work done during this thesis finalizes the first step in relation to the goal of designing a CM system for rotating machines when operating under NS regimes. We believe we have brought the basic elements for the definition of such a system, demonstrating how best to exploit the physical properties of the vibration signals for building robust indicators. We hope this contribution will lead this project to fruition.

Cette thèse est accessible à l'adresse : http://theses.insa-lyon.fr/publication/2015ISAL0106/these.pdf
© [D. Abboud], [2015], INSA Lyon, tous droits réservés

References

[Adewusi 2001] S. Adewusi, B. AI-Bedoor. Wavelet analysis of vibration signals of an overhang rotor with a propagating transverse crack. *Journal of Sound Vibrations*, 246 (5): 777–93, 20-22 Sept. 2001.

[André 2010] H. André, Z. Daher, J. Antoni, D. Rémond. Comparison between angular sampling and angular re-sampling methods applied on the vibration monitoring of a gear meshing in non-stationary conditions. *In Proceeding of ISMA 2010 Including USD 2010*, Belgium, 2010.

[Antoni 2002a] J. Antoni, J. Daniere, F. Guillet. Effective vibration analysis of IC engines using cyclostationarity. Part I: a methodology for condition monitoring. *Journal of Sound and Vibration*, 257(5): 815–837, 2002.

[Antoni 2002b] J. Antoni, R. B. Randall. Differential Diagnosis of Gear and Bearing Faults. *Journal of Sound and Vibration*, 124(2):165-171, 2002.

[Antoni 2003a] J. Antoni, R.B. Randall. Unsupervised noise cancellation for vibration signals: part I— evaluation of adaptive algorithms. *Mechanical Systems and Signal Processing*, 18(1):89–101, 2004.

[Antoni 2003b] J. Antoni, R.B. Randall. Unsupervised noise cancellation for vibration signals: part II — a novel frequency-domain algorithm. *Mechanical Systems and Signal Processing*, 18(1): 103–117, 2004.

[Antoni 2003c] J. Antoni, R.B. Randall. A stochastic model for simulation and diagnostics of rolling element bearings with localized faults. *ASME Journal of Vibration and Acoustics*, 125(3): 282-289, 2003.

[Antoni 2004a] J. Antoni, F. Bonnardot, A. Raad, M. El Badaoui. Cyclostationary modelling of rotating machine vibration sig-

Cette thèse est accessible à l'adresse : http://theses.insa-lyon.fr/publication/2015ISAL0106/these.pdf
© [D. Abboud], [2015], INSA Lyon, tous droits réservés

nals. *Mechanical Systems and Signal Processing*, 18(6): 1285–1314, 2004.

[Antoni 2004b] J. Antoni, R.B. Randall. Unsupervised noise cancellation for vibration signals: part II—a novel frequency-domain algorithm. *Mechanical Systems* and Signal Processing, 18(1):103–117, 2004.

[Antoni 2007a] J. Antoni. Cyclic spectral analysis in practice. *Mechanical Systems and Signal Processing*, 21(2):597–630, 2007.

[Antoni 2007b] J. Antoni. Cyclic spectral analysis of rolling-element bearing signals: Facts and fictions. *Journal of Sound and Vibration*, 304(3-5):497–529, 2007

[Antoni 2009] J. Antoni. Cyclostationarity by examples. *Mechanical Systems and Signal Processing*, 23(4): 987–1036, 2009.

[Antoni 2013] J. Antoni, N. Ducleaux, G. NGhiem, S.Wang. Separation of combustion noise in IC engines under cyclo-non-stationary regime. *Mechanical Systems and Signal Processing*, 38(1):223–236, 2013.

[Bardou 1994] O. Bardou, M. Sidahmed. Early detection of leakages in the exhaust and discharge systems of reciprocating machines by vibration analysis. *Mechanical Systems and Signal Processing*, 8(5): 551–570, 1994.

[Belsak 2007] A. Belsak, J. Flasker. Detecting cracks in the tooth root of gears. *Engineering Failure Analysis*, 14(8):1466–75, 2007.

[Bin 2010] Z. Bin, Z. Dong-lai. Research on Synchronous Sampling Clock Jitter of Power System. *2nd International Conference on Information Engineering and Computer Science (ICI-ECS)*, China, 25-26 Dec 2010.

[Blough 1997] J. Blough, D. Brown, H. Vold. The time variant discrete Fourier transform as an order tracking method. *SAE Technical Paper 972006*, 1997, doi:10.4271/972006.

Cette thèse est accessible à l'adresse : http://theses.insa-lyon.fr/publication/2015ISAL0106/these.pdf
© [D. Abboud], [2015], INSA Lyon, tous droits réservés

[Blough 2003] J.R. Blough. A survey of DSP methods for rotating machinery analysis, what is needed, what is available. *Journal of Sound and Vibration*, 262(3):707–720, 2003.

[Bonnardot 2005] F. Bonnardot, M. ElBadaoui, R.B. Randall, J. Daniere, F. Guillet. Use of the acceleration signal of a gearbox in order to perform angular resampling (with limited speed fluctuation), *Mechanical Systems and Signal Processing*,19(4): 766–785, 2005.

[Bouillaut 2001] L. Bouillaut, M. Sidahmed. Cyclostationary approach and bilinear approach: comparison, applications to early diagnosis for helicopter gearbox and classification method based on HOCS. *Mechanical Systems and Signal Processing*, 15(5):923–943, 2001.

[Borghesani 2012] P. Borghesani, P. Pennacchi, R.B. Randall, R. Ricci. Order tracking for discrete-random separation in variable speed conditions. *Mechanical Systems and Signal Processing*, 30:1–22, 2012.

[Borghesani 2013a] P. Borghesani, P. Pennacchi, S. Chatterton, R. Ricci. The velocity synchronous discrete Fourier transform for order tracking in the field of rotating machinery. *Mechanical Systems and Signal Processing*, 44(1): 118-133, 2014.

[Borghesani 2013b] P. Borghesani, P.Pennacchi, R.B.Randall, N.Sawalhi, R.Ricci. Application of cepstrum pre-whitening for the diagnosis of bearing faults under variable speed conditions. *Mechanical Systems and Signal Processing*, 36:370–384, 2013.

[Borghesani 2013c] P. Borghesani, R. Ricci, S. Chatterton, P. Pennacchi. A new procedure for using envelope analysis for rolling element bearing diagnostics in variable operating conditions. *Mechanical Systems and Signal Processing*, 36: 370–384, 2013.

[Braun 1975] S.G. Braun. The extraction of periodic waveforms by time domain averaging. *Acta Acustica united with Acustica*, 32(2):69–77, 1975.

Cette thèse est accessible à l'adresse : http://theses.insa-lyon.fr/publication/2015ISAL0106/these.pdf
© [D. Abboud], [2015], INSA Lyon, tous droits réservés

[Braun 1986] S. Braun. Mechanical Signature Analysis: theory and applications. *Academic Press*, (a book), 1986.

[Braun 2011] S. Braun. The synchronous (time domain) average revisited. *Mechanical Systems and Signal Processing*, 25(4):1087–1102, 2011.

[Capdessus 2000] C. Capdessus, M. Sidahmed, J. L. Lacoume. Cyclostationary processes: application in gear faults early diagnosis. *Mechanical Systems and Signal Processing*, 14(3):371–385, 2000.

[Capdessus 2013] C. Capdessus, E.Sekko. J. Antoni, Speed Transform, a New Time-Varying Frequency Analysis Technique. *Proceedings of the 3rd conference in condition monitoring of machinery in non-stationary operations*, Italia, 8-10 May 2013.

[Chaari 2011] F. Chaari, R. Zimroz, W. Bartelmus, T. Fakhfakh, M. Haddar. Modelling of local damages in spur gears and effects on dynamics response in presence of varying load conditions. *In: Proceedings of Surveillance 6*, France, 25-26 Oct. 2011.

[Coat 2009] M.D. Coats, N. Sawalhi, R.B. Randall. Extraction of tacho information from a vibration signal for improved synchronous averaging. *In: Proceedings of Acoustic 2009*, Australia, 23-25 Nov. 2009

[Cocconcelli 2012] M. Cocconcelli, L. Bassi, C. Secchi, C. Fantuzzi , R. Rubini, "An algorithm to diagnose ball bearing faults in servomotors running arbitrary motion profiles", *Mechanical Systems and Signal Processing*, 27:667–682, 2012.

[Darlow 1974] M.S. Darlow, R.H. Badgley, G.W. Hogg. Application of high frequency resonance techniques for bearing diagnostics in helicopter gearboxes. *US Army Air Mobility Research and Development Laboratory (USAAMRDL) Technical Repo*, 74–77, 1974.

[D'Elia 2010] G. D'Elia, Z. Daher, J. Antoni. A novel approach for the cyclo-nonstationary analysis of speed varying signals. *In*

Cette thèse est accessible à l'adresse : http://theses.insa-lyon.fr/publication/2015ISAL0106/these.pdf
© [D. Abboud], [2015], INSA Lyon, tous droits réservés

Proceeding of ISMA 2010 Including USD 2010, Belgium, 2010.

[Fyfe 1997] K.R. Fyfe, E.D. S. Munck, Analysis of computed order tracking, *Mechanical Systems and Signal Processing*, 11(2):187–205, 1997.

[Ferrero 1992] A. Ferrero, R. Ottoboni. High-accuracy Fourier analysis based on synchronous sampling techniques. *IEEE Transaction Instrumentation and Measurement*, 41(6):780–785, 1992.

[Feldbauer 2000] C. Feldbauer, R. Höldrich. Realization of a Vold-Kalman tracking filter - A least squares problem. *In: Proceedings of the COST G-6 Conference on Digital Audio Effects (DAFX-00)*, Ireland, 2000.

[Fair 1998] C. E. Fair. Synchronous Sampling Sideband Orders from Helical Planetary Gear Sets. *Master thesis dissertation,* faculty of the Virginia Polytechnic Institute and State University, 1998.

[Gardner 1975] W.A. Gardner, L.E. Franks. Characterization of cyclostationary random signal process. *IEEE Transactions on Information Theory*, 21(1):4–14, 1975.

[Gardner 1990] W. Gardner. Introduction to Random Processes. *2nd edition McGraw-Hill*, New York, 1990.

[George 1992] V. George, G. Gaonkar., J. Prasad, D. Schrage. Adequacy of modeling turbulence and related effects on helicopter response. *American Institute of Aeronautics and Astronautics*, 30(6):1468–1479, 1992.

[Glover 1977] J. Glover. Adaptive noise canceling applied to sinusoidal interferences. *IEEE Transactions on Acoustics Speech and Signal processing*, 25(6):485–491, 1977.

[Hamrock 1983] B. J. Hamrock, W. J. Anderson, Rolling-element bearings, *NASA reference publication 1105*, June 1983.

Cette thèse est accessible à l'adresse : http://theses.insa-lyon.fr/publication/2015ISAL0106/these.pdf
© [D. Abboud], [2015], INSA Lyon, tous droits réservés

[Heyns 2011] T. Heyns, S.J. Godsill, J.P. de Villiers and P.S. Heyns, Statistical gear health analysis which is robust to fluctuating loads and operating speeds. *Mechanical Systems and Signal Processing*, 27:651-666, 2011.

[Heyns 2012] T. Heyns, PS. Heyns, R. Zimroz, Combining discrepancy analysis with sensorless signal resampling for condition monitoring of rotating machines under fluctuating operations. *In: Proceedings of the 9th International Conference on Condition Monitoring and Machinery Failure Prevention Technologies*, UK, 12-14 June 2012.

[Ho 2000] D. Ho, R.B. Randall. Optimisation of bearing diagnostic techniques using simulated and actual bearing fault signals. *Mechanical Systems and Signal Processing*, 14(5):763–788, 2000.

[Izzo 1998] L. Izzo and A. Napolitano. The higher-order theory of generalized almost-cyclostationary time-series. *IEEE Transaction in Signal Processing*, 46:2975-2989, 1998.

[Jablonski 2013] A. Jablonski, T. Barszcz. J. Antoni. Comparison of vibration signal separation techniques for rotating machinery. *Proceeding of the conference Surveillance 7*, France, 29-30 Oct. 2013.

[Jardine 2006] A.K.S. Jardine, D. Lin and D. Banjevic. A review on machinery diagnostics and prognostics implementing condition-based maintenance. *Mechanical Systems and Signal Processing*, 20(7):1483-1510, 2006.

[Klapper 1972] J. Klapper and J. T. Frankle. Phase-Locked and Frequency-Feedback Systems. *New York: Academic Press*, 1972.

[Leuridan 1995] J. Leuridan, G. E. Kopp, N. Moshrefi, and H. Vold. High Resolution Order Tracking Using Kalman Tracking Filters – Theory and Applications. *SAE Technical Paper 951332*, 1995, doi:10.4271/951332.

Cette thèse est accessible à l'adresse : http://theses.insa-lyon.fr/publication/2015ISAL0106/these.pdf
© [D. Abboud], [2015], INSA Lyon, tous droits réservés

[Martin 1982] W. Martin. Time-frequency analysis of random signals. *International Conference on Acoustics, Speech, and Signal Processing*, France, 1982.

[McCormick 1998] A.C. McCormick, A.C. Nandi. Cyclostationarity in rotating machine vibrations. *Mechanical Systems and Signal Processing*, 12(2): 225–242, 1998.

[McFadden 1984a] P. D. McFadden, J. D. Smith. Model for the Vibration Produced by a Single Point Defect in a Rolling Element Bearing. *Journal of Sound and Vibration*, 91(1):69–82, 1984.

[McFadden 1984b] P.D. McFadden, J.D. Smith. Vibration monitoring of rolling element bearings by the high-frequency resonance technique—a review. *Tribology International*, 17(1), 3–10, 1984.

[McFadden 1985] P.D. McFadden, J. D. Smith. The Vibration Produced by Multiple Point Defects in a Rolling Element Bearing. *Journal of Sound and Vibration*, 98(2):69–82, 1985.

[McFadden 1986] P.D. McFadden. Detecting fatigue cracks in Gear by amplitude and phase demodulation of the meshing vibration. *Journal of Vibration, Acoustics, Stress, and Reliability in Design*, 108(2):165-170, 1986.

[McFadden 1989] P.D. McFadden. Interpolation techniques for time domain averaging of gear vibration. *Mechanical Systems and Signal Processing*, 3(1):87-97, 1989.

[McFadden 2000] P.D. McFadden, M. Toozhy. Application of synchronous averaging to vibration monitoring of rolling element bearing. *Mechanical Systems and Signal Processing*, 14(6):891-906, 2000.

[McGowin 2006] C. McGowin. Condition Monitoring of Wind Turbines: Technology Overview, Seeded-Fault Testing, and Cost-Benefit Analysis. *Electric Power Research Institute (EPRI), Palo Alto, Tech Report*, CA: 2006. 1010419.

Cette thèse est accessible à l'adresse : http://theses.insa-lyon.fr/publication/2015ISAL0106/these.pdf
© [D. Abboud], [2015], INSA Lyon, tous droits réservés

[Millar 1968] R.A. Millar. Digital control of shaft speed and position. *Spectrum IEEE*, 5(1):90–95, 1968.

[Morow 1952] L.C. Morow. Maintenance Engineering Hand Book. *Mc Graw Hill*, New York, 1952.

[Napolitano 2007] A. Napolitano. Generalized almost-cyclostationary processes and spectrally correlated processes: two extensions of the class of the almost cyclostationary processes. *Proceeding of 9th International Symposium on Signal Processing and its Application*, United Arab Emirates, 2007.

[Napolitano 2012] A. Napolitano. Generalizations of Cyclostationary Signal Processing: Spectral Analysis and Applications. *Wiley – IEEE Press*, 2012.

[Nice 2000] K. Nice. How Gears Work. *HowStuffWorks.com*. <http://science.howstuffworks.com/transport/engines-equipment/gear.htm> , 16 November 2000 (seen 16 Aug.2015).

[Pan 2007] M.C. Pan, C.X. Wu, Adaptive Vold–Kalman filtering order tracking, *Mechanical Systems and Signal Processing*, 21(8) (2007), pp. 2957–2969.

[Potter 1989] R. Potter, M. Gribler. Computed order tracking obsoletes older methods, *SAE Technical Paper 891131*, 1989, doi:10.4271/891131.

[Potter 1990] R. Potter, A new order tracking method for rotating machinery, *Journal of Sound and Vibration*, (24)30-34, 1990.

[Quinion 2015] M. Quinion, Preventative or preventive, *World Wide Words website*, viewed 27 Oct. 2015.

[Raad 2008] A. Raad, J. Antoni, M. Sidahmad. Indicators of cyclostationarity: Theory and application to gear fault monitoring. *Mechanical Systems and Signal Processing*, 22(3):574–587, 2008.

Cette thèse est accessible à l'adresse : http://theses.insa-lyon.fr/publication/2015ISAL0106/these.pdf
© [D. Abboud], [2015], INSA Lyon, tous droits réservés

[Randall 1982] R.B. Randall. A new method of modelling Gear faults. *Journal of Mechanical Design*, 104(2):259- 267, 1982.

[Randall 1995] R.B. Randall, L. Li. Diagnostics of planetary gear bearings in the presence of gear vibrations. *In: Proceedings of the Second International Conference on Gearbox Vibration and Diagnostics*, UK, 1995.

[Randall 2001] R.B. Randall, J. Antoni, S. Chobsaard. The relationship between spectral correlation and envelope analysis for cyclostationary machine signals, application to ball bearing diagnostics. *Mechanical Systems and System Processing*, 15(5):945–962, 2001.

[Randall 2011] R.B. Randall, J. Antoni. Rolling element bearing diagnostics— a tutorial. *Mechanical Systems and System Processing*, 25(2):485–520, 2011.

[Roussel 2013] J. Roussel, M. Haritopoulos, E. Sekko, C. Capdessus, J. Antoni, Application of Speed Transform to the Diagnosis of a Roller Bearing in Variable Speed, *Proceeding of the conference Surveillance 7*, France, 29-30 Oct. 2013.

[Sherman 1995] P.J. Sherman, L.B. White. Improved periodic spectral analysis with application to diesel vibration data. *Journal of the Acoustical Society of America*, 98(6):3285–3301, 1995.

[Stander 2006] C.J. Stander, P.S. Heyns. Transmission path phase compensation for gear monitoring under fluctuating load conditions. *Mechanical Systems and Signal Processing*, 20(7) 1511-1522, 2006.

[Staszewski 1997] W. J. Staszewski, K. Worden, G. R. Tomlinson. Time-frequency analysis in gearbox fault detection using the Wigner-Ville distribution and patter recognition. *Mechanical Systems and Signal Processing*, 11(5):673-692, 1997.

[Su 1992] Y. T. Su, S.J. Lin. On the initial fault detection of a tapered roller bearing: frequency domain analysis. *Journal of Sound and Vibration*, 155(1), 75–84, 1992.

Cette thèse est accessible à l'adresse : http://theses.insa-lyon.fr/publication/2015ISAL0106/these.pdf
© [D. Abboud], [2015], INSA Lyon, tous droits réservés

[Urbanek 2013] J. Urbanek, T. Barszcz, J. Antoni. A two-step procedure for estimation of instantaneous rotational speed with large fluctuations. *Mechanical Systems and Signal Processing*, 38(1):96-102, 2013.

[VanZante 1996] D. VanZante, R.L. Feddersen, M. Suarez, P.J. Sherman. The stochastic structure of downstream pressure from an axial compressor—I. A periodic time-frequency spectral description. *Mechanical Systems and Signal Processing*, 10(4):413–422, 1996.

[Wang 2002] W. Wang, A.K. Wong, *Autoregressive model-based gear fault diagnosis. Journal of Vibration and Acoustics*, 124(2):172-179, 2002.

[Weinberg 1974] A. Weinberg, B. Liu. Discrete time analyses of non-uniform sampling first- and second-order digital phase lock loops. *IEEE Transaction Communication*, 22(2):123–137, 1974.

[Widrow 1985] B. Widrow, S. Stearns. Adaptive Signal Processing. *Prentice-Hall, Englewood Cliffs*, NJ, 349–351, 1985.

[Zhao 2013] M. Zhao, J. Lin, X. Xu, Y. Lei. Tacholess Envelope Order Analysis and Its Application to Fault Detection of Rolling Element Bearings with Varying Speeds. *Sensors*, 13(8):10856-10875, 2013.

[Zeidler 1978] J. Zeidler, E. Satorius, D. M. Chabries, H. Wexler. Adaptive enhancement of multiple sinusoids in uncorrelated noise. *IEEE Transactions on Acoustics, Speech, and Signal Processing*, 26(3):240–254, 1978.

[Zimroz 2008] R. Zimroz. Adaptative approaches for condition monitoring of mining machines. *Gospodarka Surowami Mineralnymi*, 24 (4/3): 103-105, 2008.

Cette thèse est accessible à l'adresse : http://theses.insa-lyon.fr/publication/2015ISAL0106/these.pdf
© [D. Abboud], [2015], INSA Lyon, tous droits réservés

List of publications

Conference Papers

- D. Abboud, J. Antoni, S. Sieg-Zieba, M. Eltabach. On the extraction of rolling-element bearing fault signature in speed-varying conditions, Proceedings of the Eleventh International Conference on Condition Monitoring and. Machinery Failure Prevention Technologies, 10-12 June 2014, Manchester UK

- D. Abboud, J. Antoni, S. Sieg-Zieba, M. Eltabach, Generalization of the synchronous average for Deterministic/Random Separation under speed varying conditions, Proceedings of vibrations shocks and noise, 17-19 June 2014, Aix-en-Provence France.

- D. Abboud, J. Antoni, S. Sieg-Zieba, M. Eltabach, Speed-spectral whitening for enhancing envelope analysis in speed varying conditions, Proceedings of vibrations shocks and noise, 17-19 June 2014, Aix-en-Provence France.

- D. Abboud, J. Antoni, S. Sieg-Zieba, M. Eltabach, Angle\Time-cyclostationarity in rolling element bearing vibrations, Proceedings of the 4th conference in condition monitoring of machinery in non-stationary operations, 14-16 December 2014, Lyon France.

- D. Abboud, J. Antoni, S. Sieg-Zieba, M. Eltabach, Envelope preprocessing techniques for rolling element bearing diagnosis in variable speed conditions, Proceedings of the Twelfth International Conference on Condition Monitoring and. Machinery Failure Prevention Technologies, 9-11 June 2015, Oxford, UK

- D. Abboud, J. Antoni, S. Sieg-Zieba, M. Eltabach, The speed-dependent spectral correlation, Proceedings of the international conference on structural engineering dynamics, 22-24 June 2015, Lagos, Algarve, Portugal

- D. Abboud, J. Antoni, S. Sieg-Zieba, M. Eltabach, Order-frequency solutions for the analysis of random cyclic components, Surveillance 8, October 2015

Springer

- J. Antoni, D. Abboud, S. Baudin, Time-angle periodically correlated process, Cyclostationarity: theory and methods. Lecture notes in mechanical engineering, Springer (2014)

Cette thèse est accessible à l'adresse : http://theses.insa-lyon.fr/publication/2015ISAL0106/these.pdf
© [D. Abboud], [2015], INSA Lyon, tous droits réservés

Journal papers

- D. Abboud, J. Antoni, M. Eltabach, S. Sieg-Zieba. Deterministic-Random separation in nonstationary regime. Journal of sound and vibrations, Accepted September 21, 2015 (Actual status: waiting for publication).

- D. Abboud, S. Baudin, J. Antoni, D. Remond, M. Eltabach, O. sauvage. The spectral analysis of cyclo-non-stationary signals. Mechanical Systems and Signal Processing, Accepted September 27, 2015 (Actual status: waiting for publication).

- D. Abboud, J. Antoni, M. Eltabach, S. Sieg-Zieba. Angle\time cyclostationarity for the analysis of rolling element bearing vibrations. Measurements, Volume 75, November 2015, Pages 29–39.

- D. Abboud, J. Antoni, M. Eltabach, S. Sieg-Zieba. Envelope analysis of rotating machine vibrations in variable speed conditions: a comprehensive treatment, Mechanical Systems and Signal Processing, Submitted August 26, 2015.

Cette thèse est accessible à l'adresse : http://theses.insa-lyon.fr/publication/2015ISAL0106/these.pdf
© [D. Abboud], [2015], INSA Lyon, tous droits réservés

Appendices

Cette thèse est accessible à l'adresse : http://theses.insa-lyon.fr/publication/2015ISAL0106/these.pdf
© [D. Abboud], [2015], INSA Lyon, tous droits réservés

Appendix A - ‘Pub1’: Deterministic-Random separation in nonstationary regime

D. Abboud, J. Antoni, M. Eltabach, S. Sieg-Zieba. Deterministic-Random separation in nonstationary regime. *Journal of sound and vibrations*, Accepted September 21, 2015 (Actual status: waiting for publication).

Cette thèse est accessible à l'adresse : http://theses.insa-lyon.fr/publication/2015ISAL0106/these.pdf
© [D. Abboud], [2015], INSA Lyon, tous droits réservés

Appendix B - ‘Pub2’: The spectral analysis of cyclo-non-stationary signals

D. Abboud, S. Baudin, J. Antoni, D. Remond, M. Eltabach, O. sauvage. The spectral analysis of cyclo-non-stationary signals. *Mechanical Systems and Signal Processing*, Accepted September 27, 2015 (Actual status: waiting for publication).

Cette thèse est accessible à l'adresse : http://theses.insa-lyon.fr/publication/2015ISAL0106/these.pdf
© [D. Abboud], [2015], INSA Lyon, tous droits réservés

Appendix C - ‘Pub3’: Angle\time cyclostationarity for the analysis of rolling element bearing vibrations

D. Abboud, J. Antoni, M. Eltabach, S. Sieg-Zieba. Angle\time cyclostationarity for the analysis of rolling element bearing vibrations. *Measurements*, Volume 75, November 2015, Pages 29–39.

Cette thèse est accessible à l'adresse : http://theses.insa-lyon.fr/publication/2015ISAL0106/these.pdf
© [D. Abboud], [2015], INSA Lyon, tous droits réservés

Angle\Time cyclostationarity for the analysis of rolling element bearing vibrations

Dany Abboud[1, 2], Jerome Antoni[1], Mario Eltabach[2], Sophie Sieg-Zieba[2]

[1] LVA, INSA-Lyon, University of Lyon, France
{ dany.abboud, jerome.antoni}@insa-lyon.fr
[2] CETIM, Centre Technique des industries mécaniques, Senlis, France
{ dany.abboud, mario.eltabach, sophie.sieg-zieba}@cetim.fr

Abstract. In speed-varying conditions, the assumption of cyclostationarity of rolling-element bearing vibrations is jeopardized. The emitted signal comprises an interaction between (i) time-dependent components related to the system dynamics (e.g. transfer function) and (ii) angle-dependent mechanisms related to the system kinematics (e.g. impact, load modulations…). This necessarily implies the inadequacy of classical cyclostationary tools no matter a temporal or angular vision is adopted. This consequently calls for an angle\time approach which preserves— via the angle variable— the cyclic evolution of the signal while maintaining— via the time variable— a temporal description of the system dynamics. The first object of this paper is to analytically characterize bearing fault vibrations and explore its angle\time cyclostationary property. The second object is to experimentally validate these results on real-world vibration signals and demonstrate the optimality of the angle-time approach over classical approaches for rolling element bearing diagnosis.

Keywords: cyclostationarity, Angle\Time cyclostationarity, spectral correlation, order-frequency spectral correlation, bearing diagnosis, nonstationary conditions.

List of acronyms: REB – rolling element bearing ; AT-CS – angle\time cyclostationary; CS – cyclostationary; SC – spectral correlation; ATCF angle-time autocorrelation function; OFSC – order-frequency spectral correlation, CCF –

Cette thèse est accessible à l'adresse : http://theses.insa-lyon.fr/publication/2015ISAL0106/these.pdf
© [D. Abboud], [2015], INSA Lyon, tous droits réservés

cyclic correlation function, BPOO - ball-pass-order on the outer-race; SES squared envelope spectrum.

1 Introduction

At the beginning of the last decade, a new model of rolling element bearing (REB) vibrations has been introduced [1,2], opening the door to an insightful comprehension of REB fault signature within the cyclostationary (CS) framework. Precisely, it was shown that the produced mechanical signature is random in nature and has symptomatic properties that can be detected by means of second-order cyclostationary tools [3,4] [5]. In particular, the "spectral correlation (SC)" is a powerful second-order tool that completely describes the signal dynamics and the nature of its hidden periodicities [4]. The SC is a bispectral distribution of the *cyclic frequency* and the *spectral frequency* variables. The cyclic frequency represents the spectral content of the modulations—typically induced by the periodicity of impact, load modulations, etc.--whereas the spectral frequency represents the spectral content of the carrier—typically reflecting the transfer function of the system. This makes the SC a valuable tool for REB diagnostics: a faulty REB signal exhibits a symptomatic distribution of parallel spectral lines discretely located at the cyclic frequencies associated with the bearing fault frequencies and whose distribution along the spectral frequency axis is intensified around the system resonances. However, the SC was conceived under the assumption of constant speed with possibly slight fluctuations.

In nonstationary conditions, REB fault vibrations involve an interaction between time and angle-dependent components. In details, the emitted signal can be viewed as a series of cyclic impacts locked to the shaft angle and exciting structural resonances. Clearly, the positions of the impact excitations are described by the shaft angle while the resonance responses are governed by time differential equations that impose time-invariant resonances and relaxation times [6]. Therefore, neither a temporal nor an angular domain description[1] is sufficient alone to explore the full signal content. Precisely, if a temporal domain description is adopted, the cyclic frequency of the "temporal" SC will be unable to identify the angle-dependent modulations even though the spectral frequency would identify the carrier characteristics. Conversely, if an angular domain description is adopted, the spectral order of the "angular" SC[2] will be unable to identify the time-invariant characteristics of the carrier even though the cyclic order would identify existing modulations. Some previous attempts have been made to deal with this peculiarity. In particular, D'Elia et al. [6] proposed an order-frequency distribution aiming to jointly describe time dynamics (via the frequency variable) and angle periodicities (via the order variable) of the signal. For this purpose, some intui-

[1] It is meant by an "angular domain description" that signals are processed in the angle domain before applying classical CS tools. This strictly implies an angle-CS modeling of the vibration signal. In practice, the change of variable is commonly applied through an angular (re)sampling operation [7].

[2] In this case, the "angular" SC is an order-order distribution of the *cyclic order* and the *spectral order* variables.

Cette thèse est accessible à l'adresse : http://theses.insa-lyon.fr/publication/2015ISAL0106/these.pdf
© [D. Abboud], [2015], INSA Lyon, tous droits réservés

tive estimators were introduced based either on the SC or on the *cyclic modulation spectrum*. Later on, Urbanek et al. [8,9] proposed an angle-frequency distribution— namely the *averaged instantaneous power spectrum* -- based on a time filtering step followed by an angle averaging operation of the squared output. A similar solution was provided by Jabłoński et al. [10] who proposed the *angular-temporal spectrum* that jointly represents the angular and temporal properties of the signal. Other solutions based on the order spectrum of the squared envelope after some preprocessing steps were introduced in Refs. [11-15].

The analysis of non-stationary signals requires a formalism with rigorous statistical definitions enabling the use of estimators. Napolitano introduced the class of "spectrally correlated processes" in [16]. This formalism suffers from the restrictive conditions on the non-stationarity for the estimation of the spectral correlation density function, making it unsuitable for the particular nature of mechanical signals. Recently, a novel class of signals coined "angle\time cyclostationary (AT-CS)" was introduced in Ref. [17]. The class is defined by the angle-periodicity of the "angle\time autocorrelation function (ATCF)", that is the correlation measure at a given angle of two versions of the signals shifted by a constant time-lag. Moreover, the double Fourier transform of this quantity, namely the "order-frequency spectral correlation" (OFSC), produces an order-frequency distribution of the energy that jointly localizes angle-periodicity of the modulation signal and the frequency property of the carrier. The principal aim of this paper is to explore the AT-CS property in faulty REB vibrations and demonstrates its preference over classical approaches.
The rest of the paper is organized as follows. Section 2 reviews the AT-CS class and the order-frequency spectral correlation and proposes a Welch estimator of this quantity. Section 3 extends an existing model of REB vibrations to account for the speed variations and analytically demonstrates its AT-CS property. Section 4 aims to experimentally evidence the usefulness of the AT-CS approach over those classical for REB diagnosis. Eventually, the paper is sealed with a general conclusion in section 5.

2 Angle\Time cyclostationary signals

In this section, a brief review of second-order statistics is provided with emphasis on the angle\time (AT) vision. Then, a basic operator— namely the OFSC— is expressed by means of the classical spectral density and estimated using the Welch estimator.

2.1 Second-order statistics

The notion of time, angle and angle\time cyclostationarity are central to this paper; this first subsection provides a brief summary of their definitions with emphasis on their conceptual distinction. For the sake of simplicity but also of practical interest, only second-order statistics will be considered here. For this reason, the precision of the order will be omitted hereafter.

Cette thèse est accessible à l'adresse : http://theses.insa-lyon.fr/publication/2015ISAL0106/these.pdf
© [D. Abboud], [2015], INSA Lyon, tous droits réservés

Time-CS signals. These signals are defined by the *time-periodicity* of the *temporal correlation measure*. Formally speaking, a real signal $x(t)$ is said time-CS if its *temporal autocorrelation function* is periodic and, consequently, accepts a Fourier series of non-zero Fourier coefficients at cyclic frequencies i/T, i.e.

$$\mathrm{R}_{2x}(t,\tau) = \mathbb{E}\{x(t)x(t-\tau)\} = \sum_i \mathrm{R}_{2x}^{i}(\tau)e^{j2\pi i\frac{t}{T}} \tag{1}$$

where E{*} denotes the ensemble averaging operator, t is the time variable and coefficient $\mathrm{R}_{2x}^{i}(\tau)$ is a continuous function of the time-lag τ known as the (time) "cyclic correlation function (CCF)". This decomposition separates the autocorrelation into two sets of functions with different physical meanings: the "Fourier coefficients" and the "exponential kernels". Whereas the latter is exclusively dependent on the temporal variable and reflects the periodic evolution of the waveform, the former is exclusively dependent on the time-lag and reflects the property of a *time-stationary* carrier. The bispectral counterpart of this quantity is a frequency-frequency distribution coined ("temporal") SC.

Angle-CS signals. These signals are defined by the *angle-periodicity* of the *angular correlation measure*. Formally speaking, a real signal $x(t)$ is said angle-CS if its *angular autocorrelation function* is periodic and, consequently, accepts a Fourier series of non-zero Fourier coefficients at cyclic orders i/Θ , i.e.

$$\mathrm{R}_{2\tilde{x}}(\theta,\varphi) = \mathbb{E}\{\tilde{x}(\theta)\tilde{x}(\theta-\varphi)\} = \sum_i \mathrm{R}_{2\tilde{x}}^{i}(\varphi)e^{j2\pi i\frac{\theta}{\Theta}} \tag{2}$$

where $\theta(t) = \int_0^t \omega(t)dt$ is the angular variable (ω denotes the angular frequency), $\tilde{x}(\theta) = x\big(t(\theta)\big)$ and coefficient $\mathrm{R}_{2\tilde{x}}^{i}(\varphi)$ is a continuous function of the angle-lag φ representing the (angle) CCF [18]. This decomposition has the same interpretation as in the previous case except that the periodicity is now expressed through the angular variable θ, while the property of an *angle-stationary* carrier is expressed through the angle-lag φ. The bispectral counterpart of this quantity is an order-order distribution coined ("angular") SC.

AT-CS signals. Recently introduced [17], this class is defined by the *angle-periodicity* of the *time-correlation measure* of the signal. Formally speaking, a real signal $x(t)$ is said AT-CS if its *angle-time autocorrelation function (ATCF)* is periodic and, consequently, accepts a Fourier series of non-zero Fourier coefficients at cyclic orders i/Θ, i.e.

$$\mathfrak{R}_{2x}(\theta,\tau) = \mathbb{E}\big\{x\big(t(\theta)\big)x(t(\theta)-\tau)\big\} = \sum_i \mathfrak{R}_{2x}^{i}(\tau)e^{j2\pi i\frac{\theta}{\Theta}} \tag{3}$$

where $\mathfrak{R}_{2x}^{i}(\tau)$ is the (angle\time) CCF [17]. This function associates the cyclic evolution of the modulation signal to the angular variable (via the exponential kernels) and

Cette thèse est accessible à l'adresse : http://theses.insa-lyon.fr/publication/2015ISAL0106/these.pdf
© [D. Abboud], [2015], INSA Lyon, tous droits réservés

the waveform characteristics of the carrier to the time-lag variable (via the Fourier coefficients). The bispectral counterpart of this quantity will be the subject of the next subsection.

Discussion. In the case of constant, stationary or cyclostationary speed fluctuations, it can be shown that a time-CS signal is also angle-CS [1818]– this is the scenario often assumed in the presence of small speed fluctuations– otherwise, this equivalence does not hold in general. In particular, when speed fluctuation is of concern, *temporal* and *angular* descriptions are frequently contrasted owing to the existing interaction between angle- and time-dependent mechanisms. Actually, whereas angle-periodicity holds for mechanisms resulting from the rotation of mechanical elements whatever the rotational speed, physical phenomena governed by temporal differential equations must still be described in time. Therefore, neither a time nor an angle-domain description is sufficient alone to explore the full signal content. Hence, the optimal solution for describing such signals is to consider angle and time jointly instead of independently. This was actually the motivation for introducing the AT-CS class in Ref. [17].

2.2 Order-Frequency Spectral Correlation

Similarly to the SC [3], the bispectral counterpart of the ATCF– coined "order-frequency spectral correlation (OFSC)"– is defined as the double Fourier transform of the ATCF [17]:

$$\mathcal{S}_{2x}(\alpha, f) = \mathcal{F}_{\substack{\theta\to\alpha \\ \tau\to f}}\{\mathfrak{R}_{2x}(\theta, \tau)\} \tag{4}$$

where α stands for "order", a quantity without unit that counts the number of events occurring per rotation of the reference shaft. It is emphasized that the first Fourier transform maps angle (in radian) to order (adimensional) while the second one maps time (in seconds) to frequency (in Hertz). The above definition can be alternatively expressed with respect to temporal Fourier transforms as:

$$\mathcal{S}_{2x}(\alpha, f) = \lim_{W\to\infty} \frac{1}{\Phi(W)} \mathbb{E}\left\{\mathcal{F}_W\{x(t)\}^* . \mathcal{F}_W\left\{x(t)e^{-j\alpha\theta(t)}\omega(t)\right\}\right\} \tag{5}$$

where $\omega(t) = d\theta/dt$ is the instantaneous angular speed, $\Phi(W) = \int_W \omega(t)dt$ is the angular sector spanned during the time interval W and $\mathcal{F}_W\{*\} = \int_{-W/2}^{+W/2}(*)e^{-j2\pi tf}dt$. The proof of this equation follows similar lines as the proof provided in Ref. [17], yet replacing the time sector W by its corresponding angular sector $\Phi(W)$.
Equation (5) suggests that the OFSC can be expressed by means of the (cross-) spectral density

$$\mathcal{S}_{2x}(\alpha, f) = S_{xx_\alpha}(f), \tag{6}$$

Cette thèse est accessible à l'adresse : http://theses.insa-lyon.fr/publication/2015ISAL0106/these.pdf
© [D. Abboud], [2015], INSA Lyon, tous droits réservés

of signals x(t) and $x_\alpha(t) = x(t)e^{-j\alpha\theta(t)}\omega(t)\,W/\Phi$ (where by convention, $S_{xy}(f)$ denotes the cross spectral density of signals x and y).
For AT-CS signals, the OFSC takes the particular form

$$\mathcal{S}_{2x}(\alpha, f) = \sum_i \mathcal{S}_{2x}^i(f)\delta(\alpha - i), \tag{7}$$

where $\mathcal{S}_{2x}^i(f) = \mathcal{F}_{\tau\to f}\{\Re_{2x}^i(\tau)\}$, which clearly indicates the presence of symptomatic parallel spectral lines $\mathcal{S}_{2x}^i(f)$ at the cyclic orders i; jointly carries the cyclic information in the signal and the spectral content of the carrier.

2.3 Estimation issue

One difficulty with the spectral analysis of nonstationary signals is the non-availability of generally consistent estimators [19]. Cyclostationarity is one exception and it happens that AT-cyclostationarity, as defined in this paper, is another one to some extent. In particular, the equivalence between the OFSC and the spectral density— as indicated in Eq. (6) — also holds for their estimators, i.e.

$$\hat{\mathcal{S}}_{2x}^{(L)}(\alpha, f) = \hat{S}_{xx_\alpha}^{(L)}(f)\,, \tag{8}$$

with $x_\alpha(n) = x(n)e^{-j\alpha\theta(n)}\dot{\theta}(n)\,W/\Phi$, $\hat{S}_{xy}^{(L)}(f)$ the estimator of the cross power spectrum of x and y over L samples, and n the discrete variable of the time resampled signal with period Δ i.e. $x(t) = x(n.\Delta)$. In particular, the Welch estimator— which consists of substituting the ensemble average operator by an average over weighted blocks— is probably the most practical because of its simple implementation and low computational cost owing to the use of short-time Fourier transforms of fixed size. Precisely, let $\{w[n]\}_{n=0}^{N_w-1}$ be a short window of N_w points and $w_s[n] = w[n - sR]$ its shifted version by R samples. The increment R is set between 1 and N_w to provide the opportunity of possible overlap. The Welch estimator of the OFSC reads

$$\hat{\mathcal{S}}_{2x}^{(L)}(\alpha, f) = \frac{1}{\Phi S||w||^2}\sum_{s=0}^{S-1} \mathrm{DTFT}\{w_s(n)x(n)\}^* \,\mathrm{DTFT}\{w_s(n)x(n)\dot{\theta}(n)e^{-j\alpha\theta(n)}\}, \tag{9}$$

where S stands for the greatest integer smaller than or equal to $L - N_w/R+1$, DTFT is the discrete time Fourier transform, and $||w||^2 = \sum_{n=0}^{n=N_w-1}|w[n]|^2$ stands for the window energy.

3 AT-CS modeling of rolling element bearing vibrations

The aim of this section is to explore the nature of the vibrational component emitted by a local fault in a REB operating under speed varying conditions. To do so, a CS model of REB vibration is proposed that accounts for speed variations. Then, an analytic study is performed on the model to evaluate its statistical properties.

Cette thèse est accessible à l'adresse : http://theses.insa-lyon.fr/publication/2015ISAL0106/these.pdf
© [D. Abboud], [2015], INSA Lyon, tous droits réservés

3.1 Bearing vibration model in variable operating speed

According to Ref. [2] the excitation of a local fault in a rotating REB component is manifested by a train of short time impulses, angle-periodic on average, locked to the angular period of the fault characteristic. The inter-arrival angles of the impacts are subjected to slight random fluctuations due to existing slips (these are trivially speed-dependent); whereas the corresponding magnitude is subject to fluctuations due to the non-exactly reproducible microscopic conditions when the fault impacts a rolling surface [3]. In general, the excitation is angle-periodic modulated by the load distribution, possible REB unbalance or misalignment, and periodic changes in the impulse response as the distance and orientation of the impacts moves towards and backwards the sensor. Moreover, as a defect strikes a mating surface, an abrupt change in the contact stress occurs at the interface (also called *shock*) which corresponds to a transfer of kinetic energy into elastic potential energy. Obviously, the higher the operating speed is, the higher kinematic energy at the shock instants is and the greater the vibration response is. Thus, the dependence of the vibration magnitude on the operating speed can be fairly modeled through a speed-dependent increasing modulation function. Building on this, a faulty rolling element REB signal can be obtained by exciting the system as [11,20],

$$X(t) = M\big(\omega(t)\big).P\big(\theta(t)\big).\sum_i A_i h(t - T_i) \quad \text{with } T_i = t(i\Theta_d + \delta_i) \tag{10}$$

where $M\big(\omega(t)\big)$ is an increasing modulation function, $P(\theta) = P(\theta + \Theta_M) = \sum_l c_P^l e^{j2\pi l\frac{\theta}{\Theta_M}}$ (Θ_M is the angular period of the modulation induced by load distribution changes and c_P^l denotes the l^{th} Fourier coefficient of $P(\theta)$), $h(t)$ is linear time invariant filter expressing the impulse response of the system, Θ_d is the angular period of the defect characteristic, A_i is the amplitude modulation modelled as a delta-correlated random sequence with $\mathbb{E}\{A_i\} = 1$ and $\mathrm{Var}\{A_i\} = \sigma_A^i$, δ_i are the inter-arrival angle fluctuations modelled as a zero-mean delta-correlated random variable[3] with speed-dependent probability distribution $f_\delta(\theta, \omega)$. An illustration of the signal model is provided in Fig. 1.

3.2 Statistical evaluation of the model

A faulty REB signal can be viewed as a series of cyclic impacts locked to the shaft angle and exciting structural resonances. The positions of the impact excitations are dictated by the shaft angle while the resonance responses are governed by differential equations that impose time-invariant resonance frequencies and relaxation times. The

[3] It was shown in Ref. [21] that having uncorrelated inter-arrival time differences $T_{i+1} - T_i$ is physically more realistic than imposing uncorrelated (white) jitters on the arrival times. However, as stated in the same reference, this leads to extra complications while not fundamentally changing the resulting properties of the vibration signal. This explains the choice of this simplistic modeling of the jitter.

Cette thèse est accessible à l'adresse : http://theses.insa-lyon.fr/publication/2015ISAL0106/these.pdf
© [D. Abboud], [2015], INSA Lyon, tous droits réservés

interaction between these components makes REB vibrations prone to evidence the AT-CS property. The aim of this section is to analytically investigate this property by exploiting the model developed in the previous subsection. Since the signal is mostly random in a high frequency range [3] [21], it thus makes sense to evaluate second-order statistics in order to explore the signal properties. In particular, the temporal autocorrelation function applied to the model is

$$\Re_{2x}(t,\tau) = \left(1+\sigma_A^2\right)M\left(\omega(t)\right)M\left(\omega(t-\tau)\right).P\left(\theta(t)\right)P\left(\theta(t-\tau)\right).\sum_i \mathbb{E}\{g(t-T_i,\tau)\}\ , \qquad (11)$$

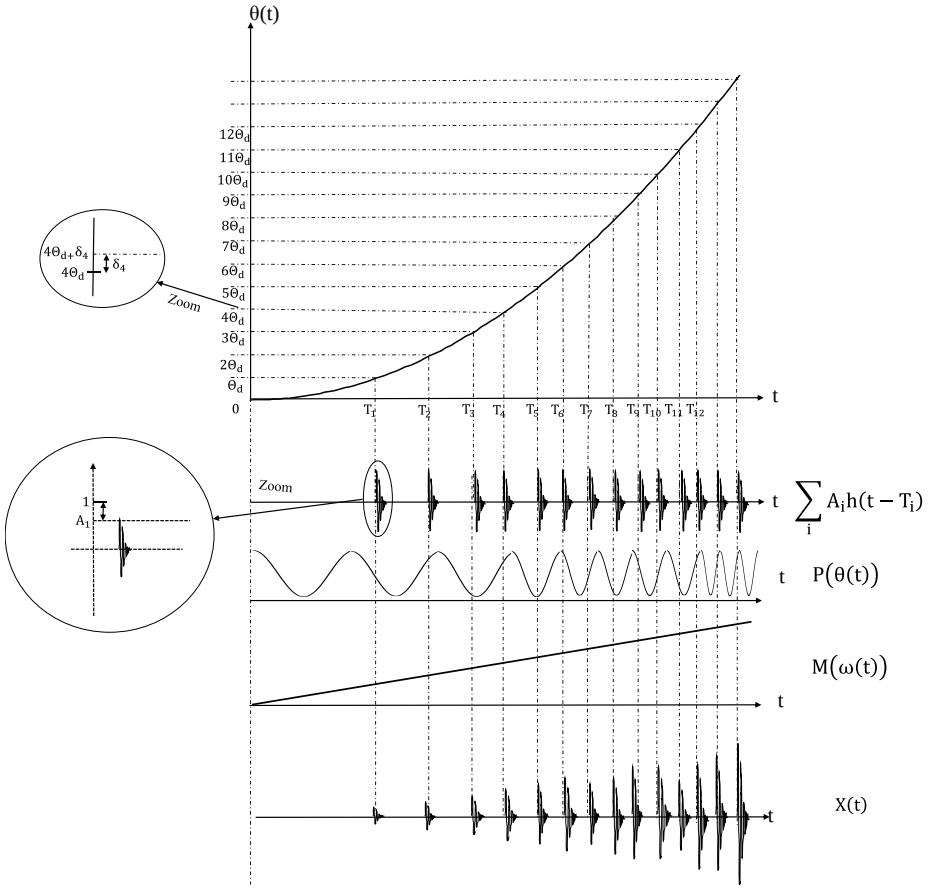

Fig. 1. REB vibration model in nonstationary speed conditions.

where $g(t,\tau) = h(t)h(t-\tau)$. Assuming that the relaxation time of the mechanical system is short compared to cycle durations and speed variations (i.e. $\tau \ll \Theta_d/\omega_{max} < \Theta_M/\omega_{max}$;ω_{max} is the maximal speed). By considering this fact and applying a variable change $\theta = \theta(t)$, one can obtain the ATCF,

$$\Re_{2x}(\theta,\tau) \approx (1+\sigma_A^2)M^2\left(\tilde{\omega}(\theta)\right).P^2(\theta)\sum_i \mathbb{E}\left\{\tilde{g}\left(\theta - i\Theta_d - \delta_i, \tau, \tilde{\omega}(i\Theta_d - \delta_i)\right)\right\}, \quad (12)$$

Cette thèse est accessible à l'adresse : http://theses.insa-lyon.fr/publication/2015ISAL0106/these.pdf
© [D. Abboud], [2015], INSA Lyon, tous droits réservés

with $\tilde{g}(\theta,\tau,\omega)=h(\theta/\omega)h(\theta/\omega-\tau)$ and $\tilde{\omega}(\theta)=\omega\big(t(\theta)\big)$. By working out the expectation operator, one obtains

$$\Re_{2x}(\theta,\tau)=(1+\sigma_A^2)M^2\big(\tilde{\omega}(\theta)\big).P^2(\theta)\sum_i G\big(\theta-i\Theta_d,\tau,\tilde{\omega}(\theta)\big) \quad (13)$$

where $G(\theta,\tau,\omega)=\int_s \tilde{g}(\theta-s,\tau,\omega)\,f_\delta(s,\omega)ds$ ($f_\delta(s,\omega)$ is the probability distribution function of the angular fluctuation at the speed ω). The sum in Eq. (13) can be replaced by a Fourier series whereof the coefficients depend on τ and $\tilde{\omega}(\theta)$, i.e. $\sum_i G\big(\theta-i\Theta_d,\tau,\tilde{\omega}(\theta)\big)=\sum_n c_G^n\big(\tau,\tilde{\omega}(\theta)\big)e^{j2\pi n\frac{\theta}{\Theta_d}}$ (where $c_G^n(\tau,\tilde{\omega})$ denotes the n^{th} Fourier coefficient of the periodic function $\sum_i G(\theta-i\Theta_d,\tau,\tilde{\omega})$). After rearranging Eq. (13) and expanding the periodic function $P^2(\theta)=\sum_m c_{2P}^m e^{j2\pi m\frac{\theta}{\Theta_M}}$ (where c_{2P}^m denotes the m^{th} Fourier coefficient of the periodic function $P^2(\theta)$),

$$\Re_{2x}(\theta,\tau)=\sum_{m,n}\gamma_{2x}^{m,n}\big(\tau,\tilde{\omega}(\theta)\big)e^{j2\pi\theta\left(\frac{n}{\Theta_d}+\frac{m}{\Theta_M}\right)} \quad (14)$$

where $\gamma_{2x}^{m,n}\big(\tau,\tilde{\omega}(\theta)\big)=(1+\sigma_A^2)M\big(\tilde{\omega}(\theta)\big)c_G^n\big(\tau,\tilde{\omega}(\theta)\big)c_{2P}^m$. By performing a Taylor expansion of the coefficients around the mean value of the speed, say ω_0, one obtains

$$\begin{aligned}&\Re_{2x}(\theta,\tau)\\&=\sum_{m,n}\gamma_{2x}^{m,n}(\tau,\omega_0)e^{j2\pi\theta\left(\frac{n}{\Theta_d}+\frac{m}{\Theta_M}\right)}\\&+\sum_{m,n}\left(\sum_k\frac{\partial^p\big(\gamma_{2x}^{m,n}(\tau,\omega)\big)}{\omega^p}\bigg|_{\omega_0}\frac{(\tilde{\omega}(\theta)-\omega_0)^k}{k!}\right)e^{j2\pi\theta\left(\frac{n}{\Theta_d}+\frac{m}{\Theta_M}\right)}\end{aligned} \quad (15)$$

where $\big(\partial^p\big(\gamma_{2x}^{m,n}(\tau,\omega)\big)/\omega^p\big)\big|_{\omega_0}$ denotes the p^{th} derivatives of $\gamma_{2x}^{m,n}(\tau,\omega)$ with respect to ω evaluated at ω_0. Obviously, the first term of Eq. (15) essentially reveals the AT-CS nature of the signal, while the second term comprises an explicit dependence on the speed via the function $\tilde{\omega}(\theta)$ making the Fourier coefficients angle-dependent and thus nonstationary. The latter dependence is principally induced by (i) the speed-dependent modulation $M\big(\omega(t)\big)$, (ii) the speed-dependent statistics of the jitter $f_\delta(\delta,\omega)$ and (iii) the convolution between angle-periodic and linear time invariant system. In practice, if AT-CS tools are considered, the average of the second term will be returned. In particular, this can be evaluated by considering $\tilde{\omega}(\theta)$ as a random variable with a given probability distribution function, $\Phi_\omega(\omega)$, leading to

$$\Re_{2x}(\theta,\tau)=\sum_{m,n}\Gamma_{2x}^{m,n}(\tau,\omega_0)e^{j2\pi\theta\left(\frac{m}{\Theta_d}+\frac{n}{\Theta_M}\right)}, \quad (16)$$

where

Cette thèse est accessible à l'adresse : http://theses.insa-lyon.fr/publication/2015ISAL0106/these.pdf
© [D. Abboud], [2015], INSA Lyon, tous droits réservés

$$\Gamma_{2x}^{m,n}(\tau,\omega_0)=\gamma_{2x}^{m,n}(\tau,\omega_0)+\left(\sum_k \frac{\int_\omega (\omega-\omega_0)^k \Phi_\omega(\omega)d\omega}{k!}\frac{\partial^p\left(\gamma_{2x}^{m,n}(\tau,\omega)\right)}{\omega^p}\bigg|_{\omega_0}\right). \quad (17)$$

Note that the second term in Eq. (17) results from working out the expectation operator on the Fourier coefficient of the second term of Eq. (15), thus resulting in the integral $\int_\omega (\omega-\omega_0)^k \Phi_\omega(\omega)d\omega$.
As a result, the OFSC reads

$$\mathcal{S}_{2x}(\alpha,f)=\sum_{m,n}\mathcal{S}_{2x}^{m,n}(f,\omega_0)\delta\left(\alpha-m\frac{2\pi}{\Theta_d}-n\frac{2\pi}{\Theta_M}\right), \quad (18)$$

with $\mathcal{S}_{2x}^{m,n}(f,\omega_0)=\mathcal{F}_{\tau\to f}\{\Gamma_{2x}^{m,n}(\tau,\omega_0)\}$, which comprises symptomatic spectral lines at the defect orders and associated sidebands. Note that $\mathcal{S}_{2x}^{m,n}(f,\omega_0)$ is a continuous function which principally depends on the transfer function of the system. This explains why a time presentation of the coefficients is actually needed to correctly reveal its spectral content. On the contrary, the 'angular' SC is inadequate in this respect albeit it can still return symptomatic spectral lines (i.e. angle-CS on average) as will be demonstrated in the experimental section. Conversely, the 'temporal' SC completely destroys the periodicities carried by the exponentials maintaining partial information about the transfer function property.
In conclusion, the vibrations emitted by faulty REBs are nonstationary in general (see Eq. (15)) and AT-CS on average (see Eq. (16)). Therefore, they produce a periodic AT-autocorrelation function and discrete spectral lines in the OFSC which constitute a symptomatic property of the fault signature in the order-frequency plane (see Eq. (18)). This indicates the usefulness of the AT vision in general and the OFSC quantity in particular for REB diagnosis. However, it is worth noting that the OFSC is dependent on the average speed ω_0 of the realization (or the record in practice).

4 Experimental validation

It has been shown that the vibrations emitted by a faulty REB operating under variable speed conditions are AT-CS and, thus, can be appropriately treated by means of AT-CS tools rather than classical angular or temporal tools. The aim of this section is to experimentally evidence the optimality of the OFSC against the classical SC and squared envelope (order) spectrum.

4.1 Benchmark

The test rig used in this paper is located at Cetim[4] and illustrated in Fig. 1. It essentially comprises an asynchronous motor supplied by a variable-speed drive to control the motor speed, followed by a spur gear with 18 teeth and reduction ratio of 1. Two

[4] Technical Center for Mechanical Industries – Senlis, France.

Cette thèse est accessible à l'adresse : http://theses.insa-lyon.fr/publication/2015ISAL0106/these.pdf
© [D. Abboud], [2015], INSA Lyon, tous droits réservés

identical REBs are installed after the spur gear whereof one among them is faulty: the first REB (B1) is closer to the gears than the second one (B2) – comprising an outer-race fault– that is branched to an alternator by means of a belt simulating a fixed load. An optical keyphasor of 'Brawn' type is fixed close to the motor output to measure the rotational shaft position. In addition, two accelerometers, Acc1 and Acc2, are mounted on REBs B1 and B2, respectively, in the vertical direction (-Z) to measure the vibrations. The characteristics of the REB are as follows: ball diameter = 6 mm, pitch diameter = 25 mm, number of elements = 8. This returns an expected ball-pass-order on the outer-race (BPOO) at 3.04 orders; that is 3.04 times the rotation speed. The sampling rate is set to 25.6 kHz.

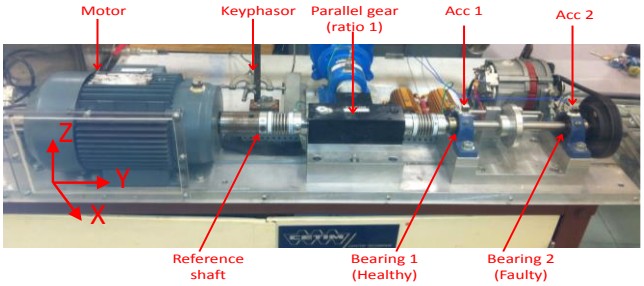

Fig. 2. The benchmark located at Cetim.

4.2 Case study 1: fault detection using nearby accelerometer

This first case study compares the OFSC with the classical SC using the vibration signal measured by the accelerometer mounted on the faulty REB (Acc2). Two experiments are implemented for this purpose.

In the first experiment, a runup from 8 to 31 Hz (see Fig. 2 (a)) is imposed to the electric motor over 40s; the acquired Acc2 signal is illustrated in Fig. 2 (b) together with its corresponding spectrogram in Fig. 2 (c). Next, the Welch estimator of the temporal SC is applied to the raw signal and the obtained result is displayed in Fig. 2 (d) (frequencies on the horizontal axis are divided by the averaged instantaneous frequency to get values close to orders). Alternatively, Fig. 2 (e) displays the angular SC of the same signal (orders on the vertical axis are multiplied by the averaged instantaneous frequency to get values close to frequencies). The latter is obtained by simply applying the Welch estimator of the SC on the angular resampled signal. Next, the Welch estimator of the OFSC is considered and the result is displayed in Fig. 2 (f). In all cases, the estimation parameters are as follows: a Hanning window with 66% overlap is used with imposed spectral resolution of 10 Hz (or its order equivalent in the case of angular SC considering the average instantaneous frequency) and a cyclic order resolution of 0.01 (or its frequency equivalent in the case of the temporal SC considering the average instantaneous frequency).

Cette thèse est accessible à l'adresse : http://theses.insa-lyon.fr/publication/2015ISAL0106/these.pdf
© [D. Abboud], [2015], INSA Lyon, tous droits réservés

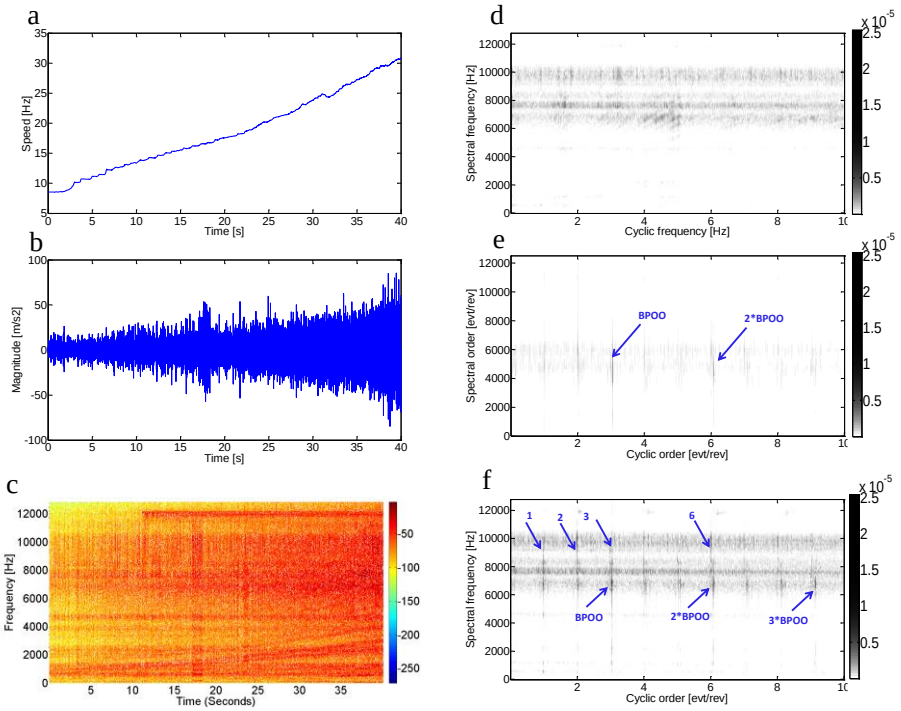

Fig. 3. (a) Runup profile, (b) Acc2 signal and (c) its spectrogram (Hamming window of 512 points, 80% overlap). Welch estimator of the (d) "temporal" SC, (e) "angular" SC and (f) OFSC applied on Acc2 signal. The same unit scale is used in (e), (f) and (g) to highlight the difference in energy among the distributions.

In the second experiment, a random speed profile ranging between 11 to 42 Hz (see Fig. 3 (a)) is imposed to the electric motor over 40s. Similarly to the runup case, the previous quantities are also applied on Acc2 signal (see Fig. 3 (b)) with the same parameters and displayed in Fig. 3 (c), (d), (e) and (f). In both experiments, an interesting energy increase is perceived in the spectrograms between 6 and 11 kHz, indicating an excitation of structural resonances along this band. The repetition rate, however, is hardly detectable and needs more sophisticated tools to be identified.

Cette thèse est accessible à l'adresse : http://theses.insa-lyon.fr/publication/2015ISAL0106/these.pdf
© [D. Abboud], [2015], INSA Lyon, tous droits réservés

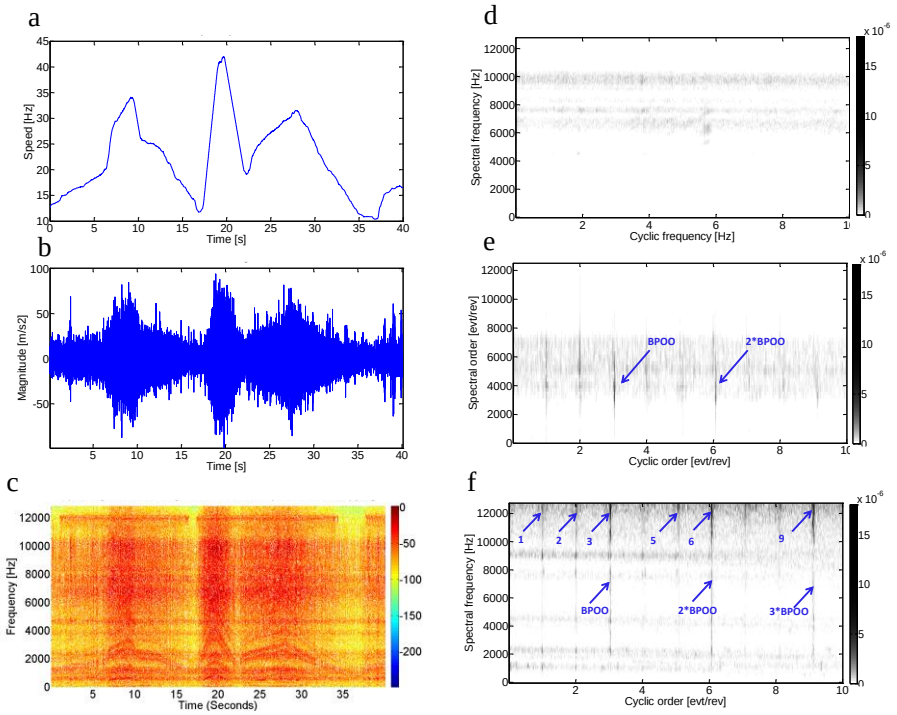

Fig. 4 (a) Random speed profile, (b) acceleration signal and (c) its spectrogram (Hamming window of 512 points, 80% overlap). Welch estimator of the (d) "temporal" SC, (e) "angular" SC and (f) OFSC applied on Acc2 signal. The same unit scale is used in (e), (f) and (g) to highlight the difference in energy among the distributions.

The observation of the results obtained from the two experiments leads to the same interpretation. It is clear that no modulations are detected by the temporal SC, yet the spectral characteristics of the resonances are partially identified. In contrast, modulations are reasonably identified by the angular SC at the BPOO (and its sidebands spaced by 1 order), but the spectral content is completely lost: the energy increase is shown below 6 kHz). Interestingly, the OFSC is able to identify both the cyclic modulations in the signal and the spectral content of its carrier. In details, the cyclic content is accurately pictured by *discrete* vertical spectral lines parallel to the spectral-frequency axis that correspond to the REB outer-race fault signature [2], while the frequency content is correctly identified by a *continuous* distribution of energy along the frequency axis with horizontal strips at the system resonances (between 6 and 8 kHz). Add to this the appearance of cyclic components at the shaft order and its harmonics in the spectral band [8 kHz; 11 kHz]. These components are random in nature and generated by gear wear [18] as opposed to the traditional deterministic nature of gear vibrations frequently generated by deterministic phenomena (e.g. meshing, a crack or spall fault…). At any rate, this highlights the power of the OFSC in identifying the source of cyclic modulations— which are likely to be carried by different time-invariant carriers— whatever the speed profile. Despite its ability to detect cy-

Cette thèse est accessible à l'adresse : http://theses.insa-lyon.fr/publication/2015ISAL0106/these.pdf
© [D. Abboud], [2015], INSA Lyon, tous droits réservés

clic components, the angular SC returns different and erroneous frequency bands for the carriers (see Fig. 2 (e) and Fig. 3 (e)).
Another interesting remark is that the OFSC reaches higher values than the temporal and angular SC. This can be explained by the fact that energy is well localized in the former or, conversely, that the energy is misdistributed in the latter. This implies that the OFSC is likely to reveal weak-energy signatures (such as those generated by incipient faults or measured by distant sensors) much better than classical operators and, particularly, the angular SC which has actually proved its ability to detect the presence of angular modulations. An example of this instance is provided in 4.3.
Note that, although they describe the same source, the OFSC of the signal from the first experiment (Fig. 2 (f)) is different from that of the second experiment (Fig. 3 (f)) due to different mean speeds ω_0 in Eq. (18).
In conclusion, performing the SC either in the time or the angle domain will not return complete information about the signal in the general scenario with large speed fluctuations: kinematic information related to angle-periodic rotations of the machine is lost in the temporal representation, whereas structural information related to time-dependent phenomena is lost in the angular representation. Being based on a joint AT vision, the OFSC provides a powerful tool to remedy this discrepancy.

4.3 Case study 2: fault detection using remoted accelerometer

The first case study asserted the superiority of the OFSC over classical tools and, particularly, the temporal SC which totally fails to reveal fault symptoms. Nevertheless, a doubt remained whether the angular SC is practically sufficient for detecting random cyclic components. The aim of this second case study is to show the need— not only the preference— of the OFSC over the angular SC in general for REB fault detection. Therefore, a comparison is made this time between these two quantities only, yet applied on a vibration signal measured by a remoted accelerometer (Acc1). This presents a challenging case since Acc1 is also close to the gears; that is the weak fault signature energy is likely to be masked by high-energy cyclic component generated by the gears. Note that this case is worth being studied because of its frequent occurrence in practice where accelerometers are remoted from the sources due to non-intrusion constraints (e.g. output REB of complex gearboxes).
Respecting the same choice of parameters as in subsection 4.2, the Welch estimator of the angular SC and OFSC are applied to Acc1 signal of the first experiment (i.e. runup regime— see Fig. 2 (a)). The angular SC is displayed in Fig. 4 (a) and its close-ups around BPOO and 2*BPOO in Figs. 4 (b) and (c) respectively. Obviously, the angular SC does not show any fault symptom; this is due to the fact that the SC stretches along the spectral order axis so that its energy falls down to the noise level. Next, The OFSC is displayed in Fig. 4 (d) and its close-ups around BPOO and 2*BPOO in (e) and (f) respectively. The OFSC successfully detects spectral lines at the fault cyclic orders in the vicinity of the spectral frequency 2 kHz, ensuring its robustness in detecting the REB fault even under this critical situation. The random contribution of the gear is, however, indicated by both operators because of its significant energy.

Cette thèse est accessible à l'adresse : http://theses.insa-lyon.fr/publication/2015ISAL0106/these.pdf
© [D. Abboud], [2015], INSA Lyon, tous droits réservés

Once again, only the OFSC is able to precisely identify cyclic sources of modulations. At the same time, the OFSC perfectly preserves structural information: it shows a structural mode between 8 and 11 kHz excited by gear wear, whereas the defect in the REB outer race excites a narrow-band structural mode around 2 kHz.
In short, the good distribution of the energy in the order-frequency plane makes the OFSC optimal not only to detect weak-energy signature, but also to identify interfering sources. The advantage of the latter feature is commonly ignored against the simplicity of the squared envelope spectrum (SES) that only returns cyclic components. The next subsection addresses the limitations of the SES and highlights the benefits brought by the OFSC in REB fault diagnosis.

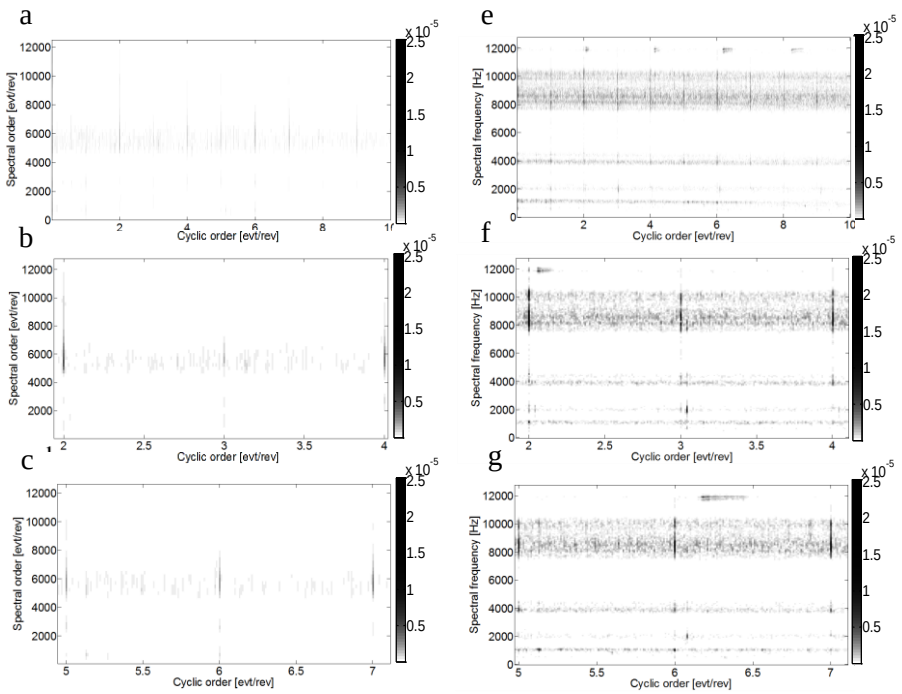

Fig. 5. Welch estimator of the (a) "angular" SC applied on Acc2 and its close-ups around (b) BPOO and (c) 2*BPOO. Welch estimator of the (d) OFSC applied on Acc2 signal and its close-ups around (e) BPOO and (f) 2*BPOO. The same unit scale is used to highlight the difference in energy among the distributions.

4.4 OFSC or SES?

For the time being, the SES technique remains the leading tool used for REB diagnosis. It can be shown that the SES is equivalent to the integration of the SC over the spectral frequency axis [2] [3].

In nonstationary conditions, the SES is combined with computed order tracking to obtain an order-domain representation [13,14]. This gives

Cette thèse est accessible à l'adresse : http://theses.insa-lyon.fr/publication/2015ISAL0106/these.pdf
© [D. Abboud], [2015], INSA Lyon, tous droits réservés

$$\mathrm{SES}_x(\alpha) = \mathcal{F}_{\theta\to\alpha}\left\{\mathbb{E}\left\{\left|\mathrm{x}\left(\mathrm{t}(\theta)\right)\right|^2\right\}\right\}. \quad (19)$$

Two main strategies are developed to cope with the non-consistency of the dynamical response in the angular domain; as well as possible interfering deterministic components. The first suggests a preprocessing step consisting of filtering the temporal signal around a high-frequency resonance band (or simply high-filtering the signal) [11]; while the second strategy eliminates the gear contribution and directly applies the SES on the residual signal [11] [Randall 2011b]. The first strategy suffers from the general ignorance of the resonance bands which, to the authors' knowledge; no existing method is currently available to determine it in variable speed conditions. Another conceptual problem of the SES technique is the possible existence of other mixed components induced by various cyclic sources of different carriers which may mask the fault signature. This latter follows from the fact that the "order tracked" SES is equivalent to the integration of the OFSC over the whole spectral frequency axis (see the proof in the appendix), i.e.

$$\int_{-\infty}^{+\infty} \mathcal{S}_{2\mathrm{x}}(\alpha, \mathrm{f})df = \mathrm{SES}_x(\alpha). \quad (20)$$

These problems make the SES an empirical technique: though being efficient for some applications, it cannot present a versatile solution in the general setting. The cases previously studied in 4.2 and 4.3 provide a practical illustration of this statement. To see this, the first strategy is applied on Acc1 and Acc2 signals obtained in the first experiment. First, the signals are high-pass filtered at 1 kHz to get rid of the gear *deterministic* components. Then, the SES is applied on the signals after angular resampling. Results are reported in Fig. 5 (a) and (b) referring to Acc2 and Acc1 respectively. The fault signature clearly appears in (a) since the random part of the signal is dominated by the REB vibrations due to the proximity of the fault with the accelerometer. The situation is reversed in (b) where the accelerometer is close to the gear system. In this case, the fault signature is masked by the *random* contribution of the gear; the SES is thus dominated by the shaft harmonics and fails to detect the symptoms of the REB fault.

In conclusion, the efficiency of the SES technique is confined to the case of one random cyclic source. This condition, however, is not generally guaranteed in rotating machine vibrations where random phenomena of different natures may simultaneously coexist. On the contrary, building on the results obtained in 4.2 and 4.3, the OFSC presents a general solution free of these shortcomings.

Cette thèse est accessible à l'adresse : http://theses.insa-lyon.fr/publication/2015ISAL0106/these.pdf
© [D. Abboud], [2015], INSA Lyon, tous droits réservés

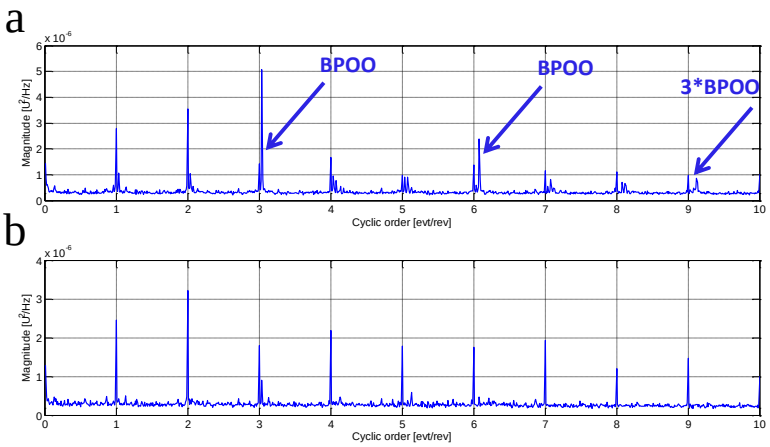

Fig. 6. The SES of (a) Acc2 and (b) Acc1 signals.

5 Conclusion

The analysis of rotating machines in nonstationary operating conditions is a current and challenging topic of research. In particular, the vibration of REB finds considerable interest in diagnostics. This paper has shown that the vibrations emitted by a local REB fault are angle\time cyclostationary on the average. The interaction between time and angle is materialized by the *angle*-periodicity of the correlation measure of two versions of the signals shifted by a constant *time*-lag. Accordingly, the inadequacy of classical cyclostationary approaches and the fruitfulness of the angle\time strategy are analytically demonstrated and experimentally validated. One limitation of this approach is that it comprises an intrinsic averaging operation of the spectral content which, in turn, may undergo substantial changes (e.g. speed dependent energy modulation, gyroscopic effects, non-linearity of the system…) as the speed severely evolves. Therefore, the authors believe that further work is to be oriented toward the consideration of this scenario.

References

1. Ho D., Randall R. B., Optimization of bearing diagnostic techniques using simulated and actual bearing fault signals. Mech. Syst. and Sign. Proc. 14, 763-788 (2000)

2. Randall R. B., Antoni J., Chobsaard S., The relationship between spectral correlation and envelope analysis for cyclostationary machine signals: application to ball bearing diagnostics. Mech. Syst. and Sign. Proc. 15, 945–962 (2001)

3. Antoni J., Cyclic spectral analysis of rolling-element bearing signals: Facts and fictions. Mech. Syst. and Sign. Proc. 304, 497–529 (2007)

Cette thèse est accessible à l'adresse : http://theses.insa-lyon.fr/publication/2015ISAL0106/these.pdf
© [D. Abboud], [2015], INSA Lyon, tous droits réservés

4. Antoni J., Cyclic spectral analysis in practice. Mech. Syst. and Sign. Proc. 21, 597–630 (2007)

5. Antoni J., Cyclostationarity by examples. Mech. Syst. and Sign. Proc., 23 (2009) 987–1036

6. D'Elia G., Daher Z., Antoni J., A novel approach for the cyclo-nonstationary analysis of speed varying signals, in: ISMA2010 International Conference on Noise and Vibration, Engineering, p. 2801–2814.

7. Fyfe K., Munk E., Analysis of computed order tracking, Mechanical Systems and Signal Processing 11 (2) (1996) 187–205.

8. Urbanek J., Barszcz T., Zimroz R., Antoni J., Application of averaged instantaneous power spectrum for diagnostics of machinery operating under non-stationary operational conditions, Measurement, Vol. 45, Issue 7, 2012, Pages 1782–1791

9. Urbanek J., Barszcz T., Antoni J., Time–frequency approach to extraction of selected second-order cyclostationary vibration components for varying operational conditions, Measurement Vol. 46, Issue 4, 2013, Pages 1454–1463

10. Jabłoński A., Urbanek J., Barszcz T., Application of angular-temporal spectrum for detection of rolling-element bearing faults operating under varying speed regime, Proceedings of the 4th conference in condition monitoring of machinery in non-stationary operations, 14-16 December 2014, Lyon France.

11. Borghesani P., Ricci; Chatterton S., R Pennacchi P., A new procedure for using envelope analysis for rolling element bearing diagnostics invariable operating conditions, Mech. Syst. and Sign. Proc. 38, 23–35 (2013)

12. Borghesani P.; Pennacchi P.; Randall R. B., Sawalhi N., Ricci R., Application of cepstrum pre-whitening for the diagnosis of bearing faults under variable speed conditions, Mech. Syst. Signal Process., 36, p. 370-384(2013)

13. Randall R.B., Antoni J., Rolling element bearing diagnostics— a tutorial, Mech. Syst. Signal Process. 25 (2) (2011) 485–520.

14. Randall R.B., Sawalhi N., Coats M., A comparison of methods for separation of deterministic and random signals, Int. J. Cond. Monit.1 (1), 11–19, (2011)

15. Randall R., Smith W., Coats M., Bearing diagnostics under widely varying speed conditions, Proceedings of the 4th conference in condition monitoring of machinery in non-stationary operations, 14-16 December 2014, Lyon France.

16. Napolitano A., Generalized almost-cyclostationary processes and spectrally correlated processes: two extensions of the class of the almost cyclostationary processes,

Cette thèse est accessible à l'adresse : http://theses.insa-lyon.fr/publication/2015ISAL0106/these.pdf
© [D. Abboud], [2015], INSA Lyon, tous droits réservés

proceeding of 9th International Symposium on Signal Processing and its Application, United Arab Emirates, Sharjah (2007)

17. Antoni J., Abboud D., Baudin S., Time-angle periodically correlated process. Cyclostationarity: theory and methods. Lecture notes in mechanical engineering, Springer (2014)

18. Antoni J., Bonnardot F., Raad A., El Badaoui M., Cyclostationary modelling of rotating machine vibration signals. Mech. Syst. And Sig. Proc. 18, 1285–1314 (2004)

19. Antonio N., Generalizations of Cyclostationary Signal Processing: Spectral Analysis and Applications, Wiley-IEEE Press (2012)

20. Abboud D., Eltabach M., Antoni J., Sieg-Zieba S.; On the extraction of rolling-element bearing fault signature in speed-varying conditions, The Eleventh International Conference on Condition Monitoring and Machinery Failure Prevention Technologies (2014)

21. Antoni J., Randall R.B., A stochastic model for simulation and diagnostics of rolling element bearings with localized faults. ASME Journal of Vibration and Acoustics, 2003: 282–289.

Appendix: Proof of Eq. (20)

By expanding Eq. (5) and integrating over the f variable, one obtains

$$\begin{aligned}
&\int_{-\infty}^{+\infty} \mathcal{S}_{2x}(\alpha, f) df \\
&= \lim_{W\to\infty} \frac{1}{\Phi(W)} \mathbb{E}\left\{ \int_{-\infty}^{+\infty} \int_{-W/2}^{+W/2} \int_{-W/2}^{+W/2} x(t)^* e^{j2\pi f t} x(t') \omega(t') e^{-j2\pi f t'} e^{-j\alpha\theta(t')} dt dt' df \right\} \\
&= \lim_{W\to\infty} \frac{1}{\Phi(W)} \mathbb{E}\left\{ \int_{-W/2}^{+W/2} \int_{-W/2}^{+W/2} x(t)^* x(t') \omega(t') e^{-j\alpha\theta(t')} \delta(t-t') dt dt' \right\} \\
&= \lim_{W\to\infty} \frac{1}{\Phi(W)} \mathbb{E}\left\{ \int_{-W/2}^{+W/2} |x(t)|^2 \omega(t) e^{-j\alpha\theta(t)} dt \right\}. \qquad \text{(A1)}
\end{aligned}$$

Since Φ is an increasing function of W, the limit of the latter equals that of the former. Exploiting the linearity of the ensemble averaging operator and applying a variable change $t = t(\theta)$, this leads to

$$\int_{-\infty}^{+\infty} \mathcal{S}_{2x}(\alpha, f) df = \lim_{\Phi\to\infty} \frac{1}{\Phi} \int_{\theta_1}^{\theta_1+\Phi} \mathbb{E}\left\{ \left| x(t(\theta)) \right|^2 \right\} e^{-j\alpha\theta} d\theta dt \,, \qquad \text{(A2)}$$

where $\theta_1 = \theta(-W/2)$; which is the order tracked SES of $x(t)$ as expressed in Eq. (19).

Cette thèse est accessible à l'adresse : http://theses.insa-lyon.fr/publication/2015ISAL0106/these.pdf
© [D. Abboud], [2015], INSA Lyon, tous droits réservés

Appendix D - 'Pub4': Envelope analysis of rotating machine vibrations in variable speed conditions: a comprehensive treatment

D. Abboud, J. Antoni, M. Eltabach, S. Sieg-Zieba. Angle\time cyclostationarity for the analysis of rolling element bearing vibrations, *Mechanical Systems and Signal Processing*, Submitted August 26, 2015.

Cette thèse est accessible à l'adresse : http://theses.insa-lyon.fr/publication/2015ISAL0106/these.pdf
© [D. Abboud], [2015], INSA Lyon, tous droits réservés

Envelope analysis of rotating machine vibrations in variable speed conditions: a comprehensive treatment

D. ABBOUD[a,b], J. ANTONI[a], S. SIEG-ZIEBA[b], M. ELTABACH[b]

[a] *Vibrations and Acoustic Laboratory (LVA), University of Lyon (INSA), F-69621 Villeurbanne CEDEX, France*

[b] *Technical Center of Mechanical industries (CETIM), CS 80067, 60304 Senlis Cedex, France*

Abstract

Nowadays, the vibration analysis of rotating machine signals is a well-established methodology, rooted on powerful tools offered in particular by the theory of cyclostationary (CS) processes. Among them, the squared envelope spectrum (SES) is probably the most popular to detect random CS components which are typical symptoms, for instance, of rolling element bearing faults. Recent researches are shifted towards the extension of existing CS tools—originally devised in constant speed conditions—to the case of variable speed conditions. Many of these works combine the SES with computed order tracking after some preprocessing steps. The principal object of this paper is to organize these dispersed researches into structured comprehensive framework. Three original features are furnished. First, a model of rotating machine signals is introduced which sheds light on the various components to be expected in the SES. Second, a critical comparison is made of three sophisticated methods, namely, the improved synchronous average, the cepstrum prewhitening, and the generalized synchronous average, used for suppressing the deterministic part. Also, a general envelope enhancement methodology which combines the latter two techniques with a time-domain filtering operation is revisited. All theoretical findings are experimentally validated on simulated and real-world vibration signals.

Keywords: Squared envelope spectrum; envelope enhancement techniques; variable speed conditions; vibration analysis; bearing diagnostic.

List of abbreviations: REB- rolling element bearings; SE- squared envelope; SES- squared envelope spectrum; CS- cyclostationary; SC- spectral correlation; VSC-variable speed conditions; ISA- improved synchronous average, CPW-cepstrum prewhitening; GSA-generalized synchronous average; SOI-source of interest; AT-CS – angle\time cyclostationary, BPOO- ball-pass-order on the outer-race

Nomenclature:

Cette thèse est accessible à l'adresse : http://theses.insa-lyon.fr/publication/2015ISAL0106/these.pdf
© [D. Abboud], [2015], INSA Lyon, tous droits réservés

t	Time variable
θ	Angle variable
α	Cyclic order variable
ω	Angular speed of the reference
$\mathcal{F}\{*\}$	Fourier transform
$\mathbb{E}\{*\}$	Ensemble average
$\mathrm{SES}_y(\alpha)$	Squared envelope spectrum of y
$\mathrm{SE}_y(t)$	Squared envelope of y
$\mathrm{cov}_{x,y}(t_1, t_2 \mid \omega)$	Covariance of x and y conditioned to ω
$\bar{\theta}$	angular location in the cycle: $\bar{\theta}\epsilon[0,2\pi]$
$m_Y(\bar{\theta}, \omega)$	GSA of Y
$m_Y(\theta)$	GSA trajectory tracked for a given speed profile $\omega = \omega(\theta)$
$\delta\omega$	Speed resolution
Φ	The angular sector spanned during the time record
$\mathbb{R}$	The set of real numbers
$\mathbb{Z}$	The set of all integer numbers

1 INTRODUCTION

Envelope analysis has been recognized for long as a powerful technique for rolling element bearing (REB) diagnosis operating at constant speed. Typically, it consists of a bandpass filtering step around a frequency band wherein the impulsive excitation is amplified followed by a demodulation that extracts the signal envelope. The spectrum of the envelope— known as the *envelope spectrum*— is expected to contain the desired diagnostic information, including the repetition rate of the fault and potential modulations [Randall 2011a]. At the time, the filtering and the demodulation operations were performed using analog techniques (e.g. [Darlow 1974]) with inherent limitations regarding the filter characteristics and the analog rectifier [Randall 2001]. Thanks to the advances of digital signal processing, considerable improvement has been made taking advantages of the Hilbert transform [Randall 1986]. This latter returns the (complex) analytic signal whose modulus uniquely defines the envelope. In this context, it has been shown in Ref. [Ho 2000] that it is preferable to use the *squared envelope (SE)* instead of the envelope inasmuch as the latter introduces extraneous components that appears as misleading peaks in the envelope spectrum. Since that time, the *squared envelope spectrum (SES)* has probably become the benchmark technique for bearing diagnostics, in particular due to its low computational cost [Randall 2011b].

During the last two decades, a wave of signal processing techniques rooted on the theory of *cyclostationary (CS)* processes [Gardner 1990] has appeared in multiple applications such as gears [Prieur 1995] [Lejeune 1997] [Rubini 1997] [Capdessus 2000] [Bouillaut 2000], REBs [Antoniadis 2001] [Randall 2001] and internal combustion engines [Konig 1994] [Konig 1995] [Antoni 2002]. In particular, a new model of REB vibrations has been introduced in Refs. [Ho

Cette thèse est accessible à l'adresse : http://theses.insa-lyon.fr/publication/2015ISAL0106/these.pdf
© [D. Abboud], [2015], INSA Lyon, tous droits réservés

2000] [Randall 2001], providing an insightful understanding of the REB fault signature within the CS framework [Antoni 2007a]. Accordingly, it has been shown that the *mechanical signature* generated by a faulty REB is random in nature and has symptomatic properties that can be detected by means of second-order CS tools such as the SES, the *spectral correlation,* the *spectral coherence,* the *cyclic modulation spectrum* and others [Randall 2001][Antoni 2007b] [Antoni 2009]. In this context, Ref. [Randall 2001] has established the relationship between the spectral correlation and the SES. Since then, the SES has become a (second-order) CS tool

All the above techniques rely on the assumption of constant— or possibly fluctuating by *stationary*— operating speed. Unfortunately, in some applications, the permanent acquisition of (quasi-) constant speed records is not available. A typical example is a wind turbine whose speed is mostly dependent on the random behavior of the wind. Evidently, the CS tools— including the SES— fail in describing such signals. Specifically, it has been shown in Refs. [Antoni 2014] [Abboud 2015c] that the vibrations emitted by rotating machines are likely to witness an interaction between time- and angle-dependent components. For instance, the REB fault signal can be viewed as a series of cyclic impacts locked to the shaft angle and exciting structural resonances [Abboud 2015c] [D'Elia 2010] [Urbanek 2012]. Clearly, the positions of the impact excitations are dictated by the shaft angle while the resonance responses are governed by differential equations that impose time-invariant properties (e.g. natural frequencies and relaxation times). Therefore, efforts have been directed toward the extension of existing diagnostic tools in variable speed conditions (VSC). The recent advances in this framework can be classified into two directions.

1) In the first one, works have been oriented toward the coupling between the SES and computed order tracking to obtain an order domain representation. In order to deal with the non-consistency of the dynamical response and to eliminate potential interfering deterministic components, two general strategies have been adopted. The first strategy filters the temporal signal around a high-frequency resonance band (or simply high-pass filtering the signal) [Borghesani 2013 a] [Zhao 2013] [Cocconcelli 2013], while the second one eliminates the gear contribution with sophisticated "deterministic/random separation" tools and directly applies the SES on the residual signal [Randall 2011b] [Borghesani 2013 c] [Abboud 2015b].

2) In the second direction, efforts have been oriented toward the generalization of existing CS. In particular, Urbanek et al. [Urbanek 2013a] [Urbanek 2013b] proposed an angle-frequency distribution— namely the averaged instantaneous power spectrum— based on a time filtering step followed by an angle averaging operation of the squared output. A similar solution was proposed by Jabłoński et al. [Jabłoński 2014] who introduced the *angular-temporal spectrum* to jointly represent the angular and temporal properties of the signal. More interestingly, a prominent solution was proposed by Delia et al. [D'Elia 2010] who explore the order-frequency approach. Their idea was to replace the frequency-frequency distribution by a frequency-order distribution that jointly describes the time-dynamics and the angle-periodicities of the signal. They proposed intuitive estimators for the spectral correlation and cyclic modulation spectrum which were coined as the *α-synchronized spectral correlation density* and *α-synchronized cyclic modulation spectrum*, respectively. Later on, a fast version of the former estimator, called "speed correlation", was proposed in Ref. [Roussel 2013] wherein the *speed transform* was used

Cette thèse est accessible à l'adresse : http://theses.insa-lyon.fr/publication/2015ISAL0106/these.pdf
© [D. Abboud], [2015], INSA Lyon, tous droits réservés

in the algorithm. Recently, Refs. [Antoni 2014] [Abboud 2015a] set up the foundations of angle\time cyclostationarity which extend the CS framework to enfold speed-varying signals. These references equally provide (i) a rigorous definition of the *order-frequency spectral correlation* together with its normalized form (namely the *order-frequency spectral coherence*), as well as a consistent Welch-based estimator.

This paper is particularly concerned with the first direction and tries to organize existing works into structured comprehensive framework. It is intended to serve as a guideline on how to exploit the SES in rotating machine diagnosis and to optimize it under given operating conditions. Overall, this paper also brings a number of original results that provide a more comprehensive view of some previously published material.

This paper is organized as follows: section 2 introduces a phenomenological signal model that describes the different components to be expected in the SES. This model will serve to formalize and illustrate the basic problem in VSC. Section 3 examines existing envelope enhancement strategies. In particular, it evaluates and compares three sophisticated deterministic random separation techniques, namely, the improved synchronous average (ISA) [Coats 2009] [Borghesani 2013a], the cepstrum prewhitening (CPW) [Borghesani 2013b] [Sawalhi 2011] and the generalized synchronous average (GSA) [Abboud 2015b]. Also, it addresses a general strategy to enhance a random source of interest—e.g. a REB fault component— and to enhance its emergence in the SES. All the theoretical findings and the qualitative comparisons are validated on simulated signals in section 5 and on real vibration signals including various case studies in section 6. Eventually, the paper is sealed with a general conclusion in section 7.

2 PROBLEM FORMULATION

The object of this section is to investigate the sources of interference which are likely to enter the SES of a vibration signal. A phenomenological model of the different possible contributions is first provided in VSC. Based on this model, the SES of a vibration signal is analytically investigated and illustrated.

2.1 Preliminaries

According to Refs. [Braun 1980][Lejeune 1997][Antoni 2003], vibration signals generated by rotating machinery can be decomposed into three contributions of different statistical natures as

$$x(t) = d(t) + r(t) + b(t), \tag{1}$$

where t stands for the time variable, $d(t)$ for the *deterministic contribution*, $r(t)$ for the (random) *cyclostationary contribution* and $b(t)$ for the stationary contribution that is neither periodic nor CS and that will be referred to subsequently as *background noise*. The deterministic part is typically related to *deterministic* excitations such as gear vibrations, misalignments, unbalances, blade rotations, reciprocating forces, etc. In (quasi-) constant speed conditions, the deterministic part is intrinsically periodic in the angular domain; thus it exhibits a discrete (order-) spectrum [Fyfe 1997] [Antoni 2004]. The CS contribution is generated by *random and repetitive* excitations such as wear, friction forces, impacting forces, fluid motions, turbulence,

Cette thèse est accessible à l'adresse : http://theses.insa-lyon.fr/publication/2015ISAL0106/these.pdf
© [D. Abboud], [2015], INSA Lyon, tous droits réservés

combustion forces, etc. [Antoni 2004]. In this context, CS components are characterized by a periodic mean instantaneous power, thus exhibiting a discrete SES [Ho 2000] [Randall 2001] [Antoni 2009]. Last, the background noise is typically generated by non-cyclostationary sources such as environmental noise, sensor measurement errors, etc.

In VSC, rotating machine vibrations undergo significant changes in their properties. In particular, the deterministic contribution $d(t)$ loses its (angle-) periodicity, the CS contribution $r(t)$ becomes *cyclo-non-stationary* (CNS) [Antoni 2013] [Abboud 2015a], and the background noise $b(t)$ becomes nonstationary (but also non-CNS). When analyzing rotating machine vibrations, the goal is typically to detect a particular vibratory component generated by a *source of interest* (SOI). The present paper is particularly concerned with the detection of a cyclo-non-stationary SOI using the envelope analysis. In the case when the component produced by the SOI is of deterministic nature, other techniques must be implemented to detect it. Let $s(t)$ be the CNS component generated by the SOI and $q_m(t)$ be the mth contribution generated by other interfering sources, so that:

$$r(t) = s(t) + \sum_{m=1}^{M} q_m(t) \tag{2}$$

where M stands for the number of interfering CNS sources. Therefore, by separating the vibrational component into *signal* and *noise*, Eq. (1) becomes

$$x(t) = s(t) + n(t), \tag{3}$$

where

$$n(t) = d(t) + \sum_{m=1}^{M} q_m(t) + b(t) \tag{4}$$

stands for the noise which comprises the sum of the deterministic interferences $d(t)$, CNS interferences $\sum_{m=1}^{M} q_m(t)$ and background noise $b(t)$.
The common practice in the literature consists of combining the SES with computed order tracking to obtain an order-domain representation [Randall 2011a] [Randall 2011b] [Zhao 2013] [Borghesani 2013c] [Cocconcelli 2013]. This follows from the fact that the periodicity of the statistics of the CNS component may be preserved to some extent in the angular domain since machine kinematics is inherently dependent on angle. In this regard, two practical difficulties are expected. The first one is related to the deterministic interference in the SES, while the second one is related to the CNS interferences. In both cases, the signature of the SOI is polluted in the SES. The present section aims to model and illustrate this issue. For this purpose, a phenomenological model of the deterministic, CNS and background noise contributions in VSCs are provided in subsections 2.2 in order to understand the structure of these components. This model will also serve to analytically investigate their contributions in the SES in subsection 2.3.

2.2 Generative model for vibration signals in variable speed conditions

This subsection models the deterministic contribution, the CNS contribution and the background noise. Note that the deterministic contribution model presented in subsection 2.2.1 is borrowed

Cette thèse est accessible à l'adresse : http://theses.insa-lyon.fr/publication/2015ISAL0106/these.pdf
© [D. Abboud], [2015], INSA Lyon, tous droits réservés

from a previous paper [Abboud 2015b], yet the interpretations and illustrations are new. The material in subsections 2.2.2 and 2.2.3 is fully original.

2.2.1 Modeling the deterministic part

In nonstationary conditions, the deterministic component is subjected to significant amplitude modulation and phase blur. These are basically induced by the variation of the machine power intake [Bartelmus 2009] [Bartelmus 2010] [Villa 2012] [Heyns 2012][Abboud 2014a] [Abboud 2015b] and the effect of time-invariant transfer functions from the excitation sources to the sensor [Stander 2006] [Borghesani 2013 a]. The first effect results in amplitude modulation, whereas the second one also induces phase blur. Provided that the speed profile is sufficiently smooth, a realistic modeling of the deterministic component is provided in Ref. [Abboud 2015b] through a Fourier decomposition whereof the coefficients have an explicit dependence on the speed, viz

$$d(t) = \sum_{\lambda_i \in \Lambda} d^{\lambda_i}\big(\omega(t)\big) e^{j\lambda_i \theta(t)}, \tag{5}$$

where θ denotes the rotational angle (in [rad]) of the machine (typically the *reference* angular period equals 2π radians), $\omega(t)$ denotes the instantaneous speed (in [rad/s]) of the machine, λ is a dimensionless index that denotes the machine cyclic orders , $\Lambda = \{\lambda_i \in \mathbb{R} / \ i = 1,2 \dots\}$ is the set of the cyclic orders associated with deterministic cyclic sources ($\mathbb{R}$ is the real set), and $d^{\lambda_i}(\omega)$ are deterministic, complex, speed-dependent Fourier coefficients. The order-domain counterpart is simply obtained by applying the variable change $t = t(\theta)$ followed by a Fourier transform with respect to θ, i.e.

$$D(\alpha) \stackrel{\text{def}}{=} \mathcal{F}_{\theta \to \alpha}\big\{d\big(t(\theta)\big)\big\} = \sum_{\lambda_i \in \Lambda} D^{\lambda_i}(\alpha - \lambda_i), \tag{6}$$

where α stands for *cyclic order* variable, a quantity without unit that counts the number of events occurring per rotation of the reference shaft (the *reference order* is 1), $\mathcal{F}_{\theta \to \alpha}\{*\} = \lim_{\Phi \to \infty} 1/\Phi \int_{-\Phi/2}^{+\Phi/2} \{*\}\, e^{j\alpha\theta} d\theta$ stands for the Fourier transform (Φ is an angular sector) , $D^{\lambda_i}(\alpha) = \mathcal{F}_{\theta \to \alpha}\big\{d^{\lambda_i}\big(\widetilde{\omega}(\theta)\big)\big\}$ is the Fourier transform of $d^{\lambda_i}\big(\widetilde{\omega}(\theta)\big)$ having an order-domain bandwidth $B_w^{\lambda_i}$ and $\widetilde{\omega}(\theta) = \omega\big(t(\theta)\big)$ is the speed profile in the angular domain. It is worth noting that $B_w^{\lambda_i}$ depends on (i) the variability of the coefficient $d^{\lambda_i}(\omega)$ with respect to the speed (i.e. higher partial derivatives of $d^{\lambda_i}(\omega)$ with respect to ω) and (ii) the variability of the speed profile itself (i.e. higher derivatives of $\widetilde{\omega}(\theta)$ with respect to θ). The more important these variabilities are, the wider the induced bandwidths are.

In a general way, these bandwidths are much narrower than the reference order (i.e. $B_w^{\lambda_i} \ll 1$) so that $D^{\lambda_i}(\alpha - \lambda_i)$ and $D^{\lambda_{i-1}}(\alpha - \lambda_{i-1})$ do not overlap over the α-axis for all $i = 1,2 \dots$. As a consequence, the order spectrum also seems discrete along the α-axis, yet undergoing an energy leakage of width $B_w^{\lambda_i}$ rather than being perfectly localized at the synchronous orders (i.e. $\lambda_i \in \Lambda$). In the particular case of constant speed the order spectrum is perfectly discrete as the bandwidths $B_w^{\lambda_i}$ tend to zero. The effect of the speed on the deterministic component is illustrated in Fig.1.

Cette thèse est accessible à l'adresse : http://theses.insa-lyon.fr/publication/2015ISAL0106/these.pdf
© [D. Abboud], [2015], INSA Lyon, tous droits réservés

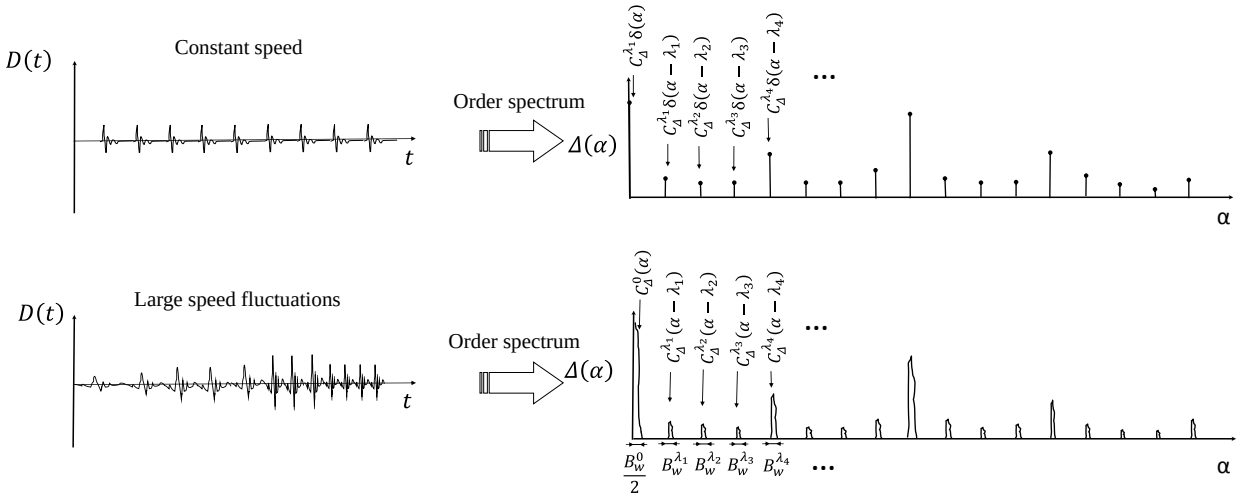

Fig.1. Academic example illustrating the effect of the speed on the deterministic component in rotating machine vibrations.

2.2.2 Modeling the cyclo-non-stationary part

In the last few years, the term "cyclo-non-stationary" has appeared in the field of rotating machine to describe the signals produced when the operating conditions are strongly NS. Similarly to CS signals, they can be produced by gears [Daher 2010] [Abboud 2014a] [Baudin 2014a][Baudin 2014b], REBs [D'Elia 2010][Abboud 2014b] [Abboud 2014c], internal combustion engines [Antoni 2013] and certainly others. A tentative definition of CNS signals was provided in [Abboud 2015a] through a Fourier series model with mutually nonstationary stochastic coefficients, $y^{\gamma_i}(t)$,

$$y(t) = \sum_{\gamma_i \in \Gamma_y} y^{\gamma_i}(t) e^{j\gamma_i \theta(t)} \tag{7}$$

where $\Gamma_y = \{\gamma_i \in \mathbb{R} / \ i = 1,2 \dots\}$ is the associated set of the cyclic orders. As admitted by the authors, the time functions entering this definition are not unique: as a consequence it comprises all nonstationary signals since modulations can either be coded by the complex exponentials or by their nonstationary coefficients. It is clear that some constraint must govern the nonstationarity of these coefficients. Inspired from the deterministic model provided in Ref. [Abboud 2015b] and reviewed in subsection 2.2.1, the nonstationarity of the coefficients will be modeled through an *explicit* dependence on the nonstationary speed profile. Precisely, a general model of CNS signal can be expressed by the following decomposition:

$$y(t) = \sum_{\gamma_i \in \Gamma_y} y^{\gamma_i}(t, \omega(t)) e^{\mathrm{j}\gamma_i \theta(t)}, \tag{8}$$

where $\mathrm{c}_Y^{\gamma}(t, \omega)$ are mutually stationary stochastic process whose joint probability density function is conditioned on ω i.e. $\mathrm{cov}_{y^{\gamma_1}, y^{\gamma_2}}(t_1, t_2 | \omega) = \sigma^2_{y^{\gamma_1}, y^{\gamma_2}}(t_1 - t_2, \omega)$. For a constant speed, the coefficients are stationary and Eq. (8) boils down to the well-known Fourier decomposition of CS processes [Antoni 2004]. Conversely, these coefficients become

Cette thèse est accessible à l'adresse : http://theses.insa-lyon.fr/publication/2015ISAL0106/these.pdf
© [D. Abboud], [2015], INSA Lyon, tous droits réservés

nonstationary when the speed varies. Loosely speaking, the long-term changes in the CNS signal are expressed by the *explicit* dependence of the Fourier coefficients on the speed, while hidden periodicities are still conserved in the form of periodic modulations carried by the complex exponentials. According to that, the CNS components emitted by the SOI and by the m[th] interfering source read:

$$\begin{cases} s(t) = \sum_{\gamma_i^{(s)} \in \Gamma_s} s^{\gamma_i^{(s)}}\big(t, \omega(t)\big) e^{j\gamma_i^{(s)}\theta(t)} \\ q_m(t) = \sum_{\gamma_i^{(m)} \in \Gamma_m} c_{q_m}^{\gamma_i^{(m)}}\big(t, \omega(t)\big) e^{j\gamma_i^{(m)}\theta(t)}, \end{cases} \tag{9}$$

where $\Gamma_s = \left\{\gamma_i^{(s)} \in \mathbb{R} / \; i = 1,2 \ldots\right\}$ and $\Gamma_m = \left\{\gamma_i^{(m)} \in \mathbb{R} / \; i = 1,2 \ldots\right\}$ stand for the set of the cyclic orders associated with the SOI and the m[th] source, respectively, and $s^{\gamma_i}(t, \omega)$ and $c_{q_m}^{\gamma_i}(t, \omega)$ are similar to the Fourier coefficients $c_Y^{\gamma}(t, \omega)$ encountered in Eq. (8).

2.2.3 Modeling the background noise

As previously pointed out, the background noise is a random contribution generated by other sources not accounted for in the model and assumed to be stationary for constant operating speed. Therefore, no periodic modulations associated with non-zero cyclic orders are expected in the model. Moreover, similarly to the CNS case, this contribution is likely to depend on the operating speed. Inspired by the CNS model introduced in subsection 2.2.1, a model of the background noise can be obtained by simply replacing the cyclic order set Γ in Eq. (8) with the singleton $\{0\}$, giving

$$b(t) = b^0(t, \omega(t)), \tag{10}$$

where $c_B^0(t, \omega))$ is a stationary stochastic process whose joint probability density function is conditioned on ω. Having modelled the deterministic contribution, the CNS contribution and the background noise, it remains to analytically investigate their contributions in the SES. The next subsection addresses this issue.

2.3 Interference of sources

The aim of this section is to analytically investigate the limitations of the SES technique in analyzing the CNS component emitted by an arbitrary SOI. Based on the model proposed in subsection 2.2, the contributions of the signal components in the SES are calculated and illustrated. Detailed calculations are provided in Appendix A. The SES is defined in the order domain as:

$$SES_x(\alpha) \stackrel{\text{def}}{=} \mathcal{F}_{\theta \to \alpha}\big\{SE_x\big(\mathrm{t}(\theta)\big)\big\}, \tag{11}$$

where $SE_x(\mathrm{t}) = \mathbb{E}\{|x(t)|^2\}$ stands for the squared envelope of $x(t)$ and the Fourier transform is to be taken in the sense of distributions. Assuming that the signal components are uncorrelated

Cette thèse est accessible à l'adresse : http://theses.insa-lyon.fr/publication/2015ISAL0106/these.pdf
© [D. Abboud], [2015], INSA Lyon, tous droits réservés

and according to Eq. (3), the SES of the vibration signal equals the sum of the SES of each component, i.e.

$$SES_x(\alpha) = SES_s(\alpha) + SES_n(\alpha). \tag{12}$$

The SES of the SOI takes the particular form

$$SES_s(\alpha) = \sum_{\gamma_i^{(s)} \in \Gamma_s} SES_s^{\gamma_i^{(s)}}\left(\alpha - \gamma_i^{(s)}\right), \tag{13}$$

where quantities $SES_s^{\gamma_i^{(s)}}$ have the same interpretation as the functions $D^{\lambda_i}(\alpha)$ encountered in Eq. (6). In other words, they evidence a discrete distribution at the synchronous orders with possible energy leakage. Nevertheless, they still provide a symptomatic and informative distribution of the cyclic content. Likewise, the SES of the noise equals the sum of the SES of its components, i.e.

$$SES_n(\alpha) = SES_d(\alpha) + \sum_{m=1}^{M} SES_{q_m}(\alpha) + SES_b(\alpha), \tag{14}$$

with

$$\begin{cases} SES_d(\alpha) = \sum_{\lambda_i \in \Lambda} SES_d^{\lambda_i}(\alpha - \lambda_i) \\ SES_{q_m}(\alpha) = \sum_{\gamma_i^{(m)} \in \Gamma_m} SES_{q_m}^{\gamma_i^{(m)}}\left(\alpha - \gamma_i^{(m)}\right) \\ SES_{\mathrm{b}}(\alpha) = SES_b^0(\alpha), \end{cases} \tag{15}$$

where $SES_d^{\lambda_i}(\alpha - \lambda)$, $SES_{q_m}^{\gamma_i^{(m)}}(\alpha - \gamma)$ and $SES_b^0(\alpha)$ again have the same interpretation as the functions $D^{\lambda_i}(\alpha)$ encountered in Eq. (6). It is obvious that the SES of a vibration signal is composed of numerous interfering sources in general. The contribution of the background noise does not have a significant impact in the SES as its corresponding distribution is localized in the vicinity of zero (see the third row in Eq. (15)). However, the presence of other components in the SES—either of deterministic (first component in Eq. (14)) or CNS nature (third component in Eq. (14)) — will certainly complicate the analysis of the SES of the SOI. This will compromise the efficiency of the SES technique in the general setting. An illustration of this effect is provided in Fig.2. Despite its presence in the SES of the random part, the contribution of the SOI component is hardly noticeable (see Fig.2 (a)): it is drowned among other CNS components from other sources. The problem is aggravated in the SES of the total vibration signal where the deterministic component also contributes to the SES (see Fig.2 (b)). These issues require the preprocessing of the signal before the application of the SES. The next section addresses this issue.

Cette thèse est accessible à l'adresse : http://theses.insa-lyon.fr/publication/2015ISAL0106/these.pdf
© [D. Abboud], [2015], INSA Lyon, tous droits réservés

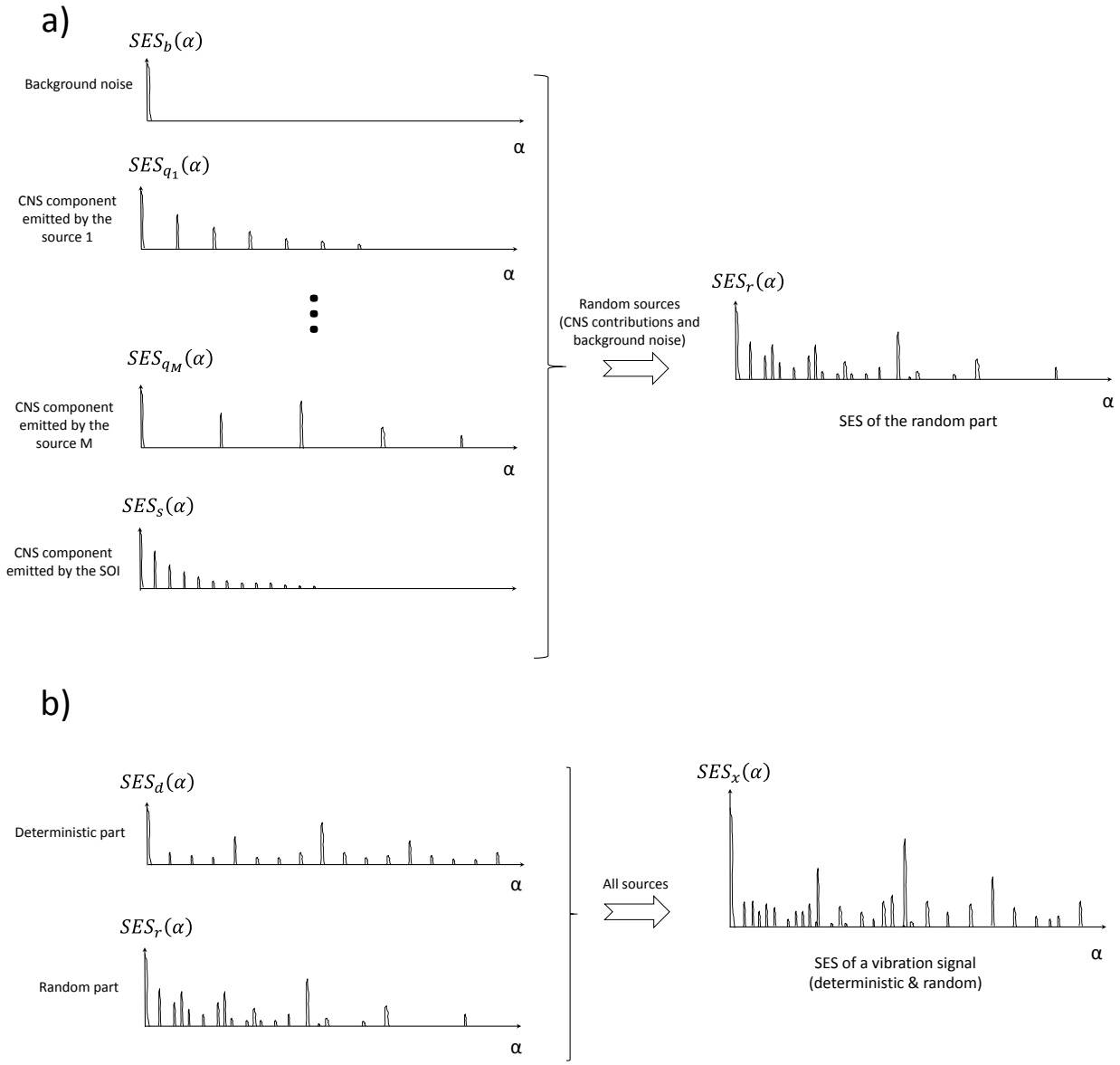

Fig.2. Academic example illustrating the interference of different sources in the SES of a vibration signal: (a) interference among random sources (CNS components and background noise) and (b) interference between deterministic and random sources.

3 ENVELOPE ENHANCEMENT STRATEGIES

A current practice in VSC is to apply the (order-domain) SES over the whole demodulation band of either the whitened [Borghesani 2013b] or the residual [Abboud 2015b] [Stander 2006] signal. Undoubtedly, the complete elimination of the deterministic component cleans the SES from its

Cette thèse est accessible à l'adresse : http://theses.insa-lyon.fr/publication/2015ISAL0106/these.pdf
© [D. Abboud], [2015], INSA Lyon, tous droits réservés

spurious contributions. For this purpose, subsection 3.1 addresses the elimination of the deterministic component in VSC through the comparison of three sophisticated techniques previously conceived for this purpose.

Removing the deterministic part is a crucial but not sufficient step to exhibit the SOI signature in the SES: the SOI signature may still be masked by other CNS components (see Fig.2 (b)) [Abboud 2015c]. For this purpose, subsection 3.2 revisits a general procedure to enhance the SOI component in the signal and, consequently, enhances its emergence in the SES.

3.1 Removing the deterministic part

As indicated in subsection 2.2.1, the deterministic component undergoes significant speed dependent changes that can jeopardize its (angle-) periodicity. This necessarily invalidates the working assumption of conventional deterministic\random separation techniques despite being applied in the angular domain. Lately, some sophisticated preprocessing techniques have been proposed to deal with this issue. This section reviews and compares three of them, namely, the ISA, the CPW and the GSA. Specifically, the fundamentals of these techniques are summarized and qualitative evaluations of their performances are given.

3.1.1 The improved synchronous average (ISA)

After inspecting the phase blur resulting from the transmission path effect, Stander and Heyns [Stander 2006] proposed an enhanced version of the SA— coined "phase domain averaging", being based on a phase domain representation. The basic idea is to order track the signal with respect to its own phase instead of that of the tachometer. The signal phase is obtained by Hilbert demodulation of a high-energy harmonic (such as a meshing order) of the angular signal. Cycles are then separately order tracked (for the second time) according to the estimated phase and then averaged together.

Later, a simpler variant was provided in Ref. [Coats 2009] — coined the "improved synchronous average" (ISA) — where the authors proposed to resample the signal with a *virtual tachometer* signal synthesized via the demodulated phase. Subsequently, the technique was used in Ref. [Borghesani 2013a] where the authors analytically tried to identify the optimal (order-domain) demodulation band and proposed it as a discrete-random separation technique in VSC. The ISA technique consists of the following steps:

1) Order track the temporal vibration signal using the tachometer signal.

2) Band-pass filter the angular signal around a high-energy harmonic (the energy leakage must be included in the filter bandwidth).

3) Compute the analytic signal.

4) Construct a second virtual tachometer signal based on the phase of the analytic signal.

5) Again, order track the angular signal using the virtual tachometer. The obtained signal is represented in the phase domain.

Cette thèse est accessible à l'adresse : http://theses.insa-lyon.fr/publication/2015ISAL0106/these.pdf
© [D. Abboud], [2015], INSA Lyon, tous droits réservés

6) Apply the SA to obtain the ISA.

The flowchart of the ISA is shown in Fig.3 (a).

In the following, the ISA is investigated on the deterministic model provided in Eq. (5). Let us restate the model after expanding its Fourier coefficients:

$$\tilde{d}(\theta) = d\big(t(\theta)\big) = \sum_{\lambda_i \in \Lambda} A_d^{\lambda_i}\big(\tilde{\omega}(\theta)\big)\mathrm{e}^{\mathrm{j}\left(\lambda_i\theta + \Psi_d^{\lambda_i}\left(\tilde{\omega}(\theta)\right)\right)}, \tag{16}$$

with $A_d^{\lambda_i}(\omega)e^{j\left(\Psi_d^{\lambda_i}(\omega)\right)} = d^{\lambda_i}(\omega)$. Let λ_m be the order of a high-energy harmonic (used for the phase demodulation), according to the first 3 steps of the ISA technique, the analytic signal of the filtered signal writes

$$\tilde{d}_f(\theta) = d^{\lambda_m}\big(\tilde{\omega}(\theta)\big)e^{j\lambda_m\theta} = A_d^{\lambda_m}\big(\tilde{\omega}(\theta)\big)e^{j\left(\lambda_m\theta + \Psi_d^{\lambda_m}\left(\tilde{\omega}(\theta)\right)\right)}, \tag{17}$$

The reference signal phase is then obtaining by dividing the demodulated phase, $\lambda_m\theta + \Psi_d^{\lambda_m}\big(\tilde{\omega}(\theta)\big)$, by the harmonic order, i.e.

$$\theta' = \theta + \frac{1}{\lambda_m}\Psi_d^{\lambda_m}\big(\tilde{\omega}(\theta)\big). \tag{18}$$

The second order tracking operation (step 5) is equivalent to represent the signal with respect to θ'. It can be shown that the phase blur of the signal can be completely compensated,

$$\tilde{d}'(\theta') = \sum_{\lambda_i \in \Lambda} A_d^{\lambda_i}\big(\tilde{\omega}'(\theta')\big)\mathrm{e}^{\mathrm{j}\lambda_i\theta'}, \tag{19}$$

where $\tilde{\omega}'(\theta')$ is the speed profile in the phase domain, only if

$$\lambda_i\Psi_d^{\lambda_m}(\omega) = \lambda_m\Psi_d^{\lambda_i}(\omega). \tag{20}$$

But, this equality implicitly assumes that the phase blurs associated with all the harmonics are linear between each other's. This assumption, however, is not always accurate; particularly when the spectral content of the harmonic coincides with a resonance. For instance, if one extracts the phase information from a meshing orders at a critical speed (i.e. in the vicinity of a structural mode); the latter is more subjected to phase blur than elsewhere [Borghesani 2013a] [Coats 2014]. As a consequence, only neighboring orders will be corrected when the speed variation is high, rather than distant ones. Note that, regardless of its capacity of correcting the signal phase, this technique ignores the long-term energy modulations in the signal. Therefore, the ISA cannot accommodate to the amplitude variations and returns an averaged result. Despite its relevance in some applications, the ISA may suffer from serious issues in large speed variations; the reason it will not be considered further. This claim is experimentally evidenced in sections 4 and 5 on simulated and real vibration signals, respectively.

Cette thèse est accessible à l'adresse : http://theses.insa-lyon.fr/publication/2015ISAL0106/these.pdf
© [D. Abboud], [2015], INSA Lyon, tous droits réservés

3.1.2 The cepstrum prewhitening (CPW)

With the aim to enhance fault detection in REBs, the authors of Refs. [Sawalhi 2011] [Randall 2011b] introduced a powerful prewhitening technique— called cepstrum prewhitening (CPW) — based on cepstral analysis. This technique enjoys a remarkable capability of blindly eliminating the deterministic content in the signal and of returning a pure random whitened signal. Recently, Borghesani et al. [Borghesani 2013b] have applied the technique in VSC after order tracking the signal. Precisely, the CPW technique consists of the following steps 1:

1) Order track the temporal signal $\tilde{y}(\theta) = y\big(t(\theta)\big)$.

2) Compute the Fourier transform,
$$Y(\alpha) = \mathcal{F}_{\theta\to\alpha}\{\tilde{y}(\theta)\} = A_Y(\alpha).\,\mathrm{e}^{\mathrm{j}\Psi_Y(\alpha)} \tag{21}$$
and save the phase $\Psi_Y(\alpha)$.

3) Compute the *real cepstrum* defined as:
$$y_{rc}(\theta) = \mathcal{F}^{-1}_{\alpha\to\theta}\{\log(|Y(\alpha)|)\} \tag{22}$$

4) Set to zero the real cepstrum except for the zero quefrency.
$$\begin{cases} y_w(\theta) = y_{rc}(\theta) \quad for\ \theta = 0 \\ y_w(\theta) = 0 \quad for\ \theta \neq 0 \end{cases} \tag{23}$$

5) Back to the order domain:
$$Y_w(\alpha) = \exp(\mathcal{F}_{\theta\to\alpha}\{\tilde{y}(\theta)\}) \tag{24}$$

6) Combine $Y_w(\alpha)$ with the original phase and back to the angle domain
$$y_{CPW}(\theta) = \mathcal{F}^{-1}_{\alpha\to\theta}\big\{Y_w(\alpha).\,\mathrm{e}^{\mathrm{j}\Psi_Y(\alpha)}\big\} \tag{25}$$

The flowchart of the CPW is shown in Fig.3 (b).

3.1.3 The generalized synchronous average (GSA)

The GSA has been proposed as an extension of the synchronous average traditionally applied in stationary regime to the case of nonstationary regime [Abboud 2015b]. Recognizing that the signal statistics are dependent on the operating speed the idea is to perform the averaging operation on cycles that belong to the same speed. Formally speaking, the GSA of a signal $y(\theta)$ with angular period Θ and operating under the speed profile $\omega(\theta)$ is defined as

$$m_y(\bar{\theta},\omega) = \lim_{\delta\omega\to 0} \lim_{card\{K_{\bar{\theta},\omega}\}\to\infty} \frac{1}{card\{K_{\bar{\theta},\omega}\}} \sum_{k\in K_{\bar{\theta},\omega}} y(\bar{\theta} + k\Theta) \tag{26}$$

Cette thèse est accessible à l'adresse : http://theses.insa-lyon.fr/publication/2015ISAL0106/these.pdf
© [D. Abboud], [2015], INSA Lyon, tous droits réservés

where $\delta\omega$ stands for the speed resolution and $K_{\bar{\theta},\omega} = \{k \in \mathbb{N} \big| \omega - \delta\omega/2 \leq \tilde{\omega}(\bar{\theta} + k\Theta) < \omega + \delta\omega/2\}$ stands for the set of samples located at $\bar{\theta}$ and coinciding with speed values in the interval $[\omega - \delta\omega/2\,; \omega + \delta\omega/2]$. Note that the GSA is in general a bivariable function of the angle and speed. The (synchronous) deterministic component associated with the profile $\omega(\theta)$ is returned by

$$m_y(\theta) = m_y\left(\bar{\theta} = \lfloor {}^{\theta}/_{\Theta} \rfloor, \omega = \tilde{\omega}(\theta)\right), \tag{27}$$

which is a function of θ only. The application of the GSA on the vibration model of subsection 2.2.1 returns,

$$m_x(\bar{\theta}, \omega) = \sum_{\lambda_i \in \Lambda} d^{\lambda_i}(\omega) e^{j\lambda_i \bar{\theta}}, \tag{28}$$

provided that $\Theta = 2\pi/\lambda_1$ and $\lambda_i = i.\lambda_1$ for all $i = 2,3 \ldots$ (see the proof in Appendix A). Interestingly, Eq. (27) perfectly returns the deterministic part:

$$m_X(\theta) = \sum_{\lambda_i \in \Lambda} d^{\lambda_i}\big(\tilde{\omega}(\theta)\big) e^{j\lambda_i \theta} = \mathrm{d}\big(\mathrm{t}(\theta)\big). \tag{29}$$

The practical implementation of the GSA can be made via the raw estimator (see Appendix B and Fig.3 (c)).

3.1.4 CPW or GSA?

Despite its simplicity and its remarkable ability to blindly eliminate the deterministic component, the CPW technique returns a whitened signal which does not constitute, in itself, the real residue. On the one hand, the whitened signal loses its absolute magnitude which may be detrimental to diagnostics. On the other hand, the whitening operation distorts the random part in which the CNS component related to the SOI (e.g. a REB fault) is embedded. Moreover, the whitening operation is made in the order domain wherein the dynamic information is effectively lost. This may result in uncontrolled amplification of low signal-to-ratio (SNR) bands, thus increasing the background noise in the SES. Interestingly, the GSA is able to systematically extract the deterministic component without affecting the CNS component. But, this technique has also some disadvantages. First, it needs (relatively) lengthy signals as (i) the speed resolution $\delta\omega$ should be chosen small enough to decrease the estimator bias and (ii) the number of averages should be sufficiently high to decrease the estimator variance. Note that the variance is inversely proportional to the power of the random part [Abboud 2015b]. Second, it is more complex than the CPW as it requires more operations as well as the choice of adequate parameter settings. Third, separate operations of different angular sampling may be needed for multiple families of harmonics. Fourth and last, each of these families should have a *commensurate* and *known* angular period. In other words, the GSA is unable to remove modulation sidebands if their angular period is incommensurate with the carrier period. Such configurations, for instance, are frequently met in planetary gearboxes [Inalpolat 2009]. To conclude, the preference between the CPW and the GSA is generally dependent on the nature of the application, recognizing that the former is likely to cover much more configurations than the latter.

Cette thèse est accessible à l'adresse : http://theses.insa-lyon.fr/publication/2015ISAL0106/these.pdf
© [D. Abboud], [2015], INSA Lyon, tous droits réservés

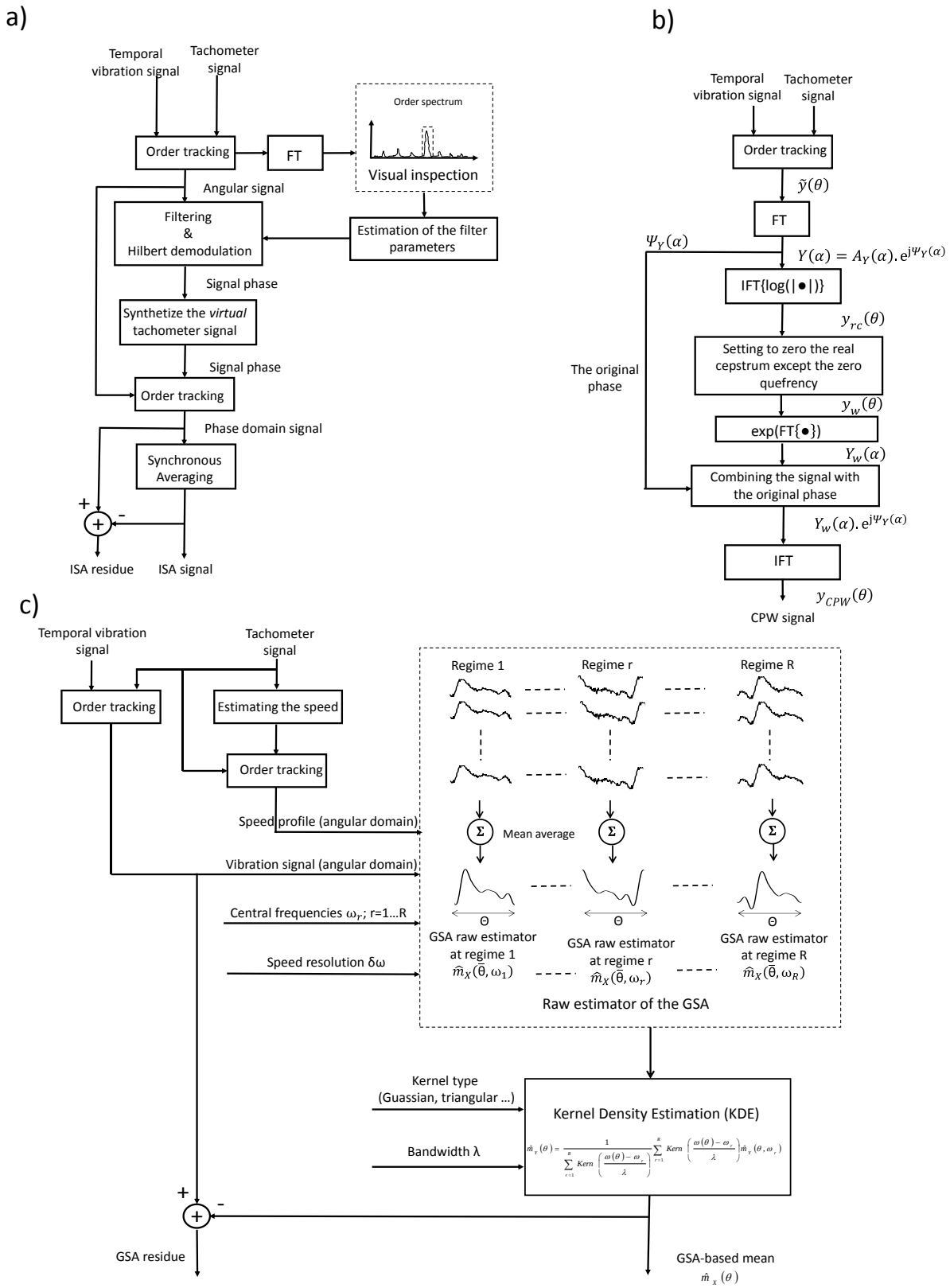

Fig.3. Flowchart of (a) the ISA, (b) the CPW and (c) the GSA.

Cette thèse est accessible à l'adresse : http://theses.insa-lyon.fr/publication/2015ISAL0106/these.pdf
© [D. Abboud], [2015], INSA Lyon, tous droits réservés

3.2 Enhancing the source of interest

In this paragraph, a general envelope enhancement methodology which combines a time-domain filtering operation with either the GSA or the CPW techniques is revised and adjusted.

3.2.1 Time-filtering operation

According to Eq.(8), each CNS component is characterized by (i) its cyclic order set which reflects the kinematic of the excitation mechanism associated with the corresponding source and (ii) the spectral content of its carrier which jointly depends on the spectral content of the excitation and on the dynamical properties of the transfer function from the source to the accelerometer. Since the final goal is to detect the signature of the SOI in the envelope, the former can be enhanced by means of some temporal band-pass filter $f(t)$. Back to the signal\noise decomposition in Eq. (3), the filtered signal reads

$$\tilde{x}(t) = \big(s(t) + \mathrm{n}(t)\big) \otimes f(t) = \tilde{s}(t) + \tilde{n}(t), \tag{30}$$

where $\otimes$ denotes the convolution product, $f(t)$ denotes the band-pass filter, $\tilde{s}(t)$ and $\tilde{n}(t)$ provide respectively an image of the signal of interest and the noise. Ideally, the filter should be conceived to maximize the SNR, i.e.

$$\underset{f(t)}{\operatorname{argmax}} \left\{ \lim_{T\to\infty} \frac{\frac{1}{T}\int_{-T/2}^{+T/2} |\tilde{s}(t)|^2 dt}{\frac{1}{T}\int_{-T/2}^{+T/2} |\tilde{n}(t)|^2 dt} \right\}. \tag{31}$$

Optimally, the energy of $\tilde{n}(t)$ would become negligible as compared to that of $\tilde{s}(t)$. In this case, the resulting SES

$$\mathrm{SES}_{\tilde{x}}(\alpha) \approx \mathrm{SES}_{\tilde{s}}(\alpha) = \sum_{\gamma_i^{(s)} \in \Gamma_s} SES_{\tilde{s}}^{\gamma_i^{(s)}} \left(\alpha - \gamma_i^{(s)}\right), \tag{32}$$

has a symptomatic discrete distribution *strictly* at the cyclic orders associated with the SOI.

3.2.2 Choice of the filter parameters

As indicated in the last subsection, the filtering operation should be performed around a high-SNR frequency band. In practice, it often happens that the SNR is high around resonance bands. Therefore, a traditional solution is to perform a *modal analysis*[1] step to explore the dynamical properties of the system [Cocconcelli 2013]. In general, modal analysis is either based on *structural testing* (e.g. "hammer impact test" [Harris 2001]) or *finite element analysis*-based simulation [Neville 2008]. The former technique (structural testing) requires a disassembly of the machine to reach the potential excitation point, whereas the latter one (finite element analysis simulation) requires a complex modelling of the system. These practical difficulties have limited the application of such techniques.

[1]to estimate the transfer function properties of the transmission path from the SOI to the acceleration.

Cette thèse est accessible à l'adresse : http://theses.insa-lyon.fr/publication/2015ISAL0106/these.pdf
© [D. Abboud], [2015], INSA Lyon, tous droits réservés

There are other *blind approaches* based on statistical signal processing which consist of finding the band that maximizes a criterion, e.g. impulsivity (e.g. kurtogram) [Antoni 2006] [Antoni 2007c] [Barszcz 2011] or cyclostationarity (e.g. spectral coherence) [Antoni 2007b]. However, these approaches rely on the assumption of constant operating speed, thus their applicability is jeopardized in VSC. The recent advances in the CS theory [Antoni 2014] have made now possible to exploit more sophisticated techniques that can adapt with the operating speed variability. In particular, the angle\time cyclostationary (AT-CS) theory has allowed the extension of the spectral coherence, to the so-called "order frequency spectral coherence" [Abboud 2015a]. The squared magnitude of the latter, when evaluated at the cyclic orders of a CNS signal, can be seen as a measure (normalized between 0 and 1) of the signal-to-noise ratio along the spectral frequency band.

3.2.3 An envelope enhancement methodology

A trivial methodology to enhance a cyclo-non-stationary SOI in a raw signal is to remove first the deterministic component and then filter the obtained signal in the time domain around a high-SNR band. This methodology consists of the following steps:

1) Remove the deterministic component using the CPW or GSA in the angular domain.
2) Order track the signal (go to the temporal domain).
3) Band-pass filter the signal around a high-SNR frequency band.
4) Order track the signal (go again to the angular domain).
5) Compute the SES.

Note that a similar procedure was proposed in [Borghesani 2013c], yet the synchronous average was used instead of the GSA.

4 NUMERICAL EVALUATION

This section validates the theoretical analysis, the different envelope enhancement approaches and the qualitative comparisons on simulated gear and bearing vibration signals. First, the corresponding models are given and their contributions in the SES are investigated. Second, a comparison between the ISA, the CPW and the GSA is provided. Third, the envelope enhancement methodology provided in 3.2.3 is applied to enhance and separate the CNS sources.

4.1 Vibration signal model in variable speed conditions

The aim of this subsection is to simulate a vibration signal of a typical powertrain constituted by a parallel gearbox and a faulty REB. The input wheel comprises $Z_1 = 56$ teeth and the output wheel $Z_2 = 60$ teeth. The former has a local defect in one of its teeth, whereas the latter is subjected to a distributed wear fault. The REB is located at the input shaft—the reference shaft—and contains an outer-race local fault with a characteristic ball-pass-order on the outer-race (BPOO) at 2.1 orders—i.e. 2.1 times the reference rotation speed. The deterministic component

Cette thèse est accessible à l'adresse : http://theses.insa-lyon.fr/publication/2015ISAL0106/these.pdf
© [D. Abboud], [2015], INSA Lyon, tous droits réservés

in the signal is principally induced by the meshing force and the local fault in the input wheel. It appears in the *order spectrum* as (widened) peaks at the orders $m.Z_1 + n$ with $m \in \mathbb{Z}, n \in \mathbb{Z}^*$. The CNS component is induced by the output gear and the input REB. The energy of the output gear contribution is principally concentrated in a resonance band centered at 4 kHz with bandwidth of 300Hz; it is expected to be discretely distributed in the SES at the output shaft order— which equals 56/60=0.933—and its harmonics. The energy of the input gear contribution is principally concentrated in a resonance band centered at 2 kHz with bandwidth of 400 Hz; it is expected to be discretely distributed in the SES at the BPOO and its harmonics. A white noise modulated by a speed-dependent increasing function is also added to the signal to model the background noise. The principal characteristics of the simulated signal are gathered in Table 1, while detailed equations of the model are provided in Appendix C.

Table 1. Characteristics of the simulated signal ($\boldsymbol{f_{res}}$: resonance frequency; $\boldsymbol{f_b}$: Bandwidth).

	Deterministic gear component	Random gear component	REB (local fault)	Background noise
Resonances	$\begin{cases} f_{res} = 3kHz \\ f_b = 2kHz \end{cases}$	$\begin{cases} f_{res} = 4kHz \\ f_b = 300Hz \end{cases}$	$\begin{cases} f_{res} = 2kHz \\ f_b = 400Hz \end{cases}$	X
Fundamental order	1	56/60=0.933	2.1	X
Energy (%)	40%	20%	15%	25%

The reference speed varies according to a raised-cosine function between 5 Hz to 15 Hz over a record duration of 20s— equivalent to 198 cycles executed by the reference (which is the input shaft associated with order 1); the corresponding profile is displayed in Fig.4 (a). The spectrograms of the different contributions are displayed in Fig.4 (b) to (f). For the REB signal (Fig.4 (b)), an energy increase is perceived at 2 kHz which corresponds to the passage on the resonance frequency. For the deterministic gear signal (Fig.4 (c)), the meshing harmonics appear as multiple curves homothetic with the speed profile, while the amplitude of the modulation induced by the local fault remains relatively small. The random gear signal (Fig.4 (d)) shows a continuous increase around the resonance frequency located at 4 kHz. The energy of the background noise (Fig.4 (f)) is uniformly distributed along the frequency axis. Last, the spectrogram of the resulting vibration signal (Fig.4 (f)) is dominated by the deterministic gear component as it constitutes 40% of the signal energy. Note that the energy distribution is intensified in the middle of the record since the speed-dependent amplitude modulation is maximal at this point.

Eventually, the SES is applied on different components of the signal and the obtained results are reported in Fig.5. The SES of the REB component shows some peaks at the BPOO and its harmonics (see Fig.5 (a)). The SES of the deterministic gear component shows peaks at the reference order and its harmonics (see Fig.5 (b)), while the random gear component shows peaks at the output wheel order (0.933) and its harmonics (see Fig.5 (c)). The SES of the noise does not show any non-zero peak (see Fig.5 (d)). The SES of the random part—constituted of the REB component, the random gear component and the background noise— is obviously equivalent to

Cette thèse est accessible à l'adresse : http://theses.insa-lyon.fr/publication/2015ISAL0106/these.pdf
© [D. Abboud], [2015], INSA Lyon, tous droits réservés

the superposition of all individual SES since the signal components are assumed uncorrelated (see Fig.5 (e)). In this case, the bearing fault component interferes with the random gear contribution. The problem is aggravated in the SES of the vibration signal as the deterministic component also contributes to the SES (see Fig.5 (f)). These preliminary results confirm the theoretical analysis of section 2.

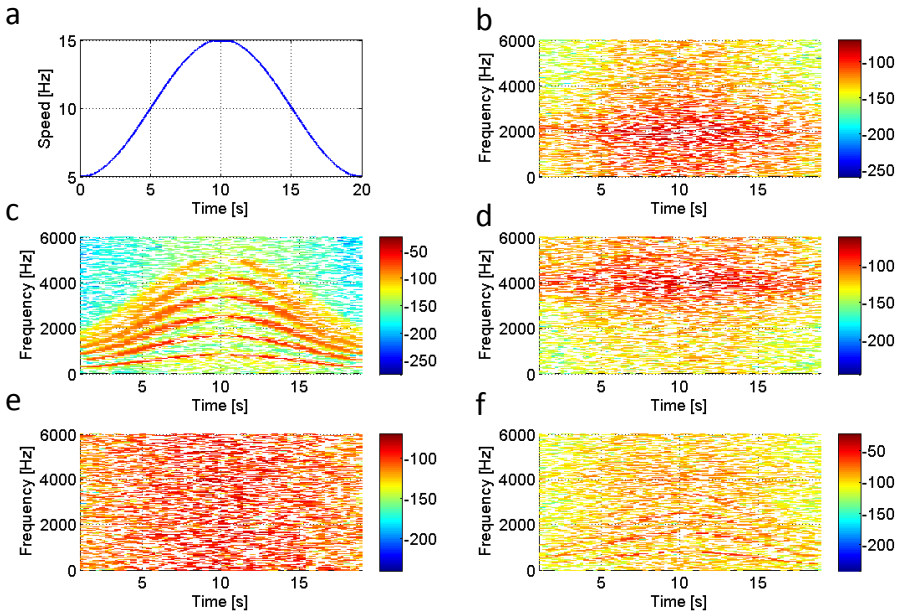

Fig.4. (a) Speed profile of the reference. Spectrograms of (b) the REB signal, (c) the deterministic gear signal, (d) the random gear signal, (e) the background noise and (f) the complete vibration signal.

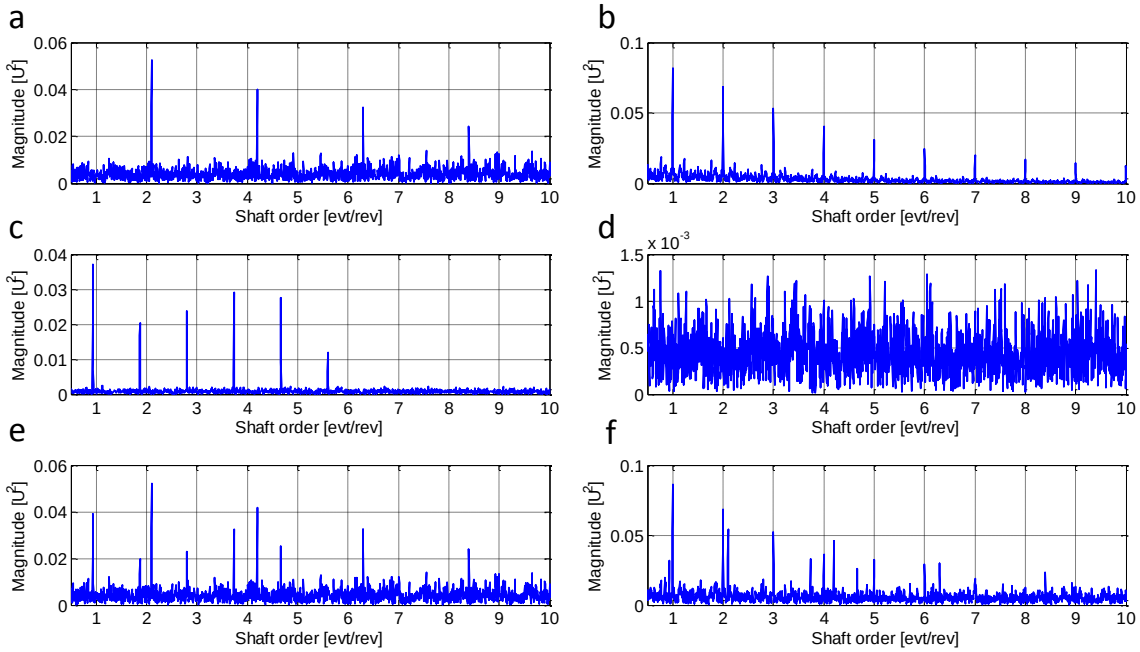

Fig.5. SES of (a) the REB signal, (b) the deterministic gear signal, (c) the random gear signal, (d) the background noise, (e) the random part and (f) the complete vibration signal.

Cette thèse est accessible à l'adresse : http://theses.insa-lyon.fr/publication/2015ISAL0106/these.pdf
© [D. Abboud], [2015], INSA Lyon, tous droits réservés

4.2 Removing the deterministic part

The goal of this subsection is to investigate the performance of the ISA, the GSA and the CPW in removing the deterministic component. In the following, the ISA is applied on the signals with a reference period equal to 2π (i.e. equivalent to the input gear order). The first meshing harmonic—located at the order 56— is used for demodulation and the filter bandwidth is visually estimated according to the existing energy leakage (the filter bandwidth is taken equal to 0.2 order). The demodulated harmonic and the equivalent order fluctuations with which the phase corrections are performed are displayed in Fig.6 (a) and (b), respectively. Next, the GSA is performed on acceleration signals to eliminate the gear component. Evidently, the reference period used in the average is also chosen equal to the input gear rotation. The speed profile is discretized with concatenated intervals of speed resolution equal to 0.4 Hz with 50% overlap. The order spectra of the resampled signal, the ISA residue and the GSA residue are displayed in Fig.6 (c) and (d). The ISA suppresses a part of the deterministic gear component energy, whereas the GSA evidences almost total suppression. Afterwards, the CPW is applied on the original signal. The SES of the original signal, the ISA residue, the GSA residue and the CPW signal are computed for both profiles and reported in Fig.7. As expected, the SES of the raw signal evidences several misleading harmonics of deterministic origin at the integer orders (see Fig.7 (a)), whereas slight enhancement is perceived after removing the ISA (see Fig.7 (b)): the amplitudes of these harmonics are attenuated but still exceeds those of the CNS components. Noticeably, the SES of the GSA residue (see Fig.7 (c)) and the CPW signal (see Fig.7 (d)) witness a complete absence of these components, yet the absolute value of the latter is totally lost. Moreover, by comparing the obtained SE spectra (see Fig.7 (c) and (d)) to the SES of the random part (see Fig.5 (e)), a significant distortion in the random part is seen in the CPW case caused by the whitening operation. In particular, the first REB fault harmonic (at the order 2.1) was the largest in the SES of the random part, while that of the output gear wear (at the order 0.933) becomes the largest in the CPW case.

Cette thèse est accessible à l'adresse : http://theses.insa-lyon.fr/publication/2015ISAL0106/these.pdf
© [D. Abboud], [2015], INSA Lyon, tous droits réservés

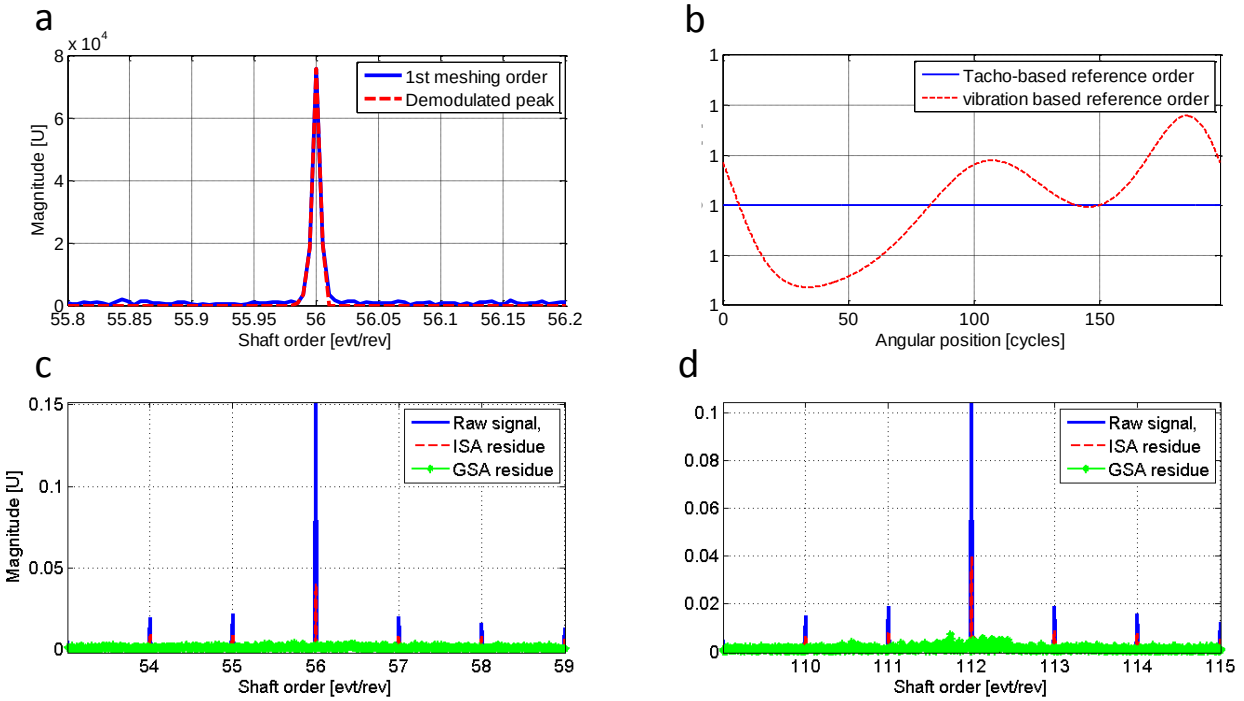

Fig.6. (a) The harmonic used for demodulation and (b) the equivalent order fluctuations used for phase correction. Comparison of the (amplitude) order spectra of the resampled signal, the ISA residue and the GSA residue: close-ups around (a) the fundamental and (b) the second meshing harmonics.

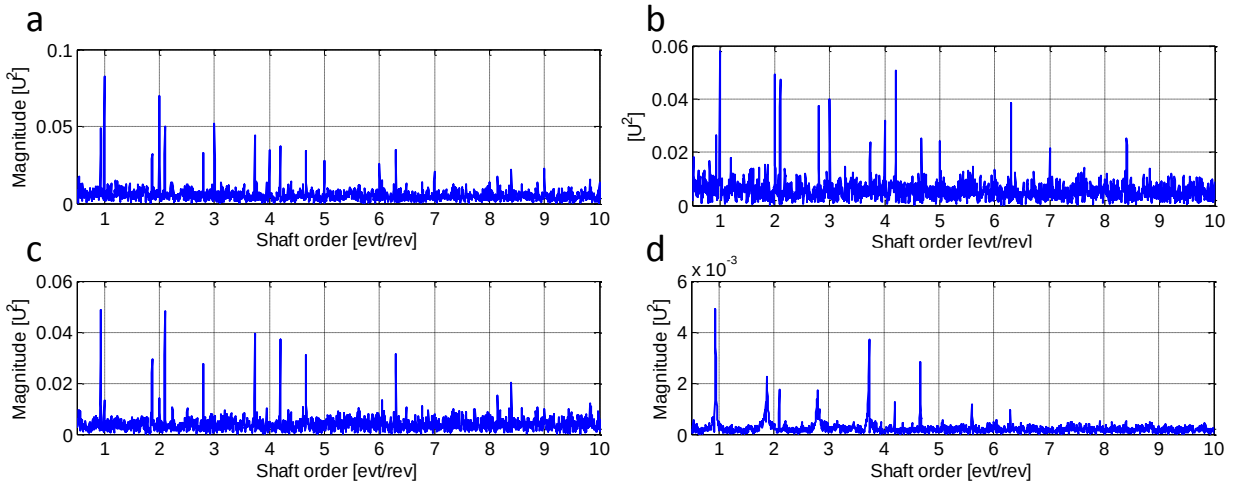

Fig.7. SES of (a) the original signal, (b) the ISA residue, (c) the GSA residue and (d) the CPW signal.

4.3 Separating CNS components

Despite their ability to reduce deterministic interferences, the GSA and the CPW were not able to clearly reveal the fault signature of neither the REB nor the output gear. Assuming a prior knowledge of the excited resonances, the methodology proposed in subsection 3.2.3 is applied to the signal to separating these two contributions. For the REB case, the central frequency of the filter is chosen equal to the corresponding resonance frequency (i.e. 2 kHz), while the filter bandwidth is set to 600 Hz. The obtained SE spectra are displayed in Fig.8 (a) and (b),

Cette thèse est accessible à l'adresse : http://theses.insa-lyon.fr/publication/2015ISAL0106/these.pdf
© [D. Abboud], [2015], INSA Lyon, tous droits réservés

respectively referring to GSA-based and CPW based strategies. Interestingly, the REB contribution is successfully enhanced and its signature becomes much clearer in the SES: the remaining peaks are strictly located at the BPOO and its harmonics. A bandpass filter was also applied to enhance the output gear contribution, with central frequency chosen equal to the corresponding resonance frequency (i.e. 4 kHz) and bandwidth set to 600 Hz. The obtained SE spectra are displayed in Fig.8 (c) and (d), respectively referring to a GSA-based and CPW-based strategies. The output gear contribution is successfully enhanced and its signature becomes much clearer in the SES: the remaining peaks are strictly located at the output gear order and its harmonics. It is worth noting that the filtering operation decreases the distortion of the cyclic components. This is due to the fact that the SNR is almost constant over the filtered band, so that the distortion affects the energy of the entire cyclic content. As a consequence, all the corresponding peaks in the SES will be attenuated uniformly. Evidently, the distortion in the signature is expected to be lower for narrow band filters.

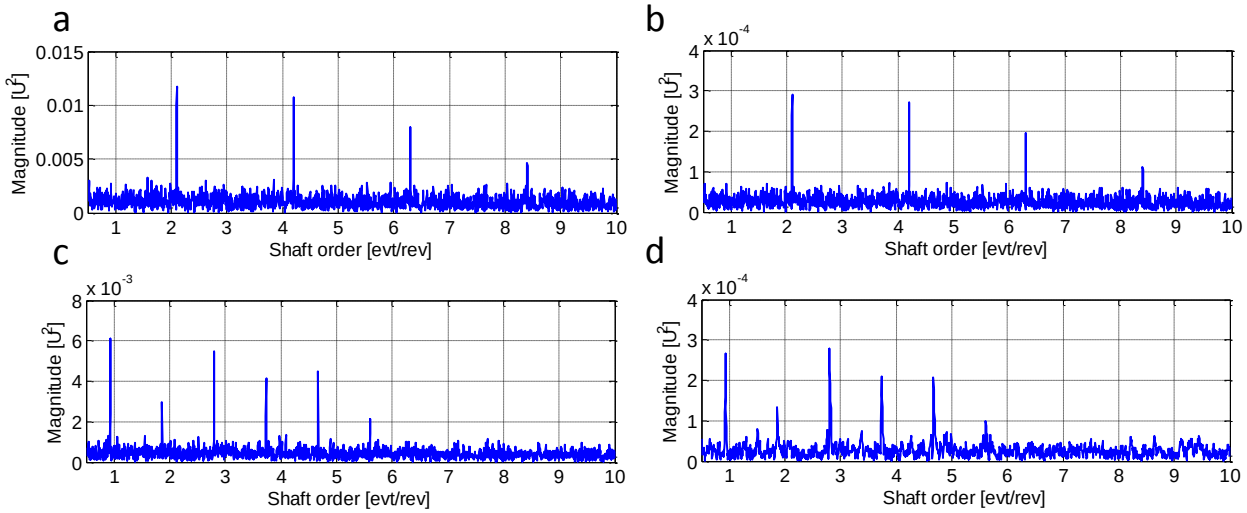

Fig.8. Envelope enhancement procedure applied on the simulated signal with filter parameter $\mathbf{f_c = 2\ kHz}$ and $\mathbf{Bw = 600\ Hz}$: (a) GSA-based strategy and (b) CPW-based strategy; filter parameters$\mathbf{f_c = 4\ kHz}$ and $\mathbf{Bw = 600\ Hz}$: (c) GSA-based strategy and (d) CPW-based strategy..

5 EXPERIMENTAL EVALUATION

The principal object of this section is to experimentally validate the theoretical analysis and qualitative comparisons on real-world gear and REB vibration signals. It reports a typical situation in the field of rotating machine diagnostics, where deterministic and random gear related components contribute to the SES and mask the REB fault signature— originally random.

5.1 Test rig and experiments

The test rig under study is located at Cetim[2] and depicted in Fig.9. It essentially comprises an asynchronous motor supplied by a variable-speed drive to control the motor speed, followed by a spur gear with 18 teeth and ratio of 1. Gears are subjected to excessive wear. This returns an

[2] Technical Center for Mechanical Industries – Senlis, France.

Cette thèse est accessible à l'adresse : http://theses.insa-lyon.fr/publication/2015ISAL0106/these.pdf
© [D. Abboud], [2015], INSA Lyon, tous droits réservés

expected meshing signature at 18 order— i.e. 18 times the rotation speed— with potential sidebands spaced by 1 order. Two identical REBs are installed behind the spur gear; the healthy one is closer to the gears than the faulty one which is coupled to an alternator by means of a belt to impose a constant load. The characteristics of the REBs are as follows: ball diameter = 6 mm, pitch diameter = 25 mm, number of elements = 8. This returns an expected ball-pass-order on the outer-race (BPOO) at 3.04 orders. An optical keyphasor of type "Brawn" is fixed close to the motor output to measure the rotational shaft position. In addition, two accelerometers, hereafter denoted as "Acc1" and "Acc2", are located on the healthy and faulty REBs in the vertical direction to measure the produced vibrations. The sampling rate is set to 25.6 kHz. Two experimental tests are conducted. In the first one, a runup from 903 to 1428 rpm (see Fig.10 (a)) is imposed to the electric motor during 15s— equivalent to 285 cycles executed by the machine. The acquired signals are illustrated in Fig.10 (b) and (c) referring to Acc1 and Acc2, respectively. In the second experiment, a random speed profile ranging between 704 to 2514rpm (see Fig.10 (d)) is imposed to the electric motor during 15s— equivalent to 392 cycles executed by the machine. The acquired signals are illustrated in Fig.10 (e) and (f) referring to Acc1 and Acc2, respectively.

The AT-CS analysis of this bench has been performed in a previous contribution [Abboud 2015a] in the case of stationary and nonstationary operating condition. Valuable information regarding the high-SNR spectral band of the CNS components emitted by the faulty REB and the gear wear were returned by the order-frequency spectral coherence. These information are summarized in Table 2 and will be subsequently used to test the envelope enhancement methodology in subsections 5.2.2 and 5.3.2.

Table 2. Principal high-SNR bands of the CNS vibration signals emitted by the faulty REB and the gear, and measured by Acc1 and Acc2. These information are based on the AT-CS analysis performed in Ref. [Abboud 2015a].

	Acc1	Acc2
High-SNR bands (faulty REB)	[1.5 kHz; 2.5 kHz]	[1.5 kHz; 2.5 kHz] and [6 kHz; 8 kHz]
High-SNR bands (gear wear)	[8 kHz; 11 kHz]	[8 kHz; 11 kHz]

Cette thèse est accessible à l'adresse : http://theses.insa-lyon.fr/publication/2015ISAL0106/these.pdf
© [D. Abboud], [2015], INSA Lyon, tous droits réservés

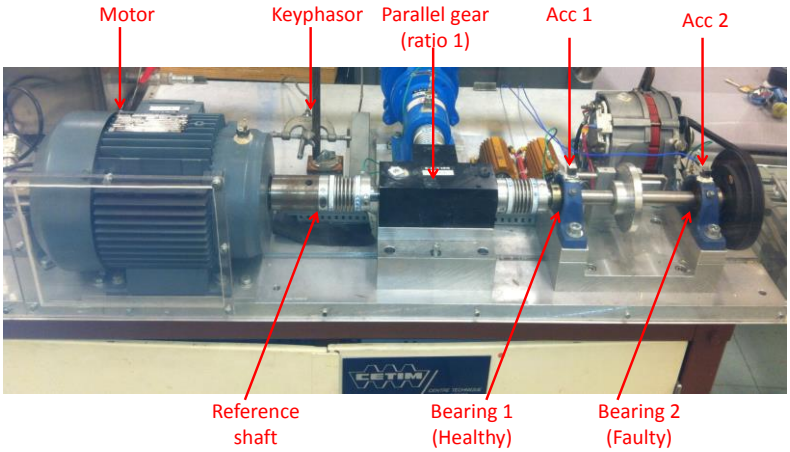

Fig.9. The test bench located at Cetim (Senlis, France).

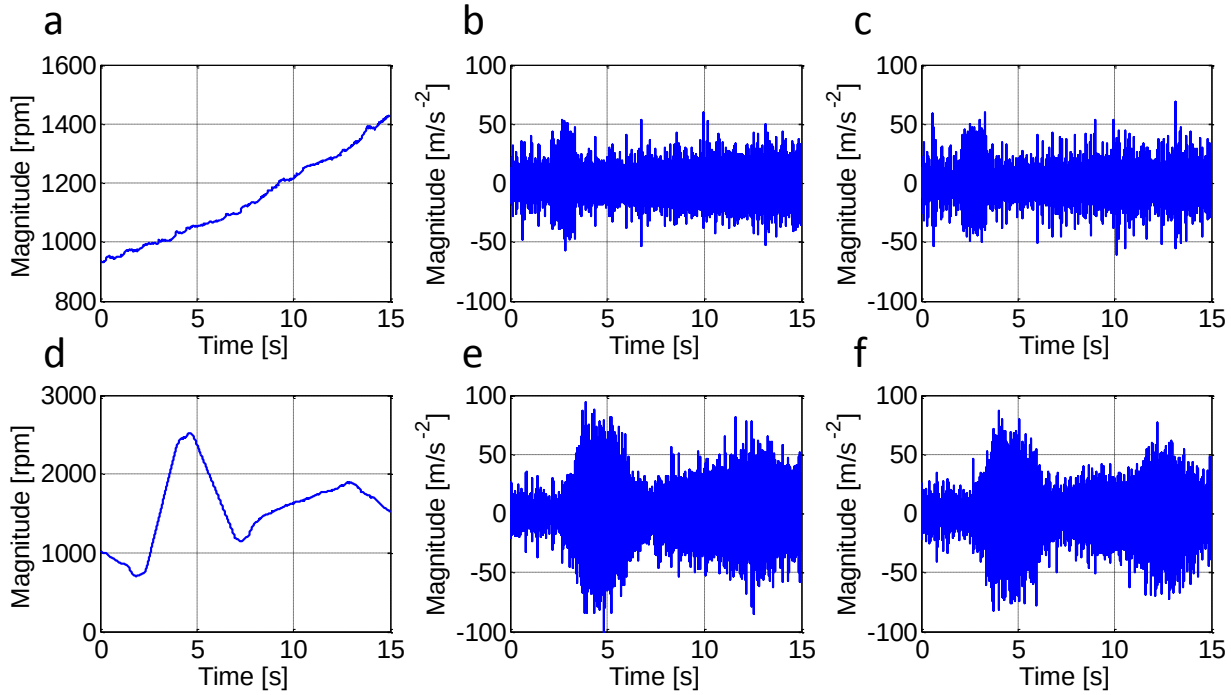

Fig.10. Experiment 1: (a) runup profile, (b) Acc1 signal and (c) Acc2 signal. Experiment 2: (d) random speed-varying profile, (e) Acc1 signal and (f) Acc2 signal.

5.2 Case study 1: the REB component dominates the random part

This paragraph treats the case where the accelerometer is mounted on the faulty REB (Acc2) and its component dominates the random part. At first, this case is exploited to compare the ISA, the CPW and the GSA for the two profiles according to their capability to improve the SES. Last, the REB component will be enhanced by the envelope enhancement methodology to return a clear presentation of its signature in the SES.

5.2.1 Removing the deterministic gear contribution

Cette thèse est accessible à l'adresse : http://theses.insa-lyon.fr/publication/2015ISAL0106/these.pdf
© [D. Abboud], [2015], INSA Lyon, tous droits réservés

This subsection compares the effectiveness of the ISA, the CPW and the GSA in removing the deterministic gear component and in enhancing the SES.

First, the ISA is applied on Acc2 signals of both experiments. Since the gears have a unit ratio, the reference period to be used for the average in the ISA is chosen equal to the gear rotation, which makes possible to account for gear modulations. The order spectra were visually inspected to choose the higher meshing harmonic for demodulation and to estimate the filtering bandwidth according to the existing energy leakage. The demodulated harmonics and the equivalent order fluctuations (see in Eq. (18)) with which the phase corrections are performed are displayed in Fig.11. Contrary to the random speed-varying case, the second meshing order is more energetic than the first one in the runup case and thus was chosen for demodulation. Note that the filter bandwidth is chosen larger in the random speed-varying (0.1 order) case than that in the runup case (0.02 order). This is explained by the fact that the high variability of the speed in the latter increases the energy leakage at the synchronous order and, thus, a wider filter is needed to filter out the component. This confirms the theoretical analysis performed in subsection 2.2.1.

Next, the GSA is performed on acceleration signals to eliminate the gear component. The reference period used for the average in the GSA is also chosen equal to the gear rotation. The speed profile is discretized with concatenated intervals of speed width equal to 30 rpm with 50% overlap. The order spectra of the resampled signal, the ISA residue and the GSA residue are displayed in Fig.12. The ISA eliminates a part of the gear contribution energy in the runup case, yet it completely fails in the random speed-varying case as the corresponding residues still contain high energy components around the synchronous orders. Note that, in the latter case, the enhancement was principally perceived at the demodulated peak (i.e. 1st meshing order—see Fig.12 (d)). This is believed to be due to the fact that, unlike the random speed-varying case, the runup profile varies in a low-speed operating margin that does not include structural resonances. The failure is principally induced by (i) the passage of the gear component in structural resonance bands and (ii) the ignorance of long-term energy modulations. Evidently, these effects are magnified in the random speed-varying case since the speed varying margin is higher and, consequently, the induced modulations are greater. On the contrary, the GSA successfully eliminates the gear component in both cases, ensuring an excellent performance even under large and random speed variations.

Finally, the CPW is applied on the acceleration signals of both profiles. The SES of the resampled (raw) signal, the ISA residue, the GSA residue and the CPW signal are computed for both profiles and displayed in Fig.13. As expected, the SES of the raw signal evidences several misleading harmonics synchronous with the reference shaft order (see Fig.13 (a) and (e)), whereas slight enhancements are perceived after removing the ISA (see Fig.13 (b) and (f)). With the exception of the first two harmonics, the CPW significantly attenuates the gear related peaks (see Fig.13 (a) and (e)), yet presenting three disadvantages. The first one is related to the increase of the noise level owing to the amplification of low signal-to-ratio spectral bands. The second one is the distortion of the REB contribution. Precisely, an attenuation of the BPOO peak relative to the second gear harmonic (to be compared with that of the GSA) is noticeable in the runup case, while a complete disappearance of the second REB fault harmonic (note the disappearance of the order 6.08 in Fig.13 (h)) is observed in the random speed-varying case. Seemingly, the CPW technique loses its efficiency as the speed variability increases. The third disadvantage is the total loss of the absolute value of the fault peaks. Noticeably, the SES of the GSA residue

Cette thèse est accessible à l'adresse : http://theses.insa-lyon.fr/publication/2015ISAL0106/these.pdf
© [D. Abboud], [2015], INSA Lyon, tous droits réservés

evidences much better the REB signature (see Fig.13 (c) and (g)), preserving the magnitude of the fault harmonics.

Note that some peaks at the gear rotation order and harmonics remain in the SES. These components are random in nature and generated by gear wear [Abboud 2015a], as opposed to the traditional deterministic nature of gear vibrations (e.g. meshing, a crack or spall fault…) [Antoni 2004].

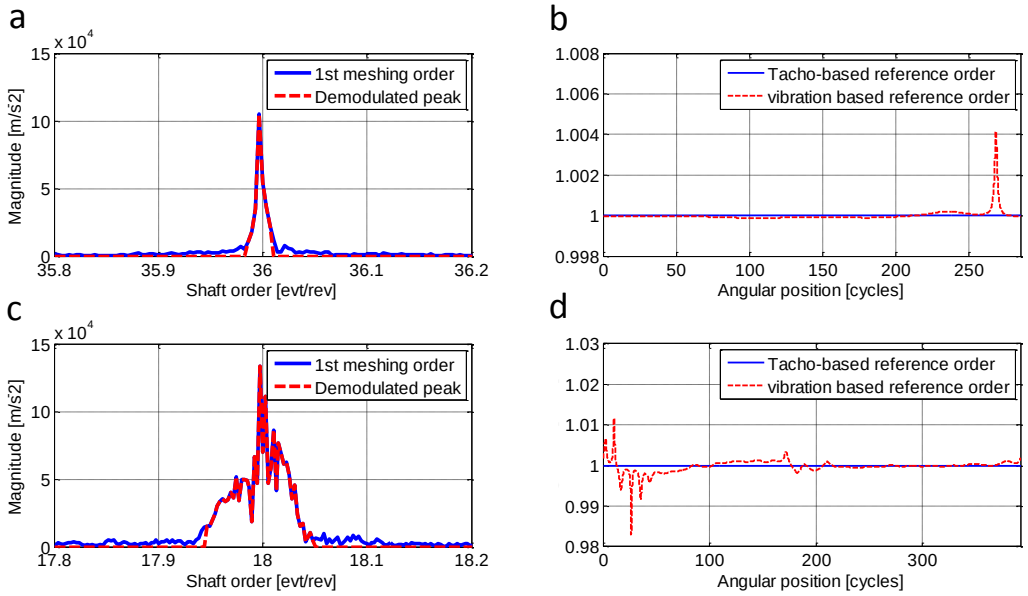

Fig.11. Runup case (Acc2 signal): (a) the harmonic used for demodulation and (b) the equivalent order fluctuations used for phase correction. Random speed-varying case: (c) the harmonic used for demodulation and (d) the equivalent order fluctuations used for phase correction.

Cette thèse est accessible à l'adresse : http://theses.insa-lyon.fr/publication/2015ISAL0106/these.pdf
© [D. Abboud], [2015], INSA Lyon, tous droits réservés

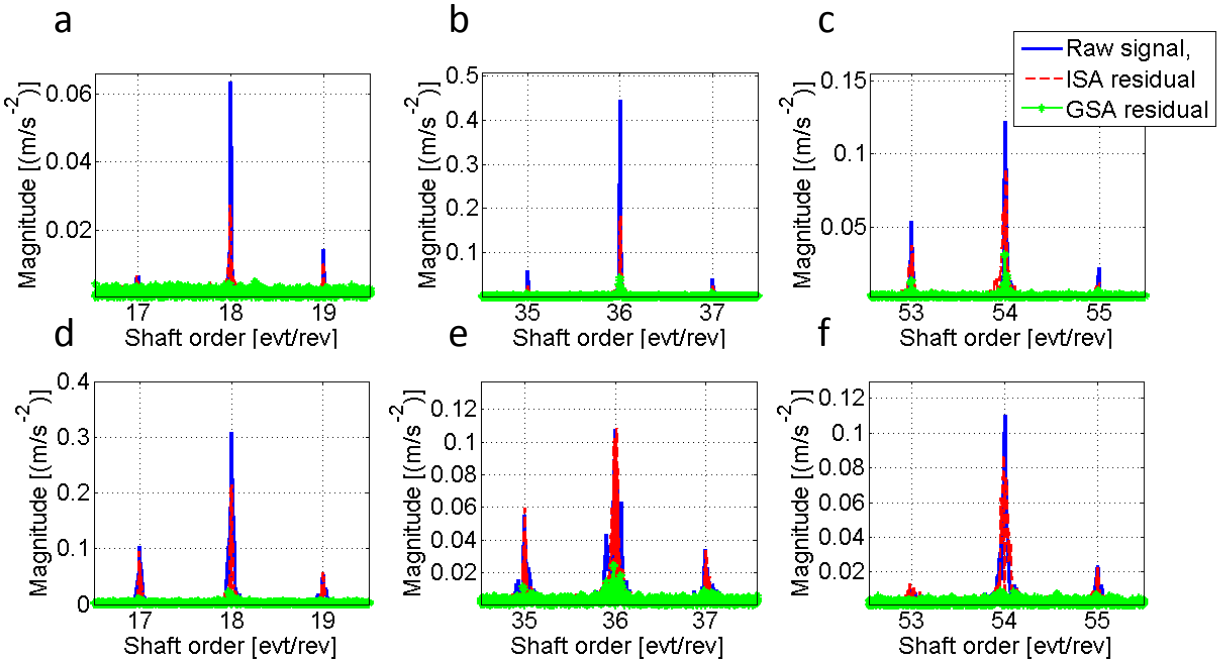

Fig.12. Comparison of the (amplitude) order spectra of the resampled signal, the ISA residue and the GSA residue (see the legend in the upper right box) on Acc2 signal; (i) in runup1 case: close-ups around (a) the fundamental, (b) the second and (c) the third harmonic of meshing order; (ii) in runup2 case: close-ups around (d) the fundamental, (e) the second and (f) the third harmonic of meshing order.

Cette thèse est accessible à l'adresse : http://theses.insa-lyon.fr/publication/2015ISAL0106/these.pdf
© [D. Abboud], [2015], INSA Lyon, tous droits réservés

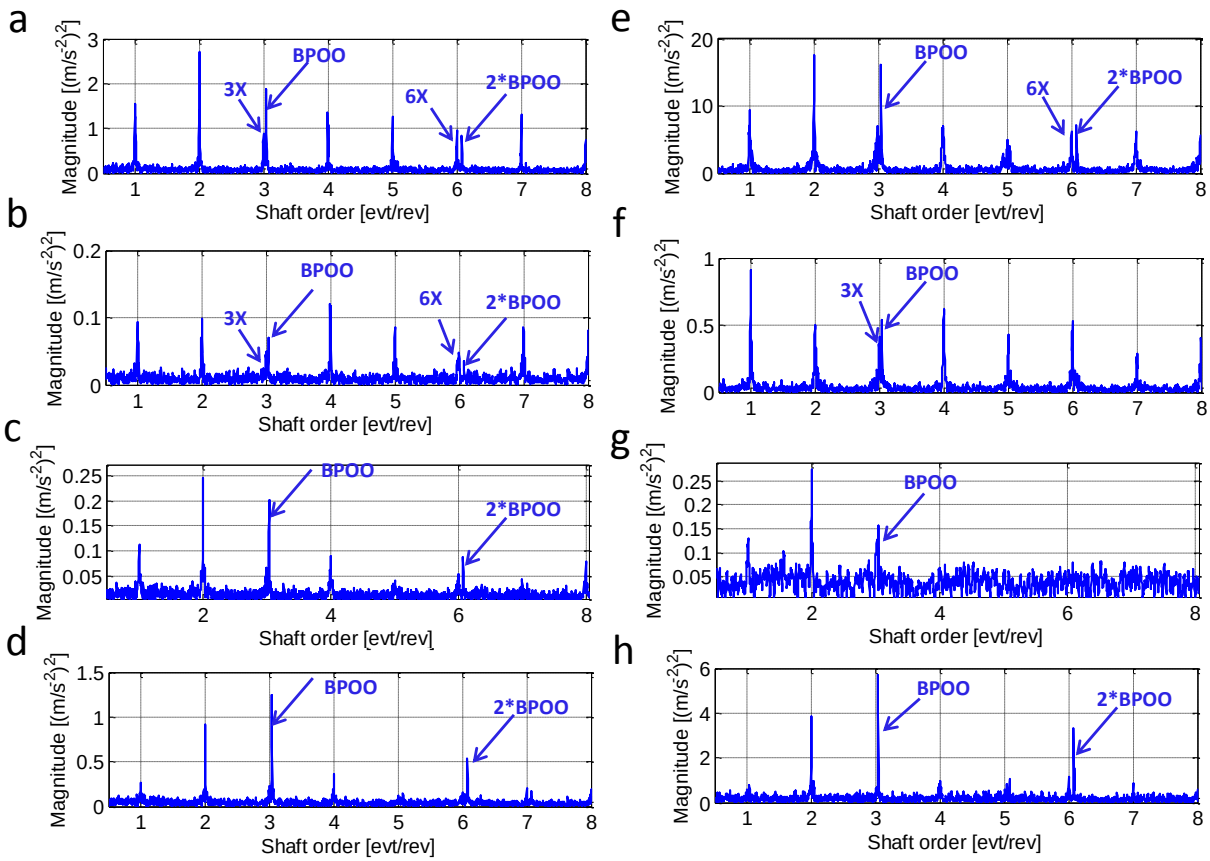

Fig.13. SES of (a) the resampled signal, (b) the ISA residue, (c) the CPW signal, and (d) the GSA residue in runup case. SES of (e) the resampled signal, (f) the ISA residue, (g) the CPW signal, and (h) the GSA residue in random speed-varying case. Signals acquired by Acc2.

5.2.2 Enhancing the REB component

Benefiting from the information on the high-SNR bands of the REB fault (see Table 2), it is useful to enhance the corresponding component by means of the methodology provided in 3.2.3. The filter parameters are chosen to account for the largest spectral band— i.e. $f_c = 7$ kHz and $Bw = 2$ kHz. Then, the SES is applied on the order tracked signal and the obtained results are displayed in Fig.14. Comparing the results to the SE spectra of the whole demodulation band (see Fig.13 (c), (g), (d) and (h)), one can remark improvement at two levels. The first one is the significant decrease in the contribution of the random gear component: the peaks synchronous with the gear rotation are weaker than those related to the REB fault. The second is the complete appearance of a clean outer-race fault signature m×BPOO+n with m=1,2; n=±1 [Randall 2001][3]. The sidebands were completely masked by noise when the SES was applied over the whole demodulation bands. Note also that the filtering operation has decreased the negative effect of the distortion in the CPW case (compare for instance Fig.13 (g) to Fig.14 (d)).

[3]The appearance of sidebands in the outer-race fault case may be due to shaft unbalance.

Cette thèse est accessible à l'adresse : http://theses.insa-lyon.fr/publication/2015ISAL0106/these.pdf
© [D. Abboud], [2015], INSA Lyon, tous droits réservés

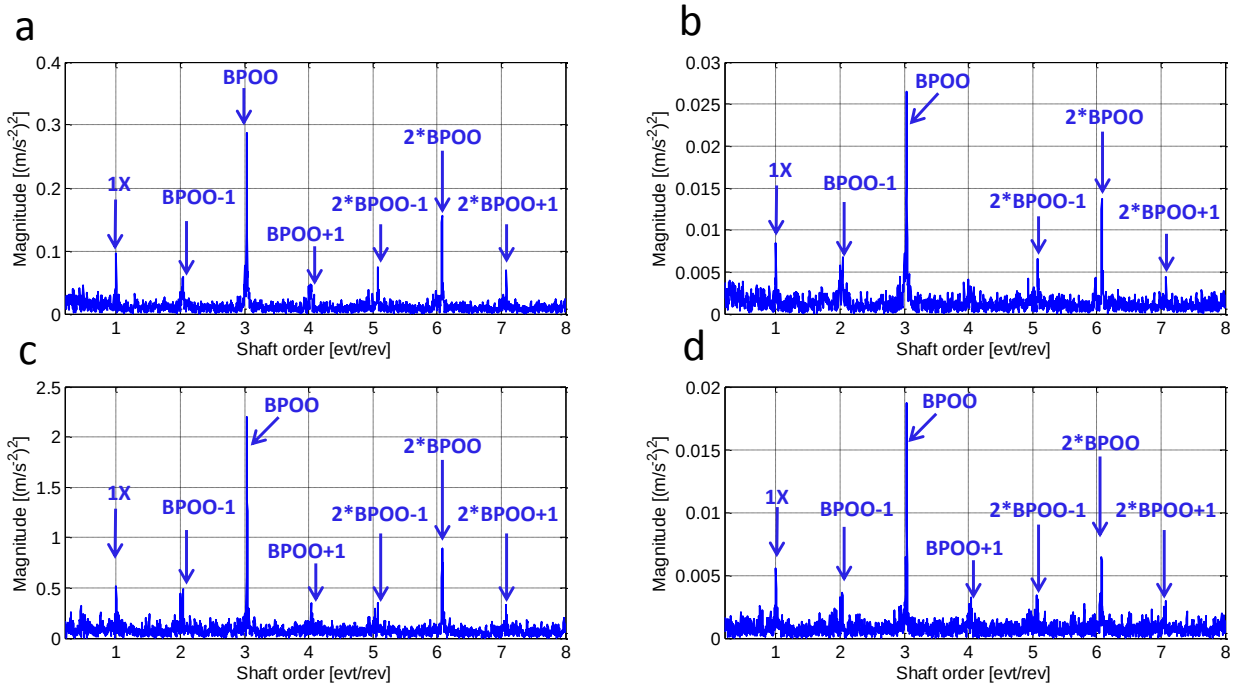

Fig.14. The envelope enhancement methodology applied on the Acc2 signals with filter parameters $\mathbf{f_c = 7\ kHz}$ and $\mathbf{Bw = 1\ kHz}$. Runup case: (a) GSA-based strategy and (b) CPW-based strategy. Random speed-varying case: (c) GSA-based strategy and (d) CPW-based strategy.

5.3 Case study 2: the gear component dominates the random part

This paragraph treats the case where the accelerometer is mounted on the healthy REB (Acc1). In practice, such cases are likely to be met in complex gearboxes where accelerometers are remoted from the sources due to non-intrusion constraints. This presents a challenging case since Acc1 is also close to the gears; that is the weak fault signature energy is likely to be masked by high-energy cyclic components generated by the gears. In fact, it will be shown that the SES is insufficient to reveal the REB fault signature even after removing the deterministic component by either the GSA or the CPW. This case demonstrates the robustness of the envelope enhancement procedure (provided in subsection 3.2.3) in highlighting a particular (very) weak signature surrounded by energetic noises and cyclic components from other sources.

5.3.1 Failure of the SES

Hereafter, the SES is applied on Acc1 signal of the two profiles after eliminating the gear component by the GSA and the CPW techniques. The GSA parameters are identical to those chosen in subsection 6.2.1. The obtained results are reported in Fig.15. For the runup profile (see in Fig.15 (a) and (c)), only a small peak at the BPOO appears in the GSA and CPW cases. However, this peak only appears in the GSA case for random-speed varying profile, while it disappears in the CPW cases. Note also that the peaks related to the random gear contribution are also distorted as most of the corresponding peaks disappear except the second harmonic (see Fig.15 (d)). Again, this is due to the high variability of the speed in the record (see subsection 5.2.1). This is a case where the SES is insufficient to accurately detect the REB fault. The next subsection addresses this issue by considering the envelope enhancement methodology.

Cette thèse est accessible à l'adresse : http://theses.insa-lyon.fr/publication/2015ISAL0106/these.pdf
© [D. Abboud], [2015], INSA Lyon, tous droits réservés

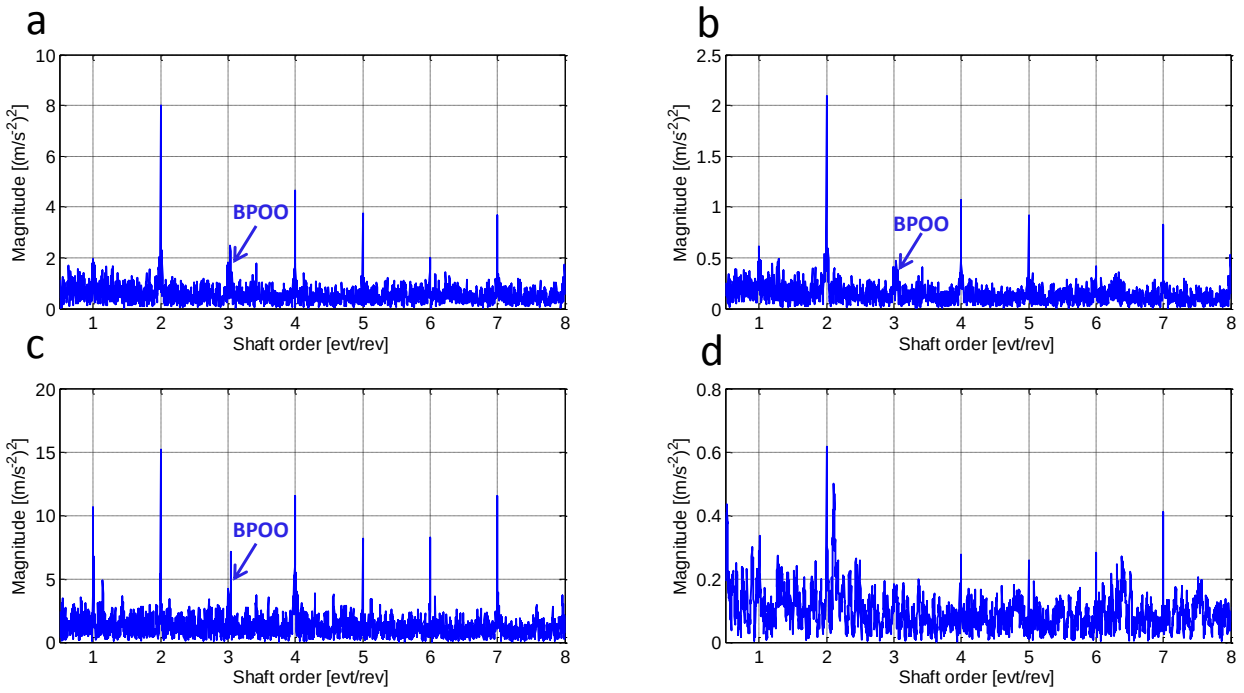

Fig.15. SES of (a) the GSA residue and (b) the CPW signal in runup case. SES of (c) the GSA residue and (d) the CPW signal in random speed-varying case. Signals acquired by Acc1.

5.3.2 Enhancing the REB component

In this subsection, the REB component is enhanced using the frequency band identified in Table 2. After eliminating the deterministic component by the GSA or the CPW, the signal is bandpass filtered with the following parameters—i.e. $f_c = 2\,\text{kHz}$ and $\text{Bw} = 1\,\text{kHz}$. Then, the SES is applied on the order tracked signal and the results are displayed in Fig.16. Interestingly, a clean outer-race fault signature appears for both profiles and strategies. In details, whereas two peaks appear in the SES at the BPOO and its second harmonic in the random speed-varying case (Fig.16 (a) and (b)), sidebands spaced by one order also appear in the runup case (Fig.16 (c) and (d)). Last, it is worth noting that the extracted signature provides an image of the excitation very similar to that obtained for Acc2 (compare Fig.16 with Fig.14).

Cette thèse est accessible à l'adresse : http://theses.insa-lyon.fr/publication/2015ISAL0106/these.pdf
© [D. Abboud], [2015], INSA Lyon, tous droits réservés

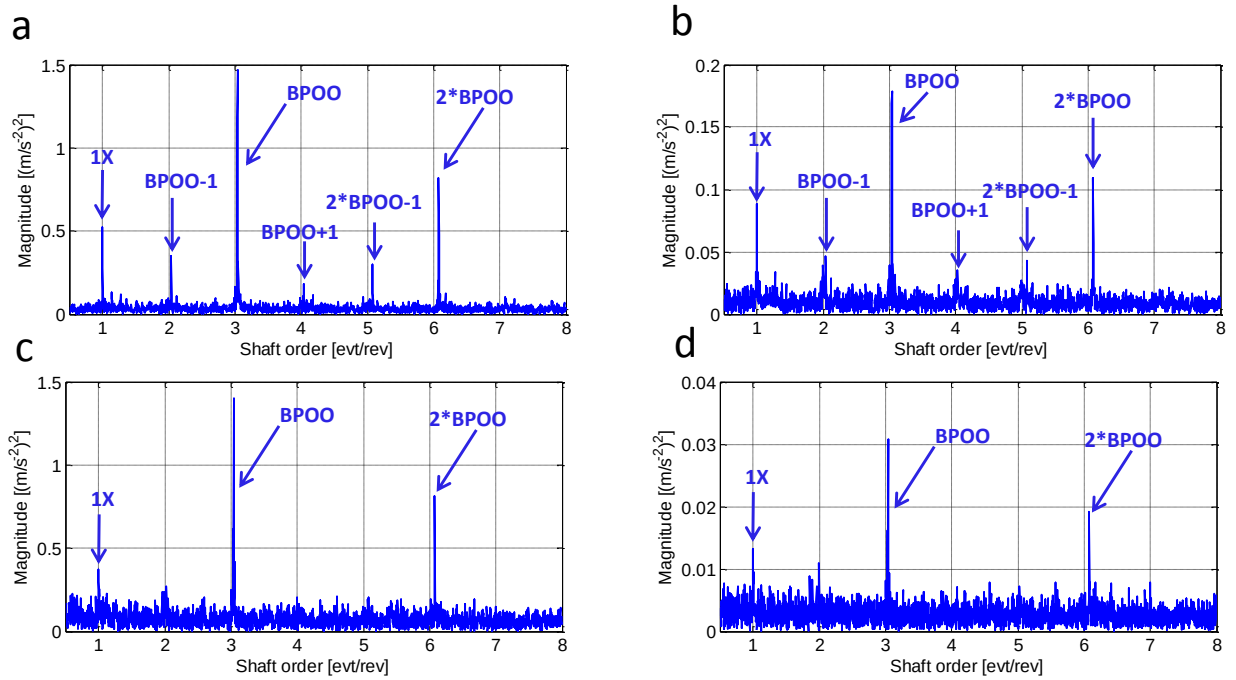

Fig.16. The envelope enhancement procedure applied on the Acc1 signal with filter parameters $\mathbf{f_c = 2\ kHz}$ and $\mathbf{Bw = 1\ kHz}$. Runup case: (a) GSA-based strategy and (b) CPW-based strategy. Random speed-varying case: (c) GSA-based strategy and (d) CPW-based strategy.

6 CONCLUSION

When dealing with random and repetitive signatures, the investigation of the squared envelope spectrum (SES) is unescapable because of its simplicity, low computational cost and implementation easiness on a hand; and the confidence gained through the decades in industries on the other hand. This paper has revised its application on rotating machine signals in variable speed conditions (VSC). It has collected previously published materials into a comprehensive framework. The aim was to provide guidelines to choose the best strategy for a given benchmark. At the onset, a phenomenological model has been proposed to describe the structure of vibration signals in VSC. This is the cornerstone towards the formalization of the subject for a comprehensive evaluation of existing strategies. Two potential challenges that may face the direct application of the SES have been identified. These are discussed hereafter together with solutions.

The first challenge is the spurious contribution of the deterministic component in the SES. The paper has addressed this issue by comparing three sophisticated methods, namely, the improved synchronous average (ISA), the cepstrum prewhitening (CPW), and the generalized synchronous average (GSA), used for suppressing the deterministic part in a vibration signal. Regarding the ISA, it has been shown that this technique suffers from serious problems as it (i) ignores the long-term energy modulation in the signal and (ii) supposes a linear relationship between phases of the harmonics. Therefore, it returns poor results in the case of modest speed variations and generally fails in large speed variations. Conversely, the CPW technique returns better results for both modest and large speed variations. Often, it suppresses completely the deterministic part, yet suffering also from some disadvantages. The most serious one is the distortion in the random

Cette thèse est accessible à l'adresse : http://theses.insa-lyon.fr/publication/2015ISAL0106/these.pdf
© [D. Abboud], [2015], INSA Lyon, tous droits réservés

part caused by the whitening operation. Such distortions also increase with the speed variability in the record. The latter case was met in a case-study with large randomly speed-varying profile where the REB fault signature almost disappeared from the envelope. On the other hand, the GSA proves an exceptional ability to systematically discriminate the deterministic part from the random part with minimal distortion of the latter. This technique also has some drawback such as its inability to remove modulation sidebands whose angular period is incommensurate with the carrier period. Note that the ISA shares the latter inconvenient. Building on this, the GSA can be an efficient alternative to the ISA. As for the preference between the GSA and the CPW, it seems strictly dependent on the nature of the application.

The second challenge is the spurious contribution of CNS components emitted by other sources. This issue has been ignored in the literature where the SES is usually computed over the whole demodulation band after removing the deterministic part. The effectiveness of this approach relies on the prominence of the source of interest (SOI) in the random part. Therefore, it can be efficient for some applications but does not present a versatile solution in the general setting. In this context, it has been shown that the best way to exhibit the mechanical signature a cyclo-non-stationary SOI in the SES is to filter (in the time domain) the signal— hypothetically purely random— around a high-SNR frequency band. In VSC, those bands may be identified, for instance, by an angle\time-cyclostationary (AT-CS) analysis of the emitted signal.

Eventually, the SES itself is an optimal diagnostic indicator in terms of simplicity and computational cost. However, regardless of the adopted strategy, a prior knowledge of high-SNR band associated with the evaluated component is required. This is a strong requirement as it calls for more complex and sophisticated techniques to identify these bands. The straightforward solution to this issue is to scan the entire frequency band while systematically sweeping the whole frequency band. This will bring back to the AT-CS framework through an order-frequency representation. The authors believe that future works are to be oriented toward the exploitation of the SES features in the AT-CS framework.

7 ACKNOWLEDGEMENTS

This work was supported by the technical center of mechanical industries (Cetim). It was performed within the framework of the LabExCeLyA (”Centre Lyonnais d’Acoustique”, ANR-10-LABX-60).

8 REFERENCES

[Darlow 1974] M.S. Darlow, R.H. Badgley, G.W. Hogg, Application of high frequency resonance techniques for bearing diagnostics in helicopter gearboxes, Technical Report, US Army Air Mobility Research and Development Laboratory, 1974, pp. 74–77.

[Ho 2000] D. Ho, R.B. Randall, Optimisation of bearing diagnostic techniques using simulated and actual bearing fault signals, Mechanical Systems and Signal Processing 14 (5) (2000) 763–788.

Cette thèse est accessible à l'adresse : http://theses.insa-lyon.fr/publication/2015ISAL0106/these.pdf
© [D. Abboud], [2015], INSA Lyon, tous droits réservés

[Randall 1986] R.B. Randall Hilbert Transform Techniques in Machine Diagnostics, IFToMM International Conference on rotordynamics, Tokyon

[Urbanek 2012] Urbanek J., Antoni J., Barszcz T., Detection of signal component modulations using modulation intensity distribution, Mech. Syst. and Sign. Proc. 28, 399–413 (2012)

[Widrow 1975] Widrow, B., Glover, J. R., McCool, J. M., Kaunitz, J., Williams, C. S., Hearn, R. H., Zeidler, J. R., Dong, E. and Goodlin, R. C. (1975). Adaptive noise cancelling: Principles and applications, Proceedings of the IEEE 63(12): 1692–1716.

[Fyfe 1997] K.R. Fyfe, E.D. S. Munck, Analysis of computed order tracking, Mech. Syst. Signal Process.11 (2) (1997)187–205.

[Antoni 2009] J. Antoni, Cyclostationary by examples, Mech. Syst. Sig. Process. 23 (4) (2009) 987–1036.

[Antoni 2007a] J. Antoni, Cyclic spectral analysis in practice, Mechanical Systems and Signal Processing 21 (2007) 597–630.

[Antoni 2004] J. Antoni, F. Bonnardot, A. Raad, M. El Badaoui, Cyclostationary modelling of rotating machine vibration signals, Mech. Syst. Sig. Process. 18 (2004,a) 1285–1314

[Randall 2001] R.B. Randall, J. Antoni, S. Chobsaard, The relationship between spectral correlation and envelope analysis for cyclostationary machine signals: application to ball bearing diagnostics. Mech. Syst. Sig. Process. 15 (5) (2001) 945–962.

[Braun 1980] S. Braun, B. Seth, "Analysis of Repetitive Mechanism Signatures", Journal of Sound and Vibration, Vol. 70, N◦. 4, 1980, p.513-522.

[Lejeune 1997] G. Lejeune, J. L. Lacoume, P. Marchand, M. Durnerin, N. Martin, J. Liénard, A. Silvent CEPHAG, "Cyclostationnarité d'ordre 1 et 2 : application à des signaux vibratoires d'engrenages", 16 i`eme colloque GRETSI, Sept. 1997, Grenoble, p.323-326 (in French).

[Antoni 2003] J. Antoni, «Apport de l'échantillonnage angulaire et de la cyclostationarite au diagnostic par analyse vibratoire des moteurs thermiques, Ph.D dissertation, 2003 (in French).

[Antoni 2013, b]J. Antoni, M. Eltabach, A KIS solution for high fidelity interpolation and resampling of signals, Mechanical Systems and Signal Processing, Volume 35, Issue 1-2, February 2013, Pages 127-136

[Abboud 2015a] D. Abboud, S. Baudin, J. Antoni, D. Remond, M. Eltabach, O. sauvage, The spectral correlation analysis of cyclo-non-stationary signals, Mechanical Systems and Signal Processing, XXXX.

[Antoni 2007a] J. Antoni, Cyclic spectral analysis of rolling-element bearing signals: Facts and fictions, Journal of Sound and Vibration 304 (2007) 497–529

Cette thèse est accessible à l'adresse : http://theses.insa-lyon.fr/publication/2015ISAL0106/these.pdf
© [D. Abboud], [2015], INSA Lyon, tous droits réservés

[Antoni 2009] J. Antoni, Cyclostationarity by examples, Mechanical Systems and Signal Processing, 23 (2009) 987–1036

[Randall 2011a] R.B. Randall, J. Antoni, Rolling element bearing diagnostics—A tutorial, Mech. Syst. Sig. Process., Volume 25, Issue 2, p. 485-520.

[Randall 2011b] R. B. Randall, Vibration-based Condition Monitoring: Industrial, Automotive and Aerospace Applications, *John Wiley and Sons*, West Sussex, (2011).

[Coats 2009] M.D. Coats, N. Sawalhi, R.B. Randall, Extraction of tacho information from a vibration signal for improved synchronous averaging, Proc. Acoust. (2009).

[Stander 2006] C.J. Stander, P.S. Heyns, Transmission path phase compensation for gear monitoring under fluctuating load conditions, Mech. Syst. Sig. Process. 20 (7) (2006) 1511-1522.

[Borghesani 2013a] P. Borghesani, P. Pennachi, R.B. Randall, R. Ricci, Order tracking for discrete-random separation in variable speed conditions, Mech. Syst. Signal Process. 30 (2012), Pages 1–22.

[Sawalhi 2011] N. Sawalhi, R.B. Randall, Signal pre-whitening using cepstrum editing (Liftering) to enhance fault detection in rolling element bearing, in: Proceedings of the 24th international Congres in condition monitoring and diagnostics engineering management (COMADEM)

[Borghesani 2013b] P. Borghesani, P.Pennacchi, R.B.Randall, N.Sawalhi, R.Ricci, Application of cepstrum pre-whitening for the diagnosis of bearing faults under variable speed conditions, Mech. Syst. Sig. Process. 36 (2013) 370–384

[Abboud 2015b] D. Abboud, J. Antoni, S. Sieg-Zieba, M. Eltabach, Deterministic-Random separation in non-stationary conditions, Journal of sounds and vibrations, (under review).

[Abboud 2015c] D. Abboud, J. Antoni, S. Sieg-Zieba, M. Eltabach, Angle\Time cyclostationarity for the analysis of rolling element bearing vibrations, Measurement, In Press, Accepted Manuscript, 75:29-39, 2015.

[Borghesani 2013c] P. Borghesani , R. Ricci, S. Chatterton, P. Pennacchi, "A new procedure for using envelope analysis for rolling element bearing diagnostics in variable operating conditions", Mech. Syst. Sig. Process. 36 (2013) 370–384

[Antoni 2014] J. Antoni, D. Abboud, S. Baudin, Time-angle periodically correlated process, Cyclostationarity: theory and methods. Lecture notes in mechanical engineering, Springer (2014)

[Antoni 2007a] J. Antoni, Cyclic spectral analysis in practice, Mechanical Systems and Signal Processing 21 (2007) 597–630.

[Antoni 2007c] J. Antoni, J. Schoukens, "A comprehensive study of the bias and variance of frequency-response-function measurements: Optimal window selection and overlapping strategies", Automatica, Volume 43, Issue 10, October 2007, Pages 1723-1736.

Cette thèse est accessible à l'adresse : http://theses.insa-lyon.fr/publication/2015ISAL0106/these.pdf
© [D. Abboud], [2015], INSA Lyon, tous droits réservés

[Baudin 2014] Sophie Baudin, Didier Rémond, Jérôme Antoni, Olivier Sauvage, Detection of rattle noise with optical encoders in run-up conditions, ISMA 2014, Sep 2014, Belgium. pp.254

[D'Elia 2010] D'Elia G., Daher Z., Antoni J., A novel approach for the cyclo-nonstationary analysis of speed varying signals. Proceedings of ISMA 2010 Including USD 2010.

[Roussel 2013] J. Roussel, M. Haritopoulos, E. Sekko, C. Capdessus, J. Antoni, Application of Speed Transform to the Diagnosis of a Roller Bearing in Variable Speed, Proceeding of the conference Surveillance 7, France, October 29-30, 2013

[Urbanek 2013] J. Urbanek, T. Barszcz , J. Antoni, "Time–frequency approach to extraction of selected second-order cyclostationary vibration components for varying operational conditions", Measurement, Measurement 46 (2013) 1454–1463

[Inalpolat 2009] Murat Inalpolat, A theoretical and experimental investigation of modulation sidebands of planetary gear sets, Dissertation Ph.D. thesis, Ohio State University, Ohio, 2009.

[Zhao 2013] M. Zhao, J. Lin, X. Xu, Y. Lei, Tacholess Envelope Order Analysis and Its Application to Fault Detection of Rolling Element Bearings with Varying Speeds, Sensors 2013, 13(8), 10856-10875.

[Cocconcelli 2013] M. Cocconcelli, L. Bassi, C. Secchi, C. Fantuzzi , R. Rubini, "An algorithm to diagnose ball bearing faults in servomotors running arbitrary motion profiles", Mech. Syst. Sig. Process., 27 (2012) 667–682.

[Gardner 1990] W. Gardner, Introduction to Random Processes, second ed., McGraw-Hill, New York, 1990.

[Prieur 1995] P. Prieur, G. D'urso, Des indices de cyclostationnarité pour la surveillance des engrenages, 15ième Colloque Gretsi, Juan les Pins (1995)1241–1244 (in French).

[Lejeune 1997] G. Lejeune, J. L. Lacoume, P. Marchand, M. Durnerin, N. Martin, J. Liénard, A. Silvent, C. Mailhes, P. Prieur, G. Goullet, Cyclostationnarités d'ordre 1 et 2: application a` des signaux vibratoires d'engrenages, 16ième Colloque GRETSI, Grenoble, France (1997) (in French).

[Rubini 1997] R. Rubini, M. Sidahmed, Diagnostics of Gear Systems Using the Spectral Correlation Density of the Vibration Signal, IFAC Fault Detection, Supervision and Safety for Technical Processes, Kingston UponHull,UK,1997.

[Capdessus 2000] C. Capdessus, M. Sidahmed, J.L. Lacoume, Cyclostationary processes: application in gear faults early diagnosis, Mechanical Systems and Signal Processing 14 (3) (2000) 371–385.

[Bouillaut 2000] L. Bouillaut, M. Sidahmed, Cyclostationary approach and bilinear approach: comparison, applications to early diagnosis for helicopter gearbox and classification method based on HOCS, Mechanical Systems and Signal Processing 15 (5) (2000) 923–943.

Cette thèse est accessible à l'adresse : http://theses.insa-lyon.fr/publication/2015ISAL0106/these.pdf
© [D. Abboud], [2015], INSA Lyon, tous droits réservés

[Antoniadis 2001] I. Antoniadis, G. Glossiotis, Cyclostationary analysis of rolling-element bearing vibration signals, Journal of Sound and Vibration 248 (5) (2001) 829–845.

[Konig 1994] D. Konig, F.Bohme, Application of cyclostationary and time–frequency analysis to car engine diagnosis, IEEE International Conference on Acoustic, Speech and Signal Processing 4 (1994) 149–152.

[Konig 1995] D. Konig, C. Tork, J. Bohme, Design of optimum periodic time varying filters for applications in combustion diagnosis of car engines, International Conference on Acoustics Speech and Signal Processing 3 (1995)1924–1927.

[Antoni 2002] J. Antoni, J. Daniere, F. Guillet, Effective vibration analysis of IC engines using cyclostationarity. Part I: a methodology for condition monitoring, Journal of Sound and Vibration 257 (5) (2002) 815–837.

[Bartelmus 2009] W. Bartelmus, R. Zimroz, A new feature for monitoring the condition of gearboxes in non-stationary operating conditions, Mech. Syst. Signal Process. 23 (5) (2009) 1528–1534.

[Bartelmus 2010] W. Bartelmus, F. Chaari, R. Zimroz, M. Haddarb, Modelling of gearbox dynamics under time-varying nonstationary load for distributed fault detection and diagnosis, European Journal of Mechanics - A/Solids, Volume 29, Issue 4, July–August 2010, Pages 637–646

[Villa 2012] L.F. Villa, A. Renones, J.R. Peran, L.J. de Miguel. Statistical fault diagnosis based on vibration analysis for gear test-bench under non-stationary conditions of speed and load. Mechanical Systems and Signal Processing, Vol. 29, 436-446, 2012

[Heyns 2012] T. Heyns, S.J. Godsill, J.P. de Villiers, P.S. Heyns, Statistical gear health analysis which is robust to fluctuating loads and operating speeds. Mechanical Systems and Signal Processing, Vol. 27, 651–666, 2012

[Baudin 2014a] S. Baudin, D. Rémond, J. Antoni, Olivier Sauvage, Detection of rattle noise with optical encoders in run-up conditions, ISMA 2014, Sep 2014, Belgium. pp.254

[Baudin 2014b] S. Baudin, J. Antoni, D. Rémond, O. Sauvage, Détection du bruit de grenaille par analyse cyclo-non-stationnaire, proceedings of CFA 2014 (in french).

[Abboud 2014a] D. Abboud, J. Antoni, S. Sieg-Zieba, M. Eltabach, Generalization of the synchronous average for Deterministic/Random Separation under speed varying conditions, Proceedings of VISHNO 2014

[Abboud 2014b] D. Abboud, J. Antoni, S. Sieg-Zieba, M. Eltabach, Speed-spectral whitening for enhancing envelope analysis in speed varying conditions, Proceedings of vibrations shocks and noise, 17-19 June 2014, Aix-en-Provence France.

[Abboud 2014c] D. Abboud, J. Antoni, S. Sieg-Zieba, M. Eltabach. On the extraction of rolling-element bearing fault signature in speed-varying conditions, Proceedings of the Eleventh

Cette thèse est accessible à l'adresse : http://theses.insa-lyon.fr/publication/2015ISAL0106/these.pdf
© [D. Abboud], [2015], INSA Lyon, tous droits réservés

International Conference on Condition Monitoring and. Machinery Failure Prevention Technologies, 10-12 June 2014, Manchester UK

[Coats 2014] M. D. Coats, R. B. Randall, Single and multi-stage phase demodulation based order-tracking, Mechanical Systems and Signal Processing 44 (2014)86–117

[Harris 2001] C. Harris, A. Persol, Harris' Shock and Vibration Handbook, McGraw Hill, 2001.

[Neville 2008] Neville F. Rieger; "the Relation between Finite Element Analysis and Modal Analysis"; Stress Technology Incorporated, Rochester, New York. 2008.

[Antoni 2006] J. Antoni, R.B. Randall, The spectral kurtosis: application to the vibratory surveillance and diagnostics of rotating machines, Mech. Syst. Sig. Process. 20 (2006) 308–331.

[Antoni 2007c] J. Antoni, Fast computation of the kurtogram for the detection of transient faults, Mech. Syst. Sig. Process. 21 (2007) 108–124

[Barszcz 2011] T. Barszcz, A. Jablonski, A novel method for the optimal band selection for vibration signal demodulation and comparison with the Kurtogram, Mech. Syst. Sig. Process. 25 (2011) 431–451.

9 APPENDICES

9.1 Appendix A: Proof of equations

A.1. SES of the deterministic component

The squared envelope of the deterministic part reads

$$SE_d(t) = \mathbb{E}\{|\mathrm{d}(\mathrm{t})|^2\} = \sum_{\lambda_j \in \Lambda} \sum_{\lambda_k \in \Lambda} d^{\lambda_j}\big(\omega(t)\big)\, d^{\lambda_k}\big(\omega(t)\big)^* e^{j(\lambda_j - \lambda_k)\theta(t)}. \tag{A1}$$

Applying the change of variable $\lambda_i = \lambda_j - \lambda_k$, one obtains

$$SE_d(t) = \sum_{\lambda_i \in \Lambda} \left(\sum_{\lambda_k \in \Lambda} d^{\lambda_i + \lambda_k}\big(\omega(t)\big)\, d^{\lambda_k}\big(\omega(t)\big)^* \right) e^{j\lambda_i \theta(t)} = \sum_{\lambda_i \in \Lambda} SE_d^{\lambda_i}\big(\omega(t)\big) e^{j\lambda_i \theta(t)} \tag{A2}$$

The corresponding SES is obtained by following the same lines as in Eq. (6), i.e.

$$SES_d(\alpha) = \mathcal{F}_{\theta \to \alpha}\big\{SE_d\big(t(\theta)\big)\big\} = \sum_{\lambda_i \in \Lambda} SES_d^{\lambda_i}(\alpha - \lambda_i), \tag{A3}$$

Cette thèse est accessible à l'adresse : http://theses.insa-lyon.fr/publication/2015ISAL0106/these.pdf
© [D. Abboud], [2015], INSA Lyon, tous droits réservés

with $SES_d^{\lambda_i}(\alpha) = \mathcal{F}_{\theta\to\alpha}\left\{SE_d^{\lambda_i}\left(\widetilde{\omega}(\theta)\right)\right\}$ and $\widetilde{\omega}(\theta) = \omega\left(t(\theta)\right)$.

A.2. SES of the CNS component

Regarding the CNS contribution, the SES is evaluated on the general model provided in Eq. (8). Accordingly, the SE of a CNS signal reads:

$$SE_y(t) = \mathbb{E}\{|y(t)|^2\} = \sum_{\gamma_j\in\Gamma_y}\sum_{\gamma_k\in\Gamma_y}\mathbb{E}\{y^{\gamma_j}(t,\omega(t))y^{\gamma_k}(t,\omega(t))^*\}\,e^{j(\gamma_j-\gamma_k)\theta(t)}. \tag{A4}$$

Applying the change of variable $\gamma_i = \gamma_j - \gamma_k$, one obtains

$$\begin{aligned} SE_y(t) &= \sum_{\gamma_i\in\Gamma_y}\left(\sum_{\gamma_k\in\Gamma_y}\mathbb{E}\{y^{\gamma_i+\gamma_k}(t,\omega(t))y^{\gamma_j}(t,\omega(t))^*\}\right)e^{j\gamma_i\theta(t)} \\ &= \sum_{\gamma_i\in\Gamma_y} SE_y^{\gamma_i}\left(\omega(t)\right)e^{j\gamma_i\theta(t)}. \end{aligned} \tag{A5}$$

The corresponding SES is obtained by following the same lines as in Eq. (6), i.e.

$$SES_y(\alpha) = \mathcal{F}_{\theta\to\alpha}\left\{SE_y\left(t(\theta)\right)\right\} = \sum_{\gamma_i\in\Gamma_y} SES_y^{\gamma_i}(\alpha-\gamma_i), \tag{A6}$$

with $\Pi_Y^{\gamma}(\alpha) = \mathcal{F}_{\theta\to\alpha}\left\{SE_y^{\gamma_i}\left(\widetilde{\omega}(\theta)\right)\right\}$. According to this, the SES of the CNS components emitted by the SOI and by the m[th] interfering source reads

$$\begin{cases} SES_s(\alpha) = \displaystyle\sum_{\gamma_i^{(s)}\in\Gamma_s} SES_s^{\gamma_i^{(s)}}\left(\alpha-\gamma_i^{(s)}\right) \\ SES_{q_m}(\alpha) = \displaystyle\sum_{\gamma_i^{(m)}\in\Gamma_m} SES_{q_m}^{\gamma_i^{(m)}}\left(\alpha-\gamma_i^{(m)}\right). \end{cases} \tag{A7}$$

A.3. SES of the background noise

Eventually, the SES of the background noise is obtained by simply replacing the cyclic order set Γ_y in Eq. (A6) by the singleton $\{0\}$, i.e.

$$SES_{\mathrm{b}}(\alpha) = \mathcal{F}_{\theta\to\alpha}\left\{SE_{\mathrm{b}}\left(t(\theta)\right)\right\} = SES_b^0(\alpha), \tag{A8}$$

with $SES_b^0(\alpha) = \mathcal{F}_{\theta\to\alpha}\left\{SE_b^0\left(\widetilde{\omega}(\theta)\right)\right\}$ and $SE_b^0(\omega) = \mathbb{E}\{|b^0(t,\omega(t))|^2\}$.

Cette thèse est accessible à l'adresse : http://theses.insa-lyon.fr/publication/2015ISAL0106/these.pdf
© [D. Abboud], [2015], INSA Lyon, tous droits réservés

Note that the properties of the functions $SES_d^{\lambda_i}(\alpha)$, $SES_y^{\gamma_i}(\alpha)$ and $SES_b^0(\alpha)$ are similar to those of function $D^{\lambda_i}(\alpha)$ encountered in Eq.(6).

A.4. Proof of Eq. (28):

Exploiting the linearity of the GSA:

$$m_x(\bar{\theta},\omega) = m_d(\bar{\theta},\omega) + m_r(\bar{\theta},\omega). \tag{A9}$$

Evidently, the GSA of the random part tend to zero as the average number increases toward the infinity. It remains to calculate the GSA on the model of the deterministic part. Inserting Eq. (5) into Eq. (26), one obtains

$$m_x(\bar{\theta},\omega) = \lim_{\delta\omega\to 0} \lim_{card\{K_{\bar{\theta},\omega}\}\to\infty} \frac{1}{card\{K_{\bar{\theta},\omega}\}} \sum_{k\in K_{\bar{\theta},\omega}} \sum_{\lambda_i\in\Lambda} d^{\lambda_i}\left(\tilde{\omega}(\bar{\theta}+k\Theta)\right) e^{j\lambda_i(\bar{\theta}+k\Theta)} \tag{A10}$$

Similarly to the classical synchronous average, the GSA also needs the cyclic orders to be multiple, i.e. $\lambda_i = i.\lambda_1 = i*2\pi/\Theta$ for all $i = 2,3$ .... By interchanging the sums, Eq. (A10) becomes

$$m_X(\bar{\theta},\omega) = \lim_{\delta\omega\to 0} \lim_{card\{K_{\bar{\theta},\omega}\}\to\infty} \sum_{\lambda_i\in\Lambda} \left[\frac{1}{card\{K_{\bar{\theta},\omega}\}} \sum_{k\in K_{\bar{\theta},\omega}} d^{\lambda_i}\left(\tilde{\omega}(\bar{\theta}+k\Theta)\right)\right] e^{j\lambda_i\bar{\theta}} \tag{A11}$$

The rest of the proof follows once recognizing that $d^{\lambda_i}\left(\tilde{\omega}(\bar{\theta}+k\Theta)\right) = d^{\lambda_i}(\omega)$ for all $k \in K_{\bar{\theta},\omega}$when $\delta\omega \to 0$.

A.5. Proof of Eq. (32):

Exploiting Eq. (9), the filtration of signal, $\tilde{S}(t)$, is expressed as:

$$\tilde{s}(t) = s(t)\otimes f(t) = \sum_{\gamma_i^{(s)}\in\Gamma_s} \tilde{s}^{\gamma_i^{(s)}}\left(t,\omega(t)\right) e^{j\gamma_i^{(s)}\theta(t)} \tag{A12}$$

where $\tilde{s}^{\gamma_i}(t,\omega) = s^{\gamma_i}(t,\omega)\otimes f(t)$ provided that the impulse response length $f(t)$ is smaller than the cycle duration. Its corresponding SES is

$$\mathrm{SES}_{\tilde{s}}(\alpha) = \sum_{\gamma_i^{(s)}\in\Gamma_s} SES_{\tilde{s}}^{\gamma_i^{(s)}}\left(\alpha-\gamma_i^{(s)}\right)$$

where $SES_{\tilde{s}}^{\gamma_i^{(s)}}(\alpha) = \mathcal{F}_{\theta\to\alpha}\left\{SE_{\tilde{s}}^{\gamma_i^{(s)}}\left(\tilde{\omega}(\theta)\right)\right\}$ and $SE_{\tilde{s}}^{\gamma}(\omega) = \sum_{\gamma'} \mathbb{E}\left\{\tilde{s}^{\gamma'+\gamma}(\omega)\tilde{s}^{\gamma'}\left(\omega(t)\right)^*\right\}$.

Cette thèse est accessible à l'adresse : http://theses.insa-lyon.fr/publication/2015ISAL0106/these.pdf
© [D. Abboud], [2015], INSA Lyon, tous droits réservés

9.2 Appendix B: Estimation of the GSA

For estimation purposes, the speed profile is divided into a predefined set of speed intervals called regimes defined by their central frequency ω_r and the speed resolution $\delta\omega$. Then, each cycle is associated to the regime that is closest to its mean speed value. Building on this, the raw estimator is then defined as,

$$\widehat{\mathrm{m}}_{\mathrm{y}}(\bar{\theta}, \omega_{\mathrm{r}}) = \frac{1}{\mathrm{card}\{\mathrm{K_r}\}} \sum_{k \in K_r} y(\bar{\theta} + k\Theta), \tag{B1}$$

where $K_r = \left\{ k \in \mathbb{N}^* \middle| \omega_r - \delta\omega/2 \leq \frac{1}{\theta} \int_{(k-1)\theta}^{k\theta} \tilde{\omega}(\theta) d\theta < \omega_r + \delta\omega/2 \right\}$ stands for the set of cycles whose mean speed falls in the speed interval centered atω_r. Note that the raw estimate of the GSA provides only estimates at the central frequencies of the predefined speed intervals. Thus, the deterministic component could not be accurately restored by Eq. (27). For this reason, an interpolation is needed to enforce the continuity along the speed axis. By applying the kernel density estimation technique, an estimation of the (synchronous) deterministic part is provided by

$$\widehat{m}_y(\bar{\theta}, \omega) = \frac{1}{\mathrm{Kern}\left(\frac{\tilde{\omega}(\theta) - \omega_r}{\sigma}\right)} \sum_{r=1}^{R} \mathrm{Kern}\left(\frac{\tilde{\omega}(\theta) - \omega_r}{\sigma}\right) \widehat{m}_y(\bar{\theta}, \omega_r) \tag{B2}$$

where $\mathrm{Kern}(*)$ is the smoothing kernel (e.g. Gaussian, Hamming…), σ is a smoothing parameter called the bandwidth,$\widehat{m}_y(\theta, \omega_r)$ is the periodized version of $\widehat{m}_y(\bar{\theta}, \omega_r)$ over the actual number of periods of $y(\theta)$.

9.3 Appendix C: Simulation models for gears and bearings

a) Deterministic contribution of gears

The deterministic gear contribution is principally induced by the meshing force and the fault impacts. The former manifests itself as a smooth angle-periodic component of fundamental order equal to the number of teeth Z_1 while the latter manifests itself as an impulsive angle-periodic component of fundamental order equal to the wheel rotation, i.e. 1. The interaction between these excitations is mostly manifested through an amplitude modulation. In turn, the resulting excitation undergoes speed-dependent energy modulation caused by the change of the machine power intake as the speed varies. Building on this, one can model the excitation of the deterministic gear vibration part as

$$\Sigma_g^{(d)}(t) = M_g^{(d)}\left(\omega_{ref}(t)\right)\left(1 + I\left(\theta_{ref}(t)\right)\right) \sum_l a_l \cos\left(Z_1.l.\theta_{ref}(t) + \varphi_l\right), \tag{D1}$$

where $\theta_{ref}(t) = \int_0^t \omega_{ref}(t) dt$ stands of the angular position of the reference shaft rotating with the angular frequency ω_{ref}, $M_g^{(d)}\left(\omega_{ref}\right)$ is a monotonally increasing modulation function with

Cette thèse est accessible à l'adresse : http://theses.insa-lyon.fr/publication/2015ISAL0106/these.pdf
© [D. Abboud], [2015], INSA Lyon, tous droits réservés

respect to the speed, a_l and φ_l are the l[th] Fourier coefficients of the angle-periodic meshing excitation, and

$$I(\theta_{ref}) = \sum_i \mathrm{I}_\xi\left(\theta_{ref} - \mathrm{i}.2\pi\right), \tag{D2}$$

models the fault impacts, where $\mathrm{I}_\xi(\theta_{ref}) = 1/\xi\sqrt{2\pi}\, e^{-j0.5(\theta_{ref})^2/\xi^2}$ is a Gaussian kernel of standard deviation, ξ, representing the angular duration of the impact. This latter is supposed to be constant in the angular domain as it may actually depend on the fault width. The deterministic gear vibration signal is then obtained after passing through an LTI system, say $h_g^{(r)}(t)$, that physically expresses the transmission path from the excitation to the sensor:

$$d(t) = \Sigma_g^{(d)}(t) \otimes h_g^{(d)}(t). \tag{D3}$$

b) Random contribution of gears

The random contribution of the output gear can be modeled as the product of white noise modulated by an angle-periodic function with period equal to that of the output gear. By adding the speed-dependent energy modulation caused by the change of the machine power intake, one can model the random contribution of the output gear as:

$$q(t) = M_g^{(r)}\left(\omega_{ref}(t)\right) W(t) \sum_m a_m \cos\left(\frac{Z_1}{Z_2}.m.\theta_{ref}(t) + \varphi_m\right) \tag{D4}$$

where $M_g^{(r)}(\omega_{ref})$ is a monotonally increasing modulation function with respect to the speed, $W(t)$ is a white noise of unit standard deviation,a_m and φ_m are the m[th] Fourier coefficients of the angle-periodic meshing excitation. The random gear signal is then obtained after passing through an LTI system, say $h_g^{(r)}(t)$, that physically expresses the transmission path from the excitation to the accelerometer:

$$X_g^{(r)}(t) = \Sigma_g^{(r)}(t) \otimes h_g^{(r)}(t). \tag{D5}$$

c) Random contribution of REB

In the following, a cyclostationary-based bearing vibration model introduced in [Randall 2001] is revisited to account for speed variation. The presence of a local fault in a REB component produces a train of short time impulses, angle periodic on the average, locked to the fault characteristic angular period. The inter-arrival angles of the impacts are subjected to slight random fluctuations due to existing slips, whereas the corresponding magnitude is subject to fluctuations due to the non-exactly reproducible microscopic conditions when a rolling surface impacts the fault. Similarly to the gear case, the excitation is also subjected to speed dependent energy changes. In this model, the modulation effects caused by the passage in the load zones are neglected. A faulty rolling element bearing signal is then obtained by exciting a wide band structural resonance as,

Cette thèse est accessible à l'adresse : http://theses.insa-lyon.fr/publication/2015ISAL0106/these.pdf
© [D. Abboud], [2015], INSA Lyon, tous droits réservés

$$s(t) = M_b\left(\omega_{ref}(t)\right)\sum_i A_i h_b\,(t - T_i);\ with\ T_i = t\left(i.\Theta_f - \mu_i\right) \tag{D6}$$

where $M_b(\omega_{ref})$ is a monotonally increasing modulation function, h_b is the system impulse response, $\Theta_f = 2\pi/BPOO$ is the fault characteristic angular period, $A_i$are the amplitude modulations modelled as mutually delta-correlated random sequence with $\mathbb{E}\{A_i\} = \bar{A}$ and $\mathrm{cov}\{A_i, A_j\} = \sigma_A^2\delta_{ij}$, μ_i are the inter-arrival angle fluctuations modelled as mutually delta-correlated random variable with $\mathbb{E}\{\mu_i\} = 0$ and $\mathrm{cov}\{\mu_i, \mu_j\} = \sigma_\mu^2\delta_{ij}$.

d) Background noise

Eventually, background noise $b(t)$ is modelled by a stationary white Gaussian noise modulated by a speed-dependent monotonically increasing function $M_N(\omega_{ref})$,

$$b(t) = W(t)M_N\left(\omega_{ref}(t)\right). \tag{D7}$$

Finally, the complete vibration signal can be then obtained by summing all contributions,

$$x(t) = \mathrm{d}(t) + \mathrm{s}(t) + q(t) + b(t). \tag{D8}$$

For simplicity, the LTI filter $h_g^{(d)}(t)$, $h_g^{(d)}(t)$ and $h_b(t)$ are chosen to be the impulse responses of single-degree-of-freedom (s.d.o.f.) systems with different parameters.

Cette thèse est accessible à l'adresse : http://theses.insa-lyon.fr/publication/2015ISAL0106/these.pdf
© [D. Abboud], [2015], INSA Lyon, tous droits réservés

Appendix E - ‘Pub5’: The speed dependent spectral correlation

D. Abboud, J. Antoni, S. Sieg-Zieba, M. Eltabach, The speed-dependent spectral correlation, Proceedings of the international conference on structural engineering dynamics, 22-24 June 2015, Lagos, Algarve, Portugal.

Cette thèse est accessible à l'adresse : http://theses.insa-lyon.fr/publication/2015ISAL0106/these.pdf
© [D. Abboud], [2015], INSA Lyon, tous droits réservés

THE SPEED DEPENDENT SPECTRAL CORRELATION

Abboud, D.[1,2], Antoni, J.[1], Sieg-Zieba, S.[2], Eltabach, M.[2]

[1]*LVA, INSA-Lyon, University of Lyon, France*
INSA de Lyon Bâtiment St. Exupéry 25 bis av. Jean Capelle, 69621 Villeurbanne cedex - FRANCE
[2] *CETIM, Centre Technique des industries mécaniques, Senlis, France*

SUMMARY: In the last decades, the vibration-based diagnosis of rotating machines has developed significantly and its applications are spreading in different industrial sectors. Some of these applications are characterized by nonstationary operating speeds making their diagnosis critical. In such cases, the emitted vibrations are likely to witness an interaction between angle-components related to the system kinematics and time-dependent components related to the system dynamics. Therefore, the angle-time cyclostationary class was designed to jointly consider these components. In accordance, the order-frequency spectral correlation (OFSC) has proven itself as a powerful diagnosis tool enjoying a symptomatic distribution of the cyclic components. However, the time-dependent components undergo structural changes as the speed varies, causing substantial changes in the frequency content of the carrier. This necessarily jeopardizes the AT-CS assumption and compromises the efficiency of the OFSC. This paper proposes a cyclo-non-stationary based solution that explicitly considers the speed as a supplementary variable. Also, the related spectral representation, namely the speed-dependent spectral correlation, is introduced as a generalization of the OFSC. This quantity, when evaluated at a given speed, returns the OFSC as if the machine was operating steadily at the corresponding speed. Eventually, the proposed strategy is evidenced on real-word rolling element bearing vibration signals.

KEYWORDS: bearing diagnosis, nonstationary conditions, cyclo-non-stationarity; speed-dependent spectral correlation.

1. Introduction

Vibration-based diagnosis of rolling element bearings (REB) is still gaining a considerable interest in many industrial sectors. In particular, it has been shown that the emitted vibrations are stochastic cyclostationary (CS) [1]. Since that time, the fault detection of REB faults has been significantly improved by this theory [2]. The validity of the CS assumption is, however, confined to the case of stationary or quasi-stationary regimes wherein the speed profile remains merely constant. In real applications, rotating machines are sometimes subjected to speed variations which jeopardize the stationary regime assumption. A typical example is a wind turbine in which rotating speed of the shaft is dictated by the random and unexpected behavior of the wind. In such cases, the emitted vibrations are likely to witness an interaction between angle- and time-dependent mechanisms [3]. The formers are dictated by system kinematics resulting in angle-periodic modulations whose periodicities are consistent in the angular domain. In turn, the latters are governed by the system transfer function that imposes time-invariant resonance frequencies and relaxation times; these are evidently constant in time. Therefore, the angle\time cyclostationary (AT-CS) was recently introduced in Ref. [4] to jointly describe the angle-kinematics and the time-dynamics of the system [5,6]. In this context, a related tool, coined as the "order-frequency spectral correlation" (OFSC), provides an order-frequency distribution of the signal energy in which the cyclic information and the spectral content of the carrier are jointly displayed. Specifically, the cyclic content is materialized by the presence of discrete spectral lines parallel to the spectral-frequency axis at the cyclic orders, while the frequency content is identified by a continuous distribution of energy along the spectral frequency axis with local strips at the system resonances. However, the proposed approach assumes that time-dependent components are independent of the operating speed. In practice, these components undergo structural changes as the speed severely varies, causing substantial changes in the frequency content of the carrier [7]. In this case, the latter assumption is violated, the AT-CS assumption is jeopardized and the efficiency of the OFSC is compromised. The aim of this paper is to (i) expose the shortcomings of the AT-CS approach in severe speed-

Cette thèse est accessible à l'adresse : http://theses.insa-lyon.fr/publication/2015ISAL0106/these.pdf
© [D. Abboud], [2015], INSA Lyon, tous droits réservés

varying conditions and (ii) provide a cyclo-non-stationary (CNS) based solution to deal with this issue. This paper is organized as follows: section 2 reviews the AT-CS class and theoretically exposes the shortcoming of the AT-CS approach. Section 3 proposes a CNS-based approach to deal with the statistical dependence on the speed. It equally generalizes the OFSC by adding the speed as a supplementary variable and proposes a consistent estimator. Then, the proposed approach is validated in section 5 on real data from test rig containing REBs. Last, the paper is sealed with a general conclusion.

2. Problem statement

The principal aim of this section is to investigate the limitations of the angle\time approach when applied on rotating machine signals in large speed-varying conditions. It starts with a brief review on the AT-CS class. Then, it evaluates the effect of applying the order-frequency spectral correlation on a CNS signal.

2.1. Angle\time cyclostationarity

The angle\time cyclostationary (AT-CS) class was originally introduced in [4] as an extension of the CS class to the case of nonstationary operating conditions. Formally speaking, a signal $X(t)$ is said AT-CS if its angle-time autocorrelation function (ATCF) is periodic and, consequently, accepts a Fourier series of non-zero Fourier coefficients at cyclic orders $k/2\pi$ (the reference angular period is 2π), i.e.

$$\Re_{2X}(\theta,\tau) \stackrel{\text{def}}{=} \mathbb{E}\{X(t(\theta))X(t(\theta)-\tau)\} = \sum_k \Re_{2X}^k(\tau)e^{j2\pi k\theta} \tag{1}$$

where $\Re_{2X}^k(\tau)$ is the (angle\time) cyclic correlation function [4]. This decomposition separates the autocorrelation into two sets of functions with different physical meanings: the "Fourier coefficients" and the "exponential kernels". Whereas the latter is exclusively dependent on the angle variable and reflects the cyclic evolution of the waveform, the former is exclusively dependent on the time-lag and reflects the property of a time-stationary carrier. The bispectral counterpart of this quantity, coined "order-frequency spectral correlation" (OFSC), was thoroughly studied in [4]. It is defined as the double Fourier transform of the ATCF:

$$\mathcal{S}_{2X}(\alpha,\mathrm{f}) \stackrel{\text{def}}{=} \mathcal{F}_{\substack{\theta\to\alpha \\ \tau\to\mathrm{f}}}\{\Re_{2X}(\theta,\tau)\} \tag{2}$$

where α denotes the *cyclic order* (adimensional) and f the *spectral frequency* (in Hertz). Equivalently, this definition can be expressed by means of temporal Fourier transforms as [5]:

$$\mathcal{S}_{2X}(\alpha,f) = \lim_{W\to\infty}\frac{1}{\Phi(W)}\mathbb{E}\left\{\mathcal{F}_W\{X(t)\}^*.\mathcal{F}_W\left\{X(t)e^{-\mathrm{j}2\pi\alpha\theta(t)}\omega(t)\right\}\right\} \tag{3}$$

where $\omega(\mathrm{t}) = \mathrm{d}\theta/\mathrm{dt}$ is the instantaneous angular speed, $\Phi(\mathrm{W}) = \int_{\mathrm{W}}\omega\mathrm{dt}$ is the angular sector spanned during the time interval W and $\mathcal{F}_{\mathrm{W}}\{*\} = \int_{-\mathrm{W}/2}^{+\mathrm{W}/2}(*)\mathrm{e}^{-\mathrm{j}2\pi\mathrm{tf}}\mathrm{dt}$. In the case of AT-CS signals, the OFSC takes the particular form

$$\mathcal{S}_{2X}(\alpha,f) = \sum_k \mathcal{S}_{2X}^k(f)\delta(\alpha-k) \tag{4}$$

where $\mathcal{S}_{2X}^k(\mathrm{f}) = \mathcal{F}_{\tau\to\mathrm{f}}\{\Re_{2X}^k(\tau)\}$, which clearly indicates the presence of symptomatic parallel spectral lines $\mathcal{S}_{2X}^k(f)$ at the cyclic orders k; jointly carries the cyclic flow of the signal energy and the spectral content of the corresponding carrier.

2.2. Practical shortcomings

The AT-CS approach assumes that time-dependent components are independent of the operating speed, which may be accurate for modest speed variations. In practice, these components undergo structural changes as the speed varies severely, causing substantial changes in the frequency content of the carrier [7]. These changes may be induced by the passage of critical speeds, change in the machine power intake, gyroscopic effects, non-

Cette thèse est accessible à l'adresse : http://theses.insa-lyon.fr/publication/2015ISAL0106/these.pdf
© [D. Abboud], [2015], INSA Lyon, tous droits réservés

linearity of the system and other phenomena. Indeed, they affect the statistical properties of the carrier which turns out speed-dependent. As a consequence, the AT-CS assumption is jeopardized and the signal turns out CNS [6]. In this case, a more realistic decomposition of the ATCF in the CNS case can be obtained by adding supplementary speed dependence to the cyclic correlation function of Eq. (1), viz,

$$\Re_{2X_{CNS}}(\theta,\tau) = \sum_k \Re^k_{2X_{CNS}}\big(\tau,\widetilde{\omega}(\theta)\big)e^{j2\pi k\theta} \tag{5}$$

with $\widetilde{\omega}(\theta) = \omega\big(t(\theta)\big)$. This necessarily invalidates the working assumption of the OFSC and compromises its efficiency [5]. This can be analytically verified by inserting Eq. (5) in Eq. (2), which returns

$$\mathcal{S}_{2X_{CNS}}(\alpha,\mathrm{f}) = \sum_{\mathrm{k}} \mathcal{S}^k_{2X_{CNS}}(\mathrm{f},\alpha-\mathrm{k}) \tag{6}$$

where $\mathcal{S}^k_{2X_{CNS}}(\mathrm{f},\alpha) = \underset{\tau\to\mathrm{f}}{\mathcal{F}_{\theta\to\alpha}}\big\{\Re^k_{2X_{CNS}}\big(\tau,\widetilde{\omega}(\theta)\big)\big\}$ is the double Fourier transform of $\Re^k_{2X_{CNS}}\big(\tau,\widetilde{\omega}(\theta)\big)$ having an order-domain bandwidth B^k_w. Obviously, B^k_w is dependent on (i) the variability of the k$^{\text{th}}$ coefficient with respect to the speed (i.e. higher partial derivatives of $\Re^k_{2X_{CNS}}\big(\tau,\widetilde{\omega}(\theta)\big)$ with respect to ω) and (ii) the variability of the speed profile itself (i.e. higher derivatives of $\widetilde{\omega}(\theta)$ with respect to θ): the more important are these variabilities, the wider the induced bandwidths are. In practice, the former dependence is dictated by the susceptibility of the machine on regimes, while the latter dependence is related to the speed profile variability within the record. Due to the nature of mechanical systems and the smooth requirement of the speed profile, these bandwidths are usually much narrower than the reference order (i.e. $\mathrm{B}^k_w \ll 1$) so that $\mathcal{S}^k_{2X_{CNS}}(\mathrm{f},\alpha-\mathrm{k})$ and $\mathcal{S}^{k+1}_{2X_{CNS}}(\mathrm{f},\alpha-\mathrm{k}-1)$ do not overlap over the α-axis for all $\mathrm{k} = 0,1,2\ldots$. As a consequence, the OFSC also seems discrete along the α-axis, yet undergoing an energy leakage of width B^k_w rather than being perfectly localized at the modulation orders. An illustration of this effect is provided in Fig. 1. Note that, in the case of modest speed variations, the bandwidths B^k_w significantly decrease and the cyclic components appear in the form of perfect spectral lines parallel to the f-axis. In this case, the AT-CS approach is optimal and returns the symptomatic distribution provided in Eq. (4). In conclusion, the dependence of the spectral lines properties (phase, magnitude and bandwidth) on the speed profile comprises the effectiveness of the AT-CS approach. Specifically, it misdistributes the energy along the f-axis and α-axis; it also returns different distributions for different speed profiles. The next subsection provides a CNS-based solution for this issue by explicitly considering the speed as a supplementary variable.

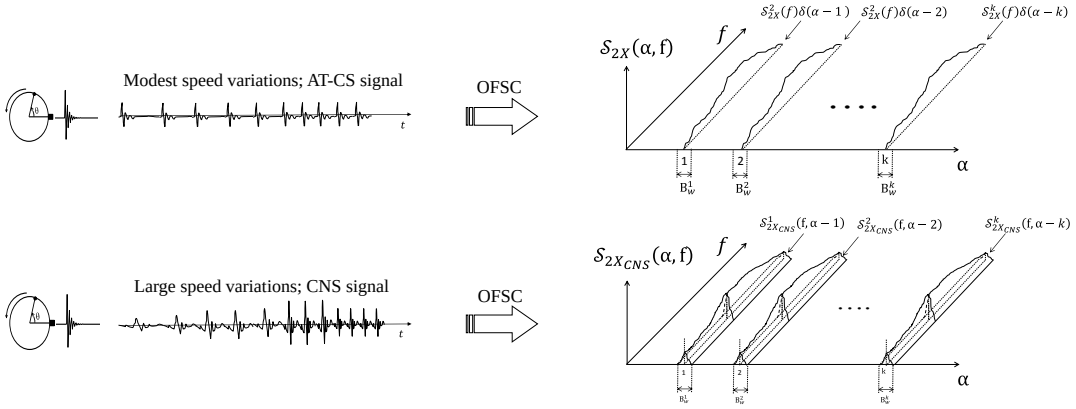

Figure 1 – Shortcoming of the OFSC in large speed variations.

3. Cyclo-non-stationary based solution

This section proposes a new strategy to deal with CNS signals. Specifically, it theoretically generalizes the ATCF and the OFSC by adding a speed variable. An estimator of the latter (i.e. the generalized form of the OFSC) is also proposed.

3.1. The cyclo-non-stationary strategy

Cette thèse est accessible à l'adresse : http://theses.insa-lyon.fr/publication/2015ISAL0106/these.pdf
© [D. Abboud], [2015], INSA Lyon, tous droits réservés

As previously pointed out, the statistical properties of a CNS signal are dependent on the speed; that is its ATCF returns different distribution for different speeds. Then, the straightforward solution to totally describe the signal is to investigate the latter for each operating regime. Therefore, the strategy in the CNS case is to restitute them from existing trajectories. At any rate, a supplementary variable is needed to express the speed variable. Building on this, one can generalize the ATCF function—to be called the "speed-dependent autocorrelation function" (SDCF)—of a random signal $Y(t)$ as,

$$\Re_{2Y}(\theta,\tau,\omega) \stackrel{\text{def}}{=} \mathbb{E}\left\{Y\left(t(\theta)\right)Y(t(\theta)-\tau)^{*}\middle|\omega(t)=\omega\right\} \tag{7}$$

where $\mathbb{E}\{*\,|\mathrm{A}\}$ stands for an ensemble average operator conditioned to event A. For CNS signals, the SDCF enjoys the following decomposition:

$$\Re_{2Y}(\theta,\tau,\omega) = \sum_k \Re_{2Y}^{k}(\tau,\omega)e^{\mathrm{j}2\pi k\frac{\theta}{\varTheta}} \tag{8}$$

where $\Re_{2Y}^{k}(\tau,\omega)$ stands for the "generalized cyclic correlation function". The next subsection investigates the bispectral counterpart of the SDCF.

3.2. The speed dependent spectral correlation

The generalization of the autocorrelation function opens the door to the generalizations of other quantities such as the cyclic autocorrelation function, the Wigner-Vile spectrum and the spectral correlation. Only the latter is investigated in this paper due to its salience in mechanical applications. In this regard, the "speed dependent spectral correlation" (SDSC) can be defined as the double Fourier transform of the SDCF:

$$\mathcal{S}_{2Y}(\alpha,\mathrm{f},\omega) \stackrel{\text{def}}{=} \underset{\tau\to\mathrm{f}}{\mathcal{F}_{\theta\to\alpha}}\{\Re_{2Y}(\theta,\tau,\omega)\}, \tag{9}$$

or equivalently through an ensemble average conditioned on the speed ω operator as:

$$\mathcal{S}_{2Y}(\alpha,\mathrm{f},\omega) = \lim_{\mathrm{W}\to\infty}\frac{1}{\mathrm{W}}\mathbb{E}\left\{\mathcal{F}_{\mathrm{W}}\{X(\mathrm{t})\}^{*}.\mathcal{F}_{\mathrm{W}}\left\{\mathrm{X(t)e}^{-\mathrm{j}2\pi\alpha\frac{\theta(\mathrm{t})}{\varTheta}}\right\}\middle|\omega(t)=\omega\right\}. \tag{10}$$

Similarly to the AT-CS case, it will be shown in the next subsection that the latter representation of the SDSC is more suitable for its estimation. For CNS signals, the SDSC takes the particular form,

$$\mathcal{S}_{2Y}(\alpha,\mathrm{f},\omega) = \sum_{\mathrm{k}}\mathcal{S}_{2Y|\omega}^{k}(\mathrm{f},\omega)\delta\left(\alpha-\mathrm{k}\frac{2\pi}{\varTheta}\right), \tag{11}$$

with $\mathcal{S}_{2Y|\omega}^{k}(\mathrm{f},\omega) = \mathcal{F}_{\tau\to f}\{\Re_{2Y}^{k}(\tau,\omega)\}$, providing a symptomatic distribution similar to that of the AT-CS case, yet being dependent on the speed.

3.3. Estimation issue

This subsection is dedicated to study a consistent estimator for the SDSC on a finite-length record $\{Y(n)\}_{n=0}^{L-1}$ sampled with period Δ having a nonstationary speed profile $\omega(n)$. Among various estimators, the averaged cyclic periodogram may be the most practical because of its easy implementation, enjoying a low computational cost while maintaining remarkable asymptotic properties [2]. Recently, it was also used for the estimation of the OFSC [5]. This estimator consists of substituting the ensemble average operator in Eq. (3) by an average over weighted blocks using short FFT's of fixed size. Let $\{\mathrm{w[n]}\}_{\mathrm{n=0}}^{\mathrm{N_w}-1}$ be a window of $\mathrm{N_w}$ points and $\mathrm{w_s[n]} = \mathrm{w[n-sR]}$ its shifted version by R samples. The increment R is set between 1 and $\mathrm{N_w}$ to provide the opportunity of possible overlap. The averaged cyclic periodogram of the OFSC reads

Cette thèse est accessible à l'adresse : http://theses.insa-lyon.fr/publication/2015ISAL0106/these.pdf
© [D. Abboud], [2015], INSA Lyon, tous droits réservés

$$\hat{\mathcal{S}}_{2Y}^{(L)}(\alpha,f)=\frac{1}{\Phi S||w||^2}\sum_{s=0}^{S-1}\mathrm{DTFT}\{w_s(n)Y(n)\}^*\ \mathrm{DTFT}\left\{w_s(n)Y(n)\omega(n)e^{-j2\pi\alpha\frac{\theta(n)}{\Theta}}\right\},\qquad(12)$$

where S stands for the greatest integer smaller than or equal to $(L-N_w)/R+1$, DTFT is the discrete time Fourier transform, and $||w||^2$ stands for the window energy. In the following, a local approach is followed to estimate the SDSC using the theoretical definition in Eq. (10). To deal with the speed variability, the conditioned ensemble average operator is substituted by a conditioned (arithmetic) mean over finite-length windows. In details, it is proposed to average the windows according to their pertinence to a *regime* r systematically defined by its *central frequency*, ω_r, and *speed resolution* $\delta\omega$. Taking this into consideration, one can relax the averaged cyclic periodogram— henceforth called the "conditioned averaged cyclic periodogram"—to estimate the SDSC of a CNS signal as

$$\hat{\mathcal{S}}_{2Y|\omega_r}^{(\delta\omega)}(\alpha,f,\omega_r)=\frac{1}{L_{eff}^{(\delta\omega)}(\omega_r)||w||^2\mathrm{card}\{M^{(\delta\omega)}(\omega_r)\}}\sum_{m\in M^{(\delta\omega)}(\omega_r)}\mathrm{DTFT}\{w_m(n)Y(n)\}^*\ \mathrm{DTFT}\left\{w_m(n)Y(n)e^{-j2\pi\alpha\frac{\theta(n)}{\Theta}}\right\},\qquad(13)$$

where $L_{eff}^{(\delta\omega)}(\omega_r)=\sum_{n=1}^{L}\mathbb{1}_{\omega_r-\frac{\delta\omega}{2}\le\omega(n)<\omega_r+\frac{\delta\omega}{2}}(n)$ stands for the effective length of regime r defined as the number of points that belong to this regime ($\mathbb{1}_A$ is the indicator function that returns 1 if the event A is true and 0 elsewhere), $M^{(\delta\omega)}(\omega_r)$ stands for the set of windows whose mean speed falls in the speed interval centered at ω_r, i.e.

$$M^{(\delta\omega)}(\omega_r)=\left\{m\in\mathbb{N}^*\ \middle|\ \left(\omega_r-\frac{\delta\omega}{2}\le\frac{1}{N_w}\sum_{n=mlR}^{mlR+N_w}\omega(n)<\omega_r+\frac{\delta\omega}{2}\right)\text{and}\ \left(m\le\left\lfloor\frac{L-1-N_w}{SR}\right\rfloor\right)\right\}\qquad(14)$$

where $\lfloor*\rfloor$ stands for the floor of the real number $*$, $\mathrm{card}\{M^{(\delta\omega)}(\omega_r)\}$ is the effective number of averaged windows. A few words should be said at the end of this subsection. First, the length of the signal does not truly reflect the actual information in the record, but rather the effective length $L_{eff}^{(\delta\omega)}(\omega_r)$ under which the speed lies within the corresponding regime. Second, the quasi-constancy of the speed for the chosen windows allows its simplification from the DTFT transform with that present in the denominator. This latter was basically embedded in the effective angular length—i.e. $\Phi_{eff}^{(\delta\omega)}(\omega_r)\approx L_{eff}^{(\delta\omega)}(\omega_r).\omega_r$. Third, the angle-dependent kernel $e^{-j2\pi\alpha\frac{\theta(n)}{\Theta}}$ was purposely maintained in order to capture slight fluctuations of the speed. Admitting these nuances, the proposed estimator asymptotically shares similar statistical properties with the conventional averaged cyclic periodogram.

4. Experimental validation

In this section, the CNS approach is validated on industrial signals. After a brief description of the test rig and experiments, the OFSC is first applied on two signals of different speed profiles in order to experimentally evidence its shortcoming. After that, the SDSC is applied on stepwise and continuous speed profiles to demonstrate (i) the dependence of the distribution properties on the speed and (b) the unicity of the cyclic signature under the CNS assumption.

4.2. Test rig and experiments

The benchmark used in this paper is located at Cetim and illustrated in Fig. 2. It essentially comprises an asynchronous motor supplied by a variable-speed drive to control the motor speed, followed by a spur gear with 18 teeth and ratio of 1. The gear is subjected to excessive wear. Two identical REB are installed behind the spur gear; the healthy one is closer to the gears than the faulty one which is coupled to an alternator by means of a belt to impose a constant load. The characteristics of the REB are as follows: ball diameter = 6 mm, pitch diameter = 25 mm, number of elements = 8. This returns an expected ball-pass-order on the outer-race (BPOO) at 3.04 orders— i.e. 3.04 times the rotation speed. The sampling rate is set to 25.6 kHz. An optical keyphasor of type "Brawn" is fixed close to the motor output to measure the rotational shaft position. In addition, accelerometer is branched on the faulty REB in the Z-direction to measure the produced vibrations.

Cette thèse est accessible à l'adresse : http://theses.insa-lyon.fr/publication/2015ISAL0106/these.pdf
© [D. Abboud], [2015], INSA Lyon, tous droits réservés

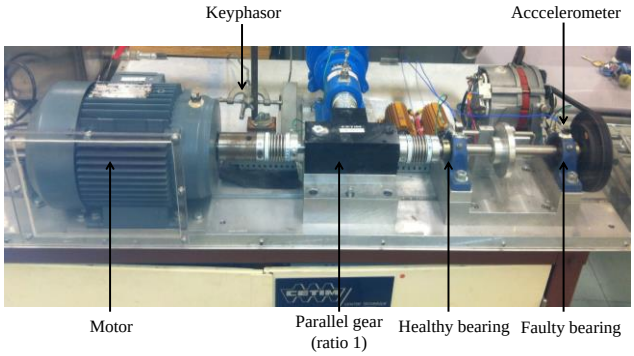

Figure 2 – The benchmark located at Cetim

Three experimental tests are conducted. In the first one, a stepwise variation is imposed to the electric motor at the speeds 950 and 1850 rpm, each for 20s. The intention behind such an experiment is to obtain an actual reference of the machine behavior at the chosen operating speeds. In the second experiment, a runup from 500 to 2000 rpm is imposed to the electric motor over 50s; while a random speed profiles between 500 to 2500 rpm is imposed to the electric motor over 100s in the third experiment. The speed profiles and the acceleration signals are displayed in Fig. 3.

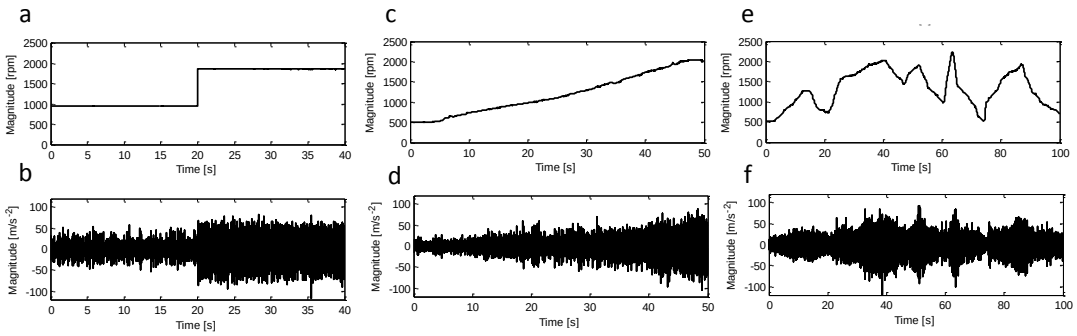

Figure 3 – Experiment 1: (a) speed profile, (b) acceleration signal. Experiment 2: (c) speed profile, (d) acceleration signal. Experiment 3: (e) speed profile, (f) acceleration signal.

4.2. Shortcoming of the OFSC

This section experimentally addresses the shortcomings of the AT approach when applied on highly speed-varying signals. The idea is to compare the OFSC of three signals issued from the same accelerometer, having different speed profiles. The aim is to show the dependence of the distribution properties on its corresponding speed profile or, equally, to demonstrate the non-unicity of mechanical signatures under the AT-CS assumption. To do so, the OFSC is applied on the acceleration signals of experiment 1 (1850 rpm), experiment 2 (runup regime) and experiment 3 (random speed-varying regime). Note that for the latter two cases, only 20s were taken from the signals in order to equals the variance of the obtained distributions. The OFSC is applied around the fundamental order to assess the REB fault signature. The averaged cyclic periodogram is used for the estimation with the following parameters: Hamming window, $N_w = 256$, 66% overlap, cyclic order resolution $\Delta\alpha$=0.001. Since the OFSCs are inversely proportional to the time durations, the distributions were multiplied by the latter to get rid of this dependence. The obtained distributions are displayed in Fig. 4 together with their integrations over the f-axis. Comparing the OFSCs (Fig. 4 (a) and (b)), one can remark a significant change in the intensity, the thickness and the distribution of the cyclic components. For instance, the spectral line of the REB fault component is thicker and less intense in the random speed case than in the runup case (see Fig. 4 (a) and (b)) which, in turn, is thicker and less intense than in the constant speed case. This is due to the fact that the energy leakage is directly related to the speed profile variability; being conform to the theoretical results obtained in subsection 2.2.. A more obvious way to reveal the dependence on the speed profile is to compare their corresponding integration over the f-axis which is actually equivalent to the squared envelope spectrum [2]. The cyclic components appear as a widened peak at the corresponding orders whose thickness is dependent on the

Cette thèse est accessible à l'adresse : http://theses.insa-lyon.fr/publication/2015ISAL0106/these.pdf
© [D. Abboud], [2015], INSA Lyon, tous droits réservés

speed variability: the energy leakage around the harmonic is more significant in the random speed case (see Fig. 4 (d)). In summary, the OFSC of a REB signal in nonstationary conditions is dependent on the corresponding speed profile. Although they provide symptomatic presentations, the existing signatures are not unique and depend on the speed variability within the record. The next subsection treats this problematic from a CNS point of view.

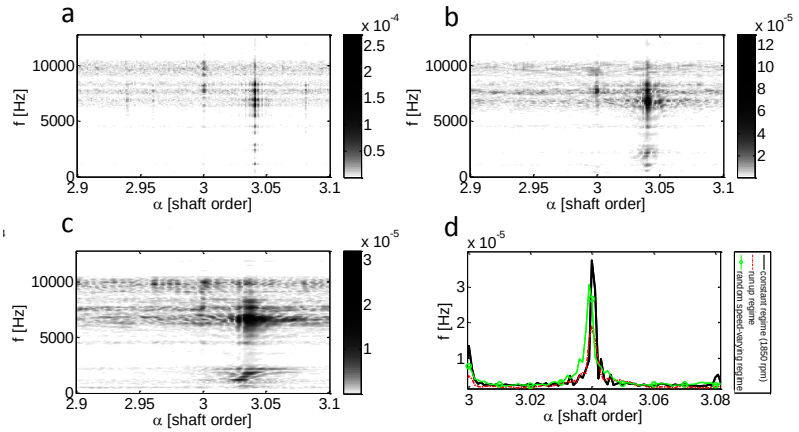

Figure 4 – Close-ups around the BPOO of the OFSC (magnitude) applied on the acceleration signals of (a) experiment 1 (constant regime—1850 rpm) (b) experiment 2 (runup regime), (c) experiment 3 (random speed varying speed) and (d) their integration over the spectral frequency axis.

4.3. Validation of the SDSC

As previously pointed out, the main shortcoming of the AT-CS assumption is the non-unicity of the cyclic signature for distinct speed profiles even though the generative source is the same. The CNS approach theoretically overcomes this problem by adding the speed as a supplementary dimension providing a unique signature independently of the speed variation in the record. The goal of this section is to practically evidence this claim. Therefore, the unicity of the SDSC and its dependence on the speed is tested hereafter. To do so, it is proposed to apply the SDSC on the acceleration signals of experiments 1, 2 and 3 at the speeds 950 and 1850 rpm. In the first case, the SDSC is perfectly equivalent to the application of the OFSC along the step (of 20 s duration) that corresponds to the evaluated regime. It is intended that these distributions stand as the reference on which the efficiency of the SDSC in the case of *continuous* and *large* speed-varying conditions (experiment 2 and 3) is tested. The conditioned averaged cyclic periodogram is used for estimation with the following parameters: Hamming window, $N_w = 256$, 66% overlap, cyclic order resolution $\Delta\alpha$=0.001, the speed resolution $\delta\omega = 150$ rpm. Since the SDSCs are inversely proportional to the effective time durations, the distributions were multiplied by the latter to get rid of this dependence. Figure 5 displays the magnitude of the SDSC applied on acceleration signal of experiment 1 (first column), experiment 2 (second column) and experiment 3 at the speeds 950 rpm (first raw), 1850 rpm (second raw). As a first remark, the distributions of the first experiment (first column) undergo considerable speed-dependent change in their energy (note the amplitude scale in Fig. (a) and (b)). This is simply explained by the fact that the whole signal power, including those of the cyclic components, increases with the speed. Comparing the SDSC of experiments 1 and 3 at each speed, one can remark the similarity in these distributions, validating the CNS approach. Note that the difference in the distribution is due to (i) the random nature of the distributions, (ii) the transfer function of the estimator and (iii) the bias induced by the regime width $\delta\omega$.

5. Conclusion

The difficulty of analyzing rotating machine vibrations in speed-varying conditions resides in the general ignorance of the properties of the induced nonstationarity. In this framework, the angle\time cyclostationary provides a simplistic solution that jointly considers the angle-kinematics and the time-dynamics of the system. A first object of this paper was to analytically demonstrate and experimentally evidence the limitations of this approach in describing such signals. In particular, it is shown that the statistical properties of these signals are dependent on the operating regime and, therefore, the order-frequency spectral correlation is likely to return different distributions for different speed profiles. The second object of this paper was to provide a cyclo-non-

Cette thèse est accessible à l'adresse : http://theses.insa-lyon.fr/publication/2015ISAL0106/these.pdf
© [D. Abboud], [2015], INSA Lyon, tous droits réservés

stationary based approach that explicitly considers the speed as a supplementary variable. In accordance, the speed-dependent spectral correlation was introduced together with its estimator, then, validated on faulty bearing signals. This quantity fully describes the statistical properties of the signal and returns a unique distribution independently of the speed profile in the record. The price to pay against this optimality is a considerable complexity inasmuch the introduced quantity is tri-variable. In light of these results, the authors believe that further work is to be oriented towards the derivation of suboptimal indicators while benefiting from the optimality of the speed-dependent spectral correlation.

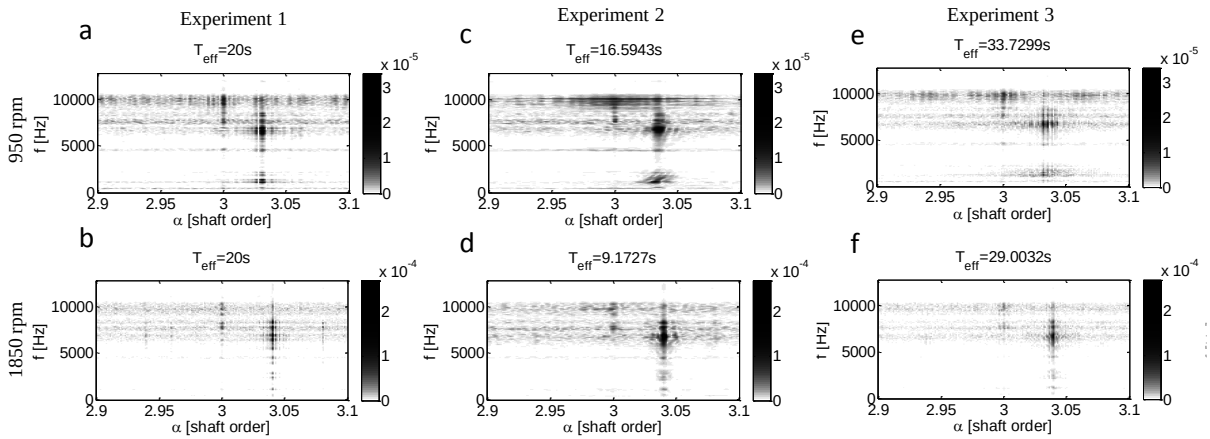

Figure 5 – The SDSC (magnitude) applied on acceleration signal of experiment 1 (first column), experiment 2 (second column) and experiment 3 at the speeds 950 rpm (first raw), 1850 rpm (second raw).

Acknowledgement: This work was supported by the technical center of mechanical industries (Cetim). It was performed within the framework of the LabEx CeLyA (”Centre Lyonnais d’Acoustique”, ANR-10-LABX-60).

6. REFERENCES

[1] Randall, R.B., Antoni, J., Chobsaard, S., “The relationship between spectral correlation and envelope analysis for cyclostationary machine signals: application to ball bearing diagnostics”, Mechanical Systems and System Processing, 15 (5), 2001, pp. 945–962.

[2] Antoni, J., “Cyclic spectral analysis of rolling-element bearing signals: Facts and fictions, Journal of Sound and Vibration”, 304, 2007, pp. 497–529.

[3] Jablonski A., Urbanek J., Barszcz T., “Application of angular-temporal spectrum for detection of rolling-element bearing faults operating under varying speed regime” , Proceedings of the 4th conference in condition monitoring of machinery in non-stationary operations, CMMNO 14-16 December 2014, Lyon France.

[4] Antoni, J, Abboud, D., Baudin, S., “Time-angle periodically correlated process, Cyclostationarity: theory and methods”. Lecture notes in mechanical engineering, Springer, 2014

[5] Abboud, D., Antoni, J., Sieg-Zieba, S., Eltabach, M., “Angle\Time-cyclostationarity in rolling element bearing vibrations”, Proceedings of the 4th conference in condition monitoring of machinery in non-stationary operations”, CMMNO 14-16 December 2014, Lyon France.

[6] Antoni, J., Ducleaux, N., NGhiem, G., Wang, S., “Separation of combustion noise in IC engines under cyclo-non-stationary regime”, Mechanical Systems and Signal Processing, 38 (1) 2009, pp. 223–236.

[7] D’Elia, G., Daher, Z., Antoni, J., “A novel approach for the cyclo-non-stationary analysis of speed varying signals”, Proceedings of ISMA 2010 Including USD 2010.

Cette thèse est accessible à l'adresse : http://theses.insa-lyon.fr/publication/2015ISAL0106/these.pdf
© [D. Abboud], [2015], INSA Lyon, tous droits réservés

FOLIO ADMINISTRATIF

THESE SOUTENUE DEVANT L'INSTITUT NATIONAL DES SCIENCES APPLIQUEES DE LYON

NOM : Abboud DATE de SOUTENANCE : 22/10/2015

Prénoms : Dany

TITRE :
Surveillance vibratoire des machines tournantes en régime non-stationnaires

NATURE : Doctorat Numéro d'ordre :
Ecole doctorale : MEGA
Spécialité : mécanique

Code B.I.U. – Lyon : T 50/210/19 / et bis CLASSE :

RESUME :

Dans les dernières décennies, la surveillance vibratoire des machines tournantes a acquis un intérêt particulier fournissant une aide efficace pour la maintenance dans l'industrie. Aujourd'hui, de nombreuses techniques efficaces sont bien établies, ancrées sur des outils puissants offerts notamment par la théorie des processus cyclostationnaires. Cependant, toutes ces techniques reposent sur l'hypothèse d'un régime de fonctionnement (c.à.d. vitesse et/ou charge) constant ou éventuellement fluctuant d'une façon stationnaire. Malheureusement, la plupart des machines surveillées dans l'industrie opèrent sous des régimes non stationnaires afin de remplir les tâches pour lesquelles elles ont été conçues. Dans ce cas, ces techniques ne parviennent pas à analyser les signaux vibratoires produits. Ce problème a occupé la communauté scientifique dans la dernière décennie et des techniques sophistiquées de traitement du signal ont été conçues pour faire face à la variabilité du régime. Mais ces tentatives restent limitées, dispersées et généralement peu sountenues par un cadre théorique. Le principal objectif de cette thèse est de combler partiellement cette lacune sur la base d'une formalisation théorique du sujet et d'un développement systématique de nouveaux outils de traitement du signal. Dans ce travail, la non-stationnarité du régime est limitée à celle de la vitesse— c.à.d. vitesse variable et charge constante— supposée connue a priori. Afin d'atteindre cet objectif, la méthodologie adoptée consiste à étendre le cadre cyclostationnaire avec ses outils dédiés. Nous avons élaboré cette stratégie en distinguant deux types de signatures. Le premier type comprend des signaux déterministes connus comme cyclostationnaires au premier ordre. La solution proposée consiste à généraliser la classe cyclostationnaire au premier ordre à la classe cyclo-non-stationnaire au premier ordre qui comprend des signaux déterministes en vitesse variable. Le second type comprend des signaux aléatoires périodiquement corrélés connus comme cyclostationnaires au deuxième ordre. Trois visions différentes mais complémentaires ont été proposées pour traiter les variations induites par la non-stationnarité de la vitesse de fonctionnement. La première adopte une approche cyclostationnaire angle\temps, la seconde une solution basée sur l'enveloppe et la troisième une approche cyclo-non-stationnaire (au second ordre). De nombreux outils ont été conçus dont les performances ont été testées avec succès sur des signaux vibratoires réels et simulés.

Cette thèse est accessible à l'adresse : http://theses.insa-lyon.fr/publication/2015ISAL0106/these.pdf
© [D. Abboud], [2015], INSA Lyon, tous droits réservés

MOTS CLES : cyclostationnaire – cyclo-non-stationnaire – cyclostationnaire en angle\temps – régime non-stationnaire – analyse vibratoire – surveillance d'état.
Laboratoire(s) de recherches : LVA
Directeur de thèse : Jérôme Antoni
Président du jury : Composition du jury M Thomas Professeur (École de Technologie Supérieure, Montréal), Rapporteur M. Elbadaoui Professeur (Université Jean Monnet), Rapporteur R. Zimroz Professeur (Université de technologie de Wroclaw) C. Capdessus Maître de conférences (IUT de Chartres) P. Borghesani Maître de conférences (Université de Queensland), invité S. Sieg-Zieba Ingénieur-docteur (CETIM), encadrant CETIM M. Eltabach Ingénieur-docteur (CETIM) , Co-directeur de thèse J. Antoni Professeur (INSA de Lyon), Directeur de thèse

Cette thèse est accessible à l'adresse : http://theses.insa-lyon.fr/publication/2015ISAL0106/these.pdf
© [D. Abboud], [2015], INSA Lyon, tous droits réservés

FOLIO ADMINISTRATIF

THESE SOUTENUE DEVANT L'INSTITUT NATIONAL DES SCIENCES APPLIQUEES DE LYON

NOM : Abboud DATE de SOUTENANCE : 22/10/2015

Prénoms : Dany

TITRE :
Vibration-based condition monitoring of rotating machines in nonstationary regimes

NATURE : Doctorat Numéro d'ordre :
Ecole doctorale : MEGA
Spécialité : mécanique

Code B.I.U. – Lyon : T 50/210/19 / et bis CLASSE :

RESUME :

In the last decades, vibration-based condition monitoring of rotating machine has gained special interest providing an efficient aid for maintenance in the industry. Nowadays, many efficient techniques are well-established, rooted on powerful tools offered in particular by the theory of cyclostationary processes. However, all these techniques rely on the assump-tion of constant— or possibly fluctuating but stationary— operating regime (i.e. speed and/or load). Unfortunately, most monitored machines used in the industry operate under nonstationary regimes in order to fulfill the task for which they have been designed. In this case, these techniques fail in analyzing the produced vibration signals. This issue, therefore, has occupied the scientific committee in the last decade and some sophisticated signal processing techniques have been conceived to deal with regime variability. But these works remain limited, dispersed and generally not supported by theoretical frameworks. The principal goal of this thesis is to partially fill in this gap on the basis of a theoretical formalization of the subject and a systematic development of new dedicated signal processing tools. In this work, the nonstationarity of the regime is confined to that of the speed— i.e. variable speed and constant load, assumed to be known *a priori*. In order to reach this goal, the adopted methodology consists in extending the cyclostationary framework together with its dedicated tools. We have elaborated this strategy by distinguishing two types of signatures. The first type includes deterministic waveforms known as first-order cyclostationary. The proposed solution consists in generalizing the first-order cyclostationary class to the more general first-order cyclo-non-stationary class which enfolds speed-varying deterministic signals. The second type includes random periodically-correlated waveforms known as second-order cyclostationary. Three different but complementary visions have been proposed to deal with the changes induced by the nonstationarity of the operating speed. The first one adopts an angle\time cyclostationary approach, the second one adopts an envelope-based solution and the third one adopts a (second-order) cyclo-non-stationary approach. Many tools have been conceived whose performances have been successfully tested on simulated and real vibration signals.

Cette thèse est accessible à l'adresse : http://theses.insa-lyon.fr/publication/2015ISAL0106/these.pdf
© [D. Abboud], [2015], INSA Lyon, tous droits réservés

MOTS CLES : cyclostationary – cyclo-non-stationary – angle\time cyclostationary – nonstationary regime – vibration analysis – condition monitoring.

Laboratoire(s) de recherches : LVA

Directeur de thèse : Jérôme Antoni

Président du jury :

Composition du jury

M Thomas	Professeur (École de Technologie Supérieure, Montréal), Rapporteur
M. Elbadaoui	Professeur (Université Jean Monnet), Rapporteur
R. Zimroz	Professeur (Université de technologie de Wroclaw)
C. Capdessus	Maître de conférences (IUT de Chartres)
P. Borghesani	Maître de conférences (Université de Queensland), invité
S. Sieg-Zieba	Ingénieur-docteur (CETIM), encadrant CETIM
M. Eltabach	Ingénieur-docteur (CETIM) , Co-directeur de thèse
J. Antoni	Professeur (INSA de Lyon), Directeur de thèse

Cette thèse est accessible à l'adresse : http://theses.insa-lyon.fr/publication/2015ISAL0106/these.pdf
© [D. Abboud], [2015], INSA Lyon, tous droits réservés